FE-15529-3

MHD ELECTRODE DEVELOPMENT

Quarterly Report, April—June 30, 1979

By
John W. Sadler
Jeff Bein
David L. Black
Laurence H. Cadoff
James A. Dilmore
Alfred G. Eggers
Edsel W. Frantti
Edgar L. Kochka
Jack A. Kuszyk
S. K. Lau
Joseph Lempert
Barry R. Rossing
Stephen J. Schneider

August 1979

Work Performed Under Contract No. AC01-79ET15529

Westinghouse Electric Corporation
Advanced Energy Systems Division
Pittsburgh, Pennsylvania

U. S. DEPARTMENT OF ENERGY

DISCLAIMER

Available from the National Technical Information Service, U. S. Department of Commerce, Springfield, Virginia 22161.

Price: Paper Copy $9.00
Microfiche $3.50

FE-15529-3
Distribution Categories UC-90g and UC-93

MHD ELECTRODE DEVELOPMENT

Quarterly Report for the Period

APRIL-JUNE 30, 1979

John W. Sadler
Jeff Bein
David L. Black
Laurence H. Cadoff*
James A. Dilmore*
Alfred G. Eggers
Edsel W. Frantti
Edgar L. Kochka
Jack A. Kuszyk
S. K. Lau
Joseph Lempert**
Barry R. Rossing*
Stephen J. Schneider*

*Westinghouse Research & Development Center
**Consultant

WESTINGHOUSE ELECTRIC CORPORATION
Advanced Energy Systems Division
P. O. Box 10864
Pittsburgh, Pa. 15236

AUGUST 1979

PREPARED FOR THE
UNITED STATES DEPARTMENT OF ENERGY

Under Contract No. DE-AC-01-79-ET-15529

APPROVED:

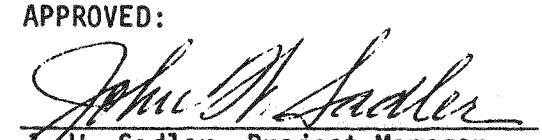

J. W. Sadler, Project Manager
Advanced Energy Systems Division

TABLE OF CONTENTS

TABLE OF CONTENTS (Continued)

LIST OF TABLES

LIST OF FIGURES

LIST OF FIGURES (Continued)

LIST OF FIGURES (Continued)

I. ABSTRACT

Technical progress under DOE Contract DE-AC-01-79-ET-15529 during the April to June 1979 quarter is reported.

Additional zirconia based electrode compositions have been identified as alternates for the non-slagging super-hot WESTF Test 42. Fabrication and processing details are presented for these alternate materials. Results are presented for slag compatibility tests of additional candidate ceramic insulating materials.

Laboratory screening tests, electrochemical and anode arc erosion tests, have continued. Electrochemical corrosion tests of single and polycrystalline zirconia have been completed. The single crystal samples showed recession rates lower by a factor of 5 to 10 when compared with the polycrystalline samples. This data provides further support to the observation that grain boundaries act as sites for corrosion of these materials. Anode arc tests completed with copper samples showed that the highest copper erosion losses were associated with the K_2SO_4 slurry coating.

Test planning and detailed experiment design activities have continued in support of the upcoming WESTF tests. As part of this activity plans are being implemented to add alternative test sections to the planned WESTF tests. Two additional test sections have been defined, a Materials Test Section and a Mini-WESTF Test Section. These test sections provide an opportunity to increase use of WESTF and to obtain critical data on the effects of the various MHD environments, including slag/seed chemistry, on candidate electrode and insulator materials.

The test section for WESTF Test 41 Run 2, reference AVCO electrodes, has been rebuilt and installed in preparation for continuation of the test.

Detailed planning is continuing concerning the mini-computer/DAS expansion and the magnet addition to WESTF. Long lead procurements have been initiated.

II. OBJECTIVE AND SCOPE OF WORK

In continuation of the program to develop MHD power generation to commercial feasibility, Westinghouse is conducting a program to develop improved electrode designs for open-cycle coal-fired MHD generator applications. The program includes the link between basic and supportive materials development and testing in an engineering test rig that offers an adverse MHD environment for extended periods of time.

Specific development activities of this program are as follows:

(a) Laboratory screening tests to provide preliminary electrochemical stability data on selected advanced or modified ceramic candidate electrode and insulation materials.

(b) Laboratory screening tests to evaluate the resistance of selected candidate anode materials to simulated arc impingements under a representative range of chemical and thermal conditions.

(c) Engineering rig tests of preferred electrode designs, selected on the basis of the screening test results and/or pertinent outside data, under simulated open-cycle coal-fired MHD operating conditions.

(d) Preparation and fabrication of experimental electrode materials, as warranted by favorable laboratory screening test results, to provide samples for engineering rig tests.

In addition to these four main development activities, this project includes providing such laboratory, design, test and analytical support as necessary to characterize test materials, and to determine such essential physical and chemical properties as are required to properly design the test specimens and to interpret and analyze test data. Dependent on development results, preferred electrode materials will be prepared for advanced testing in other DOE contractor facilities.

These objectives are being pursued in accordance with a statement of work which is consistent with the National Plan for MHD development formulated by DOE.

The major elements of the program are presented in a Work Breakdown Structure which is presented in Table 1. The Level I effort is the MHD Electrode Development Contract, and Level II consists of the following four tasks.

WBS 1.1 ELECTRODE AND INSULATOR MATERIALS
WBS 1.2 ENGINEERING TESTS
WBS 1.3 WESTF MODIFICATION
WBS 1.4 PROJECT MANAGEMENT AND DOCUMENTATION

WBS 1.1 - ELECTRODE AND INSULATOR MATERIALS

The objective of this task is to provide for the development, laboratory evaluation and fabrication of electrode and insulator materials. All necessary experimental material preparation, as well as fabrication of test samples for laboratory screening tests, engineering rig tests in the Westinghouse Electrode System Test Facility, WESTF (WBS 1.2), or other tests will be completed under this task. This task also includes supporting pre-test material characterization and laboratory screening tests used to evaluate the relative performance of candidate materials. These screening tests include electrochemical and anode arc impingement tests.

WBS 1.2 - ENGINEERING TESTS

The objective of this task is to provide for the engineering tests of promising electrode/insulator materials resulting from the WBS 1.1 activity. In particular, this task provides for the supporting design, test and post-test analysis effort as well as maintenance and operation of the engineering test rig, WESTF. Table 2 summarizes WESTF test capabilities.

This task incorporates the elements of planning, experiment design, test operations and post-test analysis and provide the close engineering design and test discipline necessary to effect successful electrode/insulating wall system development. In addition, final fabrication and assembly operations necessary to incorporate electrode and interelectrode insulating elements fabricated under WBS 1.1 into a complete assembly ready for testing in WESTF

TABLE 1

WORK BREAKDOWN STRUCTURE

(SUBELEMENTS TO DOE WBS 2.2.2)

WBS 1.0 MHD ELECTRODE DEVELOPMENT

- WBS 1.1 ELECTRODE AND INSULATOR MATERIALS
  - WBS 1.1.1 EXPERIMENTAL MATERIALS FABRICATION
    - MATERIAL DEVELOPMENT
    - MATERIAL CHARACTERIZATION
    - MATERIAL FABRICATION
  - WBS 1.1.2 LABORATORY SCREENING TESTS
    - ELECTROCHEMICAL TESTS
    - ANODE ARC TESTS
- WBS 1.2 ENGINEERING TESTS
  - WBS 1.2.1 TEST ENGINEERING
    - DEVELOPMENT REQUIREMENTS
    - EXPERIMENT DESIGN
    - POST-TEST ANALYSIS
  - WBS 1.2.2 TEST ASSEMBLY FABRICATION
  - WBS 1.2.3 WESTF OPERATIONS
    - PRE-TEST ACTIVITY
    - TEST OPERATIONS
- WBS 1.3 WESTF MODIFICATION
- WBS 1.4 PROJECT MANAGEMENT AND DOCUMENTATION

I II III - SYSTEMS LEVEL

TABLE 2

WESTF TEST CAPABILITIES

Mass Flow	To 0.5 lb/sec
Combustion Temperature	To 2850^{o}K
Combustor Pressure	1 to 5 atm
Channel Velocity	Subsonic, 500 to 800 m/sec
Seeding	K_2CO_3 or K_2SO_4 wet with ash or char additions (Rosebud)
B Field	3 Tesla, nominal - 3.3 Tesla, objective
Fuel	Toluene/#2 Fuel Oil
Oxidant	Preheated air with oxygen enrichment
Data Collection	240 channels coupled with minicomputer
Test Duration	Up to 100 hours
Test Frequency	Up to 2 per month
Channel Configuration	12.5 cm^2 flow cross section
Startup Ramp, Minimum	$\approx$25^{o}K/min

will be provided under this task. Required test documentation and facility opeating procedures will also be prepared.

WBS 1.3 - WESTF MODIFICATION

This task has been established to provide for the planned modification of WESTF. The primary element of this task is the addition of a conventional 3.0 Tesla magnet.

WBS 1.4 - PROJECT MANAGEMENT AND DOCUMENTATION

This centralized management task provides the focal point for directing the activities which comprise the full project effort. The Project Manager is responsible for the proper definition, integration and implementation of the technical, schedule, contractual, and financial aspects of the program. Coordination of the preparation of required documentation will also be completed under this task.

III SUMMARY OF PROGRESS TO DATE

Figure 1 summarizes the overall program schedule and status based on the approved Project Management Summary Baseline Report.

During the April to June 1979 quarter, the principal areas of activity were as follows:

- Continuation of electrode and insulator material development activities.
- Continuation of electrochemical corrosion tests of single crystal and polycrystal zirconia.
- Rebuilding of the WESTF test section for WESTF Test 41 - Run 2.
- Continuation of design activities in support of WESTF Test 42/44 (zironia and hafnia coupons) and WESTF Test 43 (Pt-Fe).
- Initiation of design of the modified WESTF Test Section (magnet), the Materials Test Section and the Mini-WESTF Test Section.
- Continuation of activities, including long lead procurement actions, in support of the magnet installation in WESTF.

1.0 WBS 1.1 -- ELECTRODE AND INSULATOR MATERIALS

In support of WESTF Tests 42 and 44 (non-slagging super-hot electrode coupons) the processing for the additional zirconia based materials was defined and the material characterized. Additional slag corrosion tests of insulator materials which are candidates for use in slagging hot or non-slagging super-hot generators were completed. Of these a spinel and magnesia material have been selected for further tests. Details relative to the above are presented in Section IV - 1.1.

Additional electrochemical corrosion tests have been completed to evaluate the intrinsic corrosion resistance of zirconia based materials under hot slagging conditions. Fully stabilized single crystal ZrO_2-12m/oY_2O_3 and partially

U.S. DEPARTMENT OF ENERGY

DOE Form CR-535 (1-78)

MILESTONE SCHEDULE AND STATUS REPORT

1. Contract Identification: MHD ELECTRODE DEVELOPMENT PROGRAM	2. Reporting Period through 6/30/79	3. Contract Number: DE-AC-01-79-ET-15529
4. Contractor (name, address): WESTINGHOUSE ELECTRIC CORPORATION ADVANCED ENERFY SYSTEMS DIVISION P. O. Box 10864 Pittsburgh, Pa. 15236		5. Contract Start Date: April 23, 1979 6. Contract Completion Date: September 30, 1980

7. Identification Number WBS	8. Reporting Category (e.g. contract line item or work breakdown structure element)	9. Fiscal Years and Months: 79 (O N D J F M A M J J A S) 80 (10 20 30 40)	10. Percent Complete a) Planned	b) Actual
1.1	ELECTRODE AND INSULATOR MATERIALS			
1.1.1	EXPERIMENTAL MATERIALS FABRICATION			
1.1.2	LABORATORY SCREENING TESTS			
1.2	ENGINEERING TESTS			
1.2.1	TEST ENGINEERING			
1.2.2	TEST ASSEMBLY FABRICATION			
1.2.3	WESTF OPERATIONS			
1.3	WESTF MODIFICATION			
1.4	PROJECT MANAGEMENT AND DOCUMENTATION			

11. Remarks

12. Signature of Contractor's Project Manager and Date	13. Signature of Government Technical Representative and Date
John W. Sadler	

Figure 1. Program Schedule and Status

stabilized polycrystalline ZrO_2-8m/oY_2O_3 were evaluated. The single crystal ZrO_2 anodes demonstrated the lowest corrosion rate obtained to date. A series of anode arc tests were completed with copper samples and a variety of coatings. As expected, the highest copper erosion losses were associated with the K_2SO_4 slurry coating and involved formation of complex sulfates with the copper substrate. Specific details are presented in Section IV - 1.2.

2.0 WBS 1.2 -- ENGINEERING TESTS

Test Specification revisions have been issued for WESTF Test 41 - Run 2 (AVCO reference electrodes) and WESTF Test 42 (zirconia/hafnia electrode coupons). Summaries of the above are presented in Section IV - 2.1.1. Two alternative WESTF Test Sections, a Materials Test Section and a Mini-WESTF Test Section, are discussed in Section IV - 2.1.1.

Section IV - 2.1.2 presents the results of detailed thermal analyses completed for WESTF Tests 42/44 and 43. This section also reports the results of general purpose thermal analyses. Additional results of the post-test analysis of WESTF Test 41 - Run 1, slag chemical analysis and electrical performance analysis, are discussed in Section IV - 2.1.3.

Details of the rebuilding of the WESTF Test 41 test section for run 2, as well as the results of final assembly electrical measurements, are presented in Section IV - 2.2.

Table 3 provides a summary of WESTF tests. No tests were completed during this quarter.

3.0 WBS 1.3 -- WESTF MODIFICATION

As presented in Section IV-3.0, a number of procurements have been initiated concerning expansion of the mini-computer/DAS and modifications to support the magnet addition.

TABLE 3

WESTF TEST SUMMARY

OPERATING MODE	SLAG COLD	SLAG COLD	SLAGGING	NON-SLAG-SH	SLAG HOT	NON-SLAG-SH	SLAG HOT	NON-SLAG-SH	SLAG HOT
Facility	WESTF	WESTF	WESTF	WESTF	WESTF	WESTF	WESTF	WESTF	WESTF
Test ID	W-40	W-41	D-9	W-42	W-43	W-44	TBD	TBD	TBD
Approx. Date	11/78-1/79	3/79-8/79	9/79	9/79	10/79	12/79	TBD	TBD	TBD
Electrode Material	Cu	Cu-Pt (+) Cu-W/Cu (-)	NA	ZrO_2 Based[1] HfO_2 Based Perovskite	Pt (+) Fe (-)	ZrO_2 Based[1] HfO_2 Based Perovskite	SiC	ZrO_2 Based HfO_2 Based Perovskite	$MgCr_2O_4$
Insulator Material	$MgAl_2O_4$	BN	NA	NA	$MgAl_2O_4$ Al_2O_3	NA	Si_3N_4	NA	$MgAL_2O_4$ Al_2O_3
T_E, ^oC	150/275	150	NA	1700-1900	1000-1300	1700-1900	1000-1300	1700-1900	1000-1400
J, amp/cm^2	To 1.25	0.9	NA	NA	To 1.25	NA	To 1.25	To 1.25	To 1.25
$\dot{Q}$, w/cm^2	~125	~125	NA	<60	~80	<60	~80	<60	~80
Axial Field, Kv/m	Yes	Yes	NA	NA	Yes	NA	Yes	TBD	Yes
Coal Type	Eastern	Eastern	Rosebud	Rosebud	Rosebud	Rosebud	Rosebud	Rosebud	Rosebud
Duration-Hrs.[2]	15	20+	NA	8/Increm.	~20	8/Increm.	~20	8/Increm.	~20
Status	Complete	In Process							

(1) Coupons

(2) Seen On to Seed Off

4.0 WBS 1.4 -- PROJECT MANAGEMENT AND DOCUMENTATION

Significant project documentation issued included the following:

- Quarterly Report - January - March 1979
- Project Management Summary Baseline Report.

The Project Management Summary Baseline Report was approved by DOE.

IV. DETAILED DESCRIPTION OF TECHNICAL PROGRESS

1. WBS 1.1 ELECTRODE AND INSULATOR MATERIALS

1.1 WBS 1.1.1 - Experimental Materials Fabrication

1.1.1 Material Development

Zirconia - Based Electrodes

WESTF-42 and 44 will consist of 'coupons' of electrode materials suitable for use under non-slagging super-hot conditions and will be tested initially in the absence of electrical or magnetic fields. ZrO_2 and HfO_2-based electrode compositions have been identified as promising candidate materials. The ZrO_2-based electrodes are to be processed and fabricated by Westinghouse while the HfO_2 based electrodes will be supplied by Battelle Northwest Laboratories (BNW). WESTF-42 will tentatively consist of one wall of ZrO_2 based electrodes and the other wall of the HfO_2-based materials supplied by BNW. Two ZrO_2 compositions have been identified for the test and will be positioned in the channel wall to achieve three different surface temperatures. Specifically, the compositions are:

(1) 85 m/o ZrO_2 - 15 m/o $(Mg_{.625}Ca_{.375})O$

(2) 88 m/o ZrO_2 - 12 m/o Y_2O_3

(3) 88 m/o ZrO_2 - 12 m/o Y_2O_3 (Phase I U-02 Electrode)

The virgin Yttria-stabilized electrodes from the U-02 Phase I program will be run as a comparison with the newly processed electrodes. Since there may not be a sufficient number of the hafnia-based compositions to fill half a channel, a third ZrO_2-based material was processed as a possible substitute material. This composition consisted of 85 m/o ZrO_2 - 12 m/o CeO_2 - 3 m/o Y_2O_3

The processing and characterization scheme for fabricating this ZrO_2-based electrode was identical to the previously processed electrodes, as reported

in the previous Quarterly Report, Reference 1. All of the starting powders were of very pure quality and very fine grain size. They were obtained from commercial sources with a purity of greater than 99.9 percent. The individual powders were blended together to a specific molar composition in a large V-blender until a good mechanical mixture was obtained. The batch was then combined with a mixture of distilled water, polyvinyl alcohol, and carbowax to form a slurry. Homogeneity was achieved by milling these constituents together for four hours in a rubber lined ball mill using yttria-stabilized zirconia balls. The slurry was then introduced into a centrifugal disk type spray dryer to produce free flowing spherical powder. A SEM photomicrograph of the powder after spray-drying is shown in Figure 2. The different oxide constitutents have agglomerated into spherical particles as observed by the other ZrO_2-based powders. A bimodel distribution of the spheres is also observed, presumably due to the large particle size difference between the starting powders. Analysis of the surface area of the 85 m/o ZrO_2 - 12 m/o CeO_2 - 3 m/o Y_2O_3 powder was also acquired using a Micromeritics Surface Area Analyzer. A value of 1.38 m^2/gm was obtained, which was of the same order of magnitude as the previous ZrO_2-based powders.

The material was then cold pressed at 30,000 psi into 50 gm bars approximately 9 cm x 1.2 cm x 1.2 cm. They were subsequently sintered for ten hours at 1500°C and then at 1900 °C for 2.5 hours.

Linear shrinkage was measured at ~12 percent. The bars will be final machined to the proper design dimensions using diamond cutting tools.

General Insulating Materials

As a continuation of insulating materials evaluations reported in Reference 1, tests were completed on the slag corrosion resistance of three more ceramic insulators considered suitable for use in slagging hot or non-slagging super-hot generators. The simple static immersion test, previously described, was used to evaluate the materials. Photographs of the three sectioned insulators are shown in Figures 3 to 5. Macrophotographs of the sectioned "mini-crucibles" are shown on the left side of the pages along with higher magnification photos

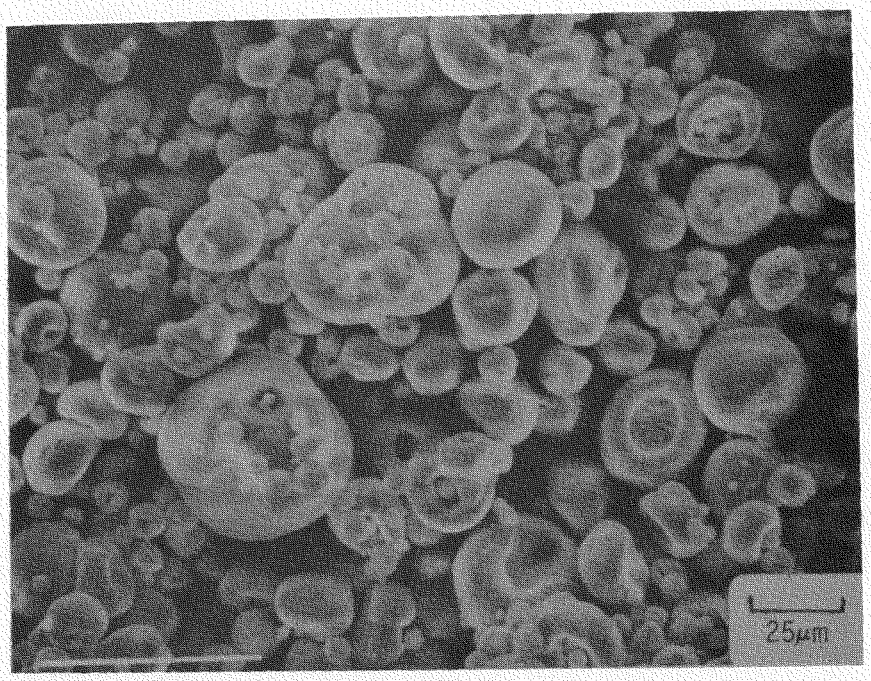

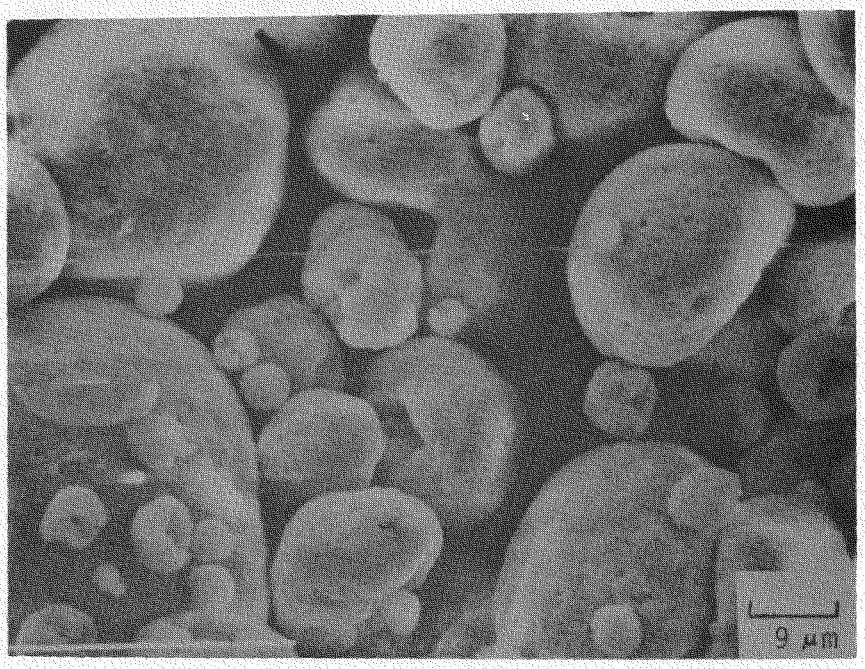

Figure 2. SEM Microphotographs of 85 m/o - ZrO_2 - 12 m/o CeO_2 - 3 m/o Y_2O_3 Powder after Spray-Drying

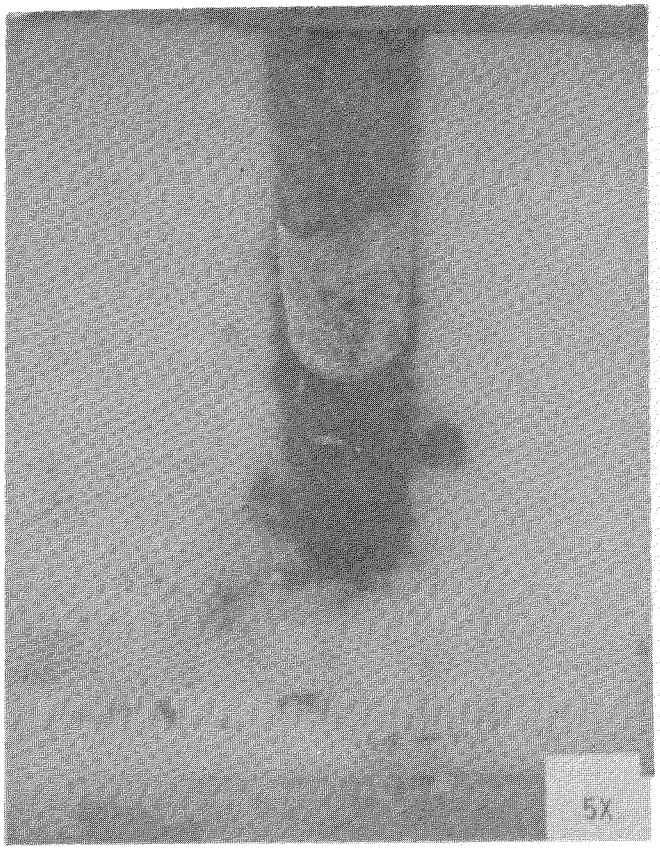

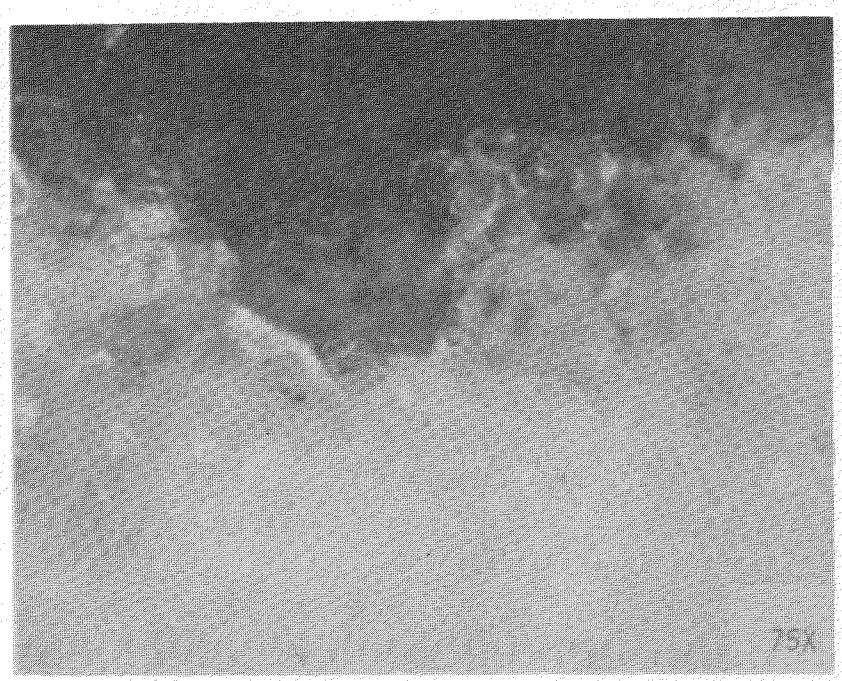

Figure 3. Appearance of $MgAl_2O_4$ (Fused Cast) from CORHART after Exposure to Western Coal Slag at 1400°C for 20 Hours

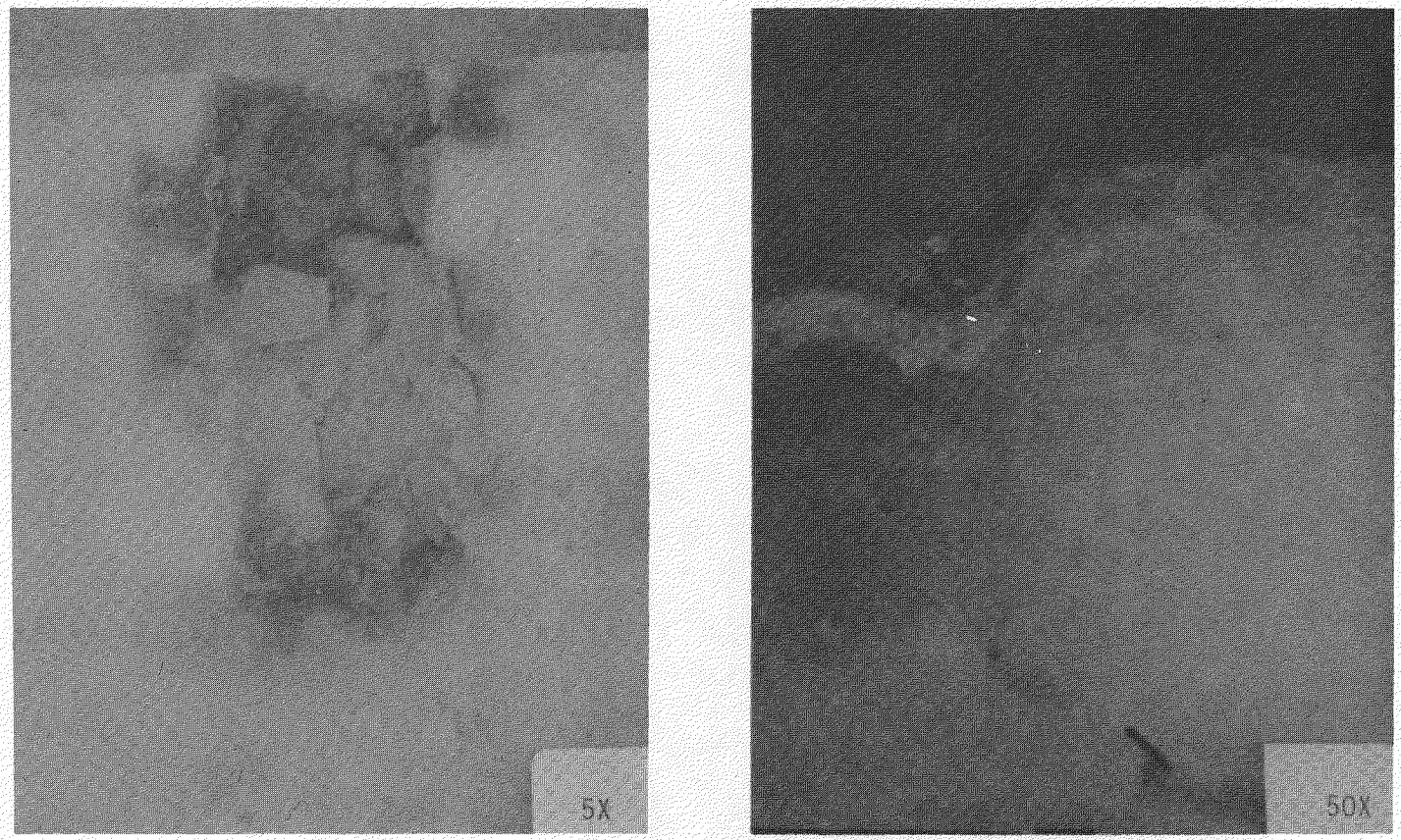

Figure 4. Appearance of MgO (Experimental High Sintered) from North American Refractories after Exposure to Western Coal Slag at 1400°C for 20 Hours

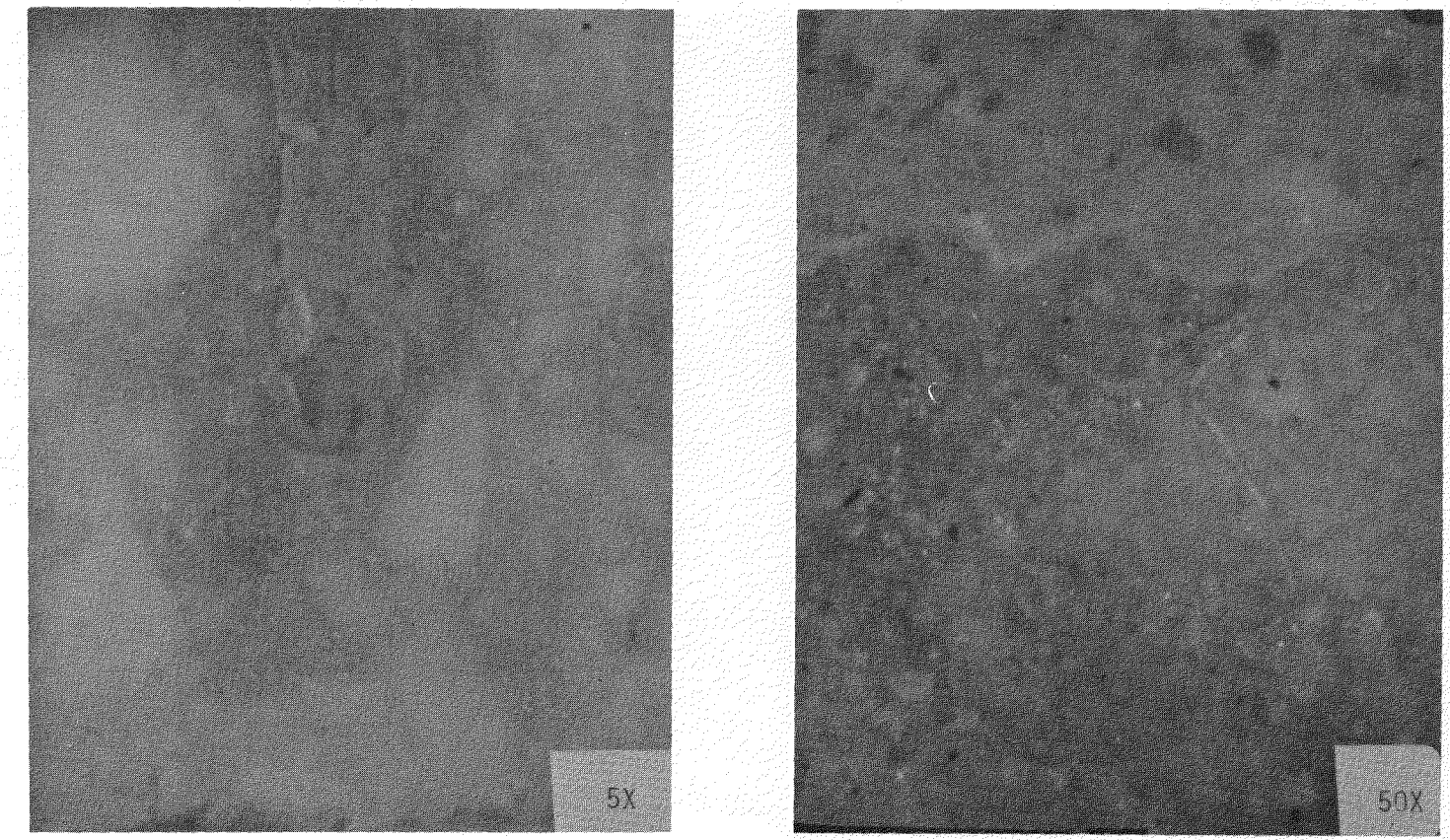

Figure 5. Appearance of MgO (Experimental High Sintered w/Pitch Impregnation) from North American Refractories after Exposure to Western Coal Slag at 1400°C for 20 Hours

of the insulator/slag interface on the right-hand side. Table 4 lists the three insulators along with their density, source, processing history and relative observations of their corrosion resistance.

The fused-cast spinel ($MgAl_2O_4$) from Corhart in Figure 3, appeared to be reasonably resistive to Western coal slag for the twenty hour exposure. Wetting of the insulator's surface was observed but no boundary layer or attack zone was detected. The only possible detrimental aspect of the material was the large macro voids present in the structure. These cavities can be passageways for slag penetration if they are open to the exposed surface. Another fused-cast spinel refractory has just recently been obtained from Carborundum and will undergo the same slag corrosion test as a comparison with the Corhart product. This experimental insulator is a 'true' spinel unlike the Corhart material which consists of large MgO grains imbedded in an Al_2O_3 matrix. It is also much denser, with no large pores scattered throughout the structure. Figure 6 displays the fractured surfaces of these two spinels. It is easily observed that the Corhart material has fractured intergranularly - between the large MgO grains. The Carborundum spinel, in complete contrast, shows a transgranular mode of fracture across a very smooth fine grained structure.

An experimental high sintered MgO refractory from North American Refractories, with and without pitch impregnation, was tested for slag corrosion, as shown in Figures 4 and 5. This refractory was made with Dead Sea periclase grain which has a very low SiO_2 content and presumably a better corrosion rate than the commercial MgO refractories. The MgO without pitch impregnation showed only fair resistance to the coal slag. The slag was observed to penetrate through the bonding phase of the refractory which as a result loosened many of the MgO grog grains. The pitch impregnated refractory, on the other hand, displayed very little grain pullout. The structural integrity of the bonding phase appears stronger and there seems to be less detectable slag penetration.

Both insulators, the spinel and magnesia (with and without pitch), will join the four other selected insulators found superior in this "mini-crucible" test for further evaluation. This will include laboratory slag testing at higher

TABLE 4

COMPATIBILITY OF CERAMIC INSULATORS WITH WESTERN COAL SLAG*
(MINI-CRUCIBLE TEST AT 1400°C FOR 20 HOURS)

Material	% Theoretical Density	Source	Processing History	Relative Observations
$MgAl_2O_4$	85	CORHART	Fused Cast	Slag has wet the surface of the material to average depth of 1 mm; there is no extensive structural damage, large open voids in microstructure could be sink for slag penetration; at slag/insulator interface slag has shown to have coated glassy grains, but no boundary layer or attack zone is present. [Sample run for 100 hours shows no added damage to insulator.]
MgO	82	North American Refractories	Cold Pressed, Sintered to 1500°C	Slag has penetrated into the matrix of the insulator to a depth of 1-2 mm in some areas; penetration is through the bonding phase in and around the grog grains; some of the grains have been loosened by the corrosion of the slag; some areas show a boundary layer noted by a brownish discoloration.
MgO	82	North American Refractories	Cold Pressed, Sintered to 1500°C and Impregnated with Pitch	Slag has wet surface and penetrated to depth of 1 mm; boundary between slag and insulator is glassy, no apparent pull out of grog grains observed; pitch seems to have increased the structural integrity and increased strength of bonding phase, less detectable chemical activity with pitch.

* Montana Flyash/K_2CO_3

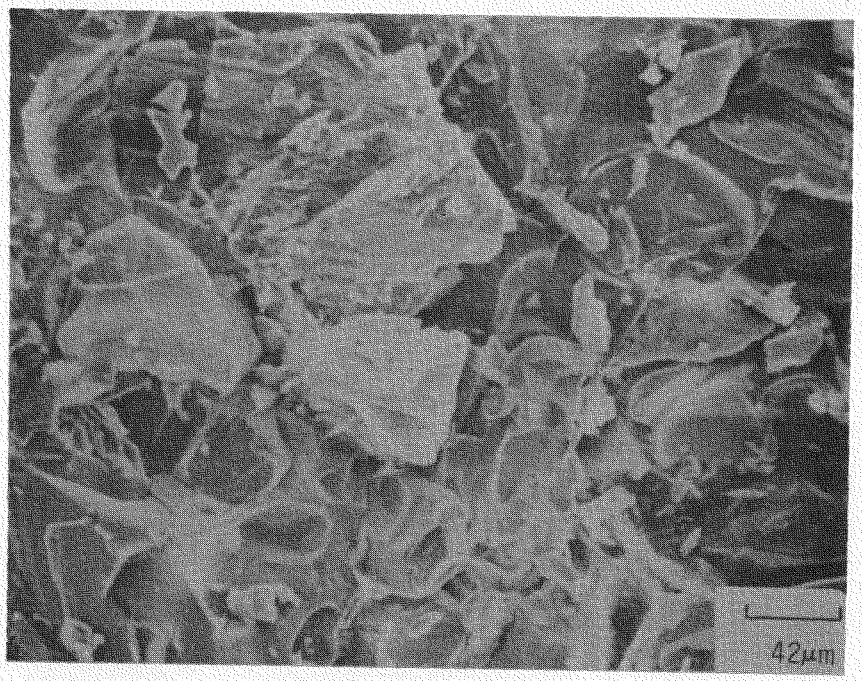

(A)

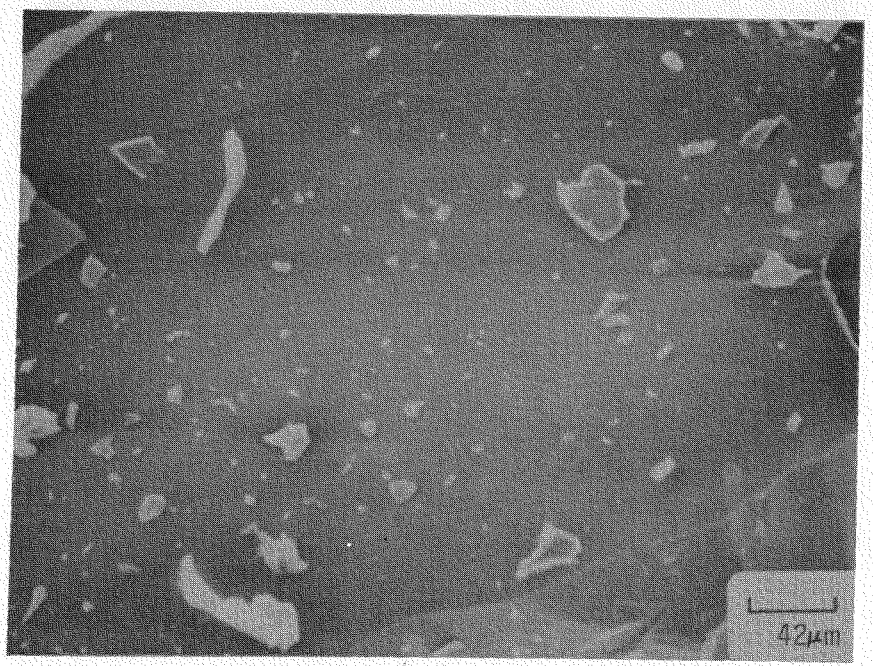

(B)

Figure 6. SEM Microphotographs of Fractured Surface of (A) Fused Cast $MgAl_2O_4$ (CORHART), (B) Fused Cast $MgAl_2O_4$ (Carborundum)

temperatures (1500-1650°C) along with insertion in the insulating walls or transition sections in future WESTF tests.

1.1.2 Material Characterization

Zirconia-Based Electrodes

The ZrO_2-based electrode (85 m/o ZrO_2 - 12 m/o CeO_2 - 3 m/o Y_2O_3) which was processed for consideration in WESTF 42 or 44 was characterized for a number of material properties. This pre-test analysis was undertaken to properly evaluate the performance of this electrode under the design conditions. Small samples were cut from the as-processed sintered bars for the analyses.

The densities, porosities, and phase analysis of 85 m/o ZrO_2 - 12 w/o CeO_2 - 3 m/o Y_2O_3 is presented in Table 5. It should be observed that the density of this composition did not increase significantly after the 1900°C firing. What did change dramatically was the percent of open pores in the material. A decrease from 4.83 to 0.13 percent open porosity was noted, which is very advantageous for a MHD electrode material in combatting the corrosive nature of a coal slag. X-ray diffraction methods were employed for determing the phases present, the crystallinity, and the lattice parameters of 85 m/o ZrO_2 - 12 m/o CeO_2 - 3 m/o Y_2O_3. The results, as presented in Table 5, shows the material with poor crystallinity and a tetragonal lattice structure rather than the expected stable cubic form. Other ZrO_2 compositions with CeO_2 as one of the constituents have also shown the same poor crystallinity and tetragonal or distorted cubic lattice.

The microstructure of 85 m/o ZrO_2 - 12 m/o CeO_2 - 3 m/o Y_2O_3 was evaluated from both fracture surface samples and from samples which had been mounted and polished. Figure 7 depicts scanning electron micrographs of the electrodes fractured surface and Figure 8 displays an optical metallographic photograph of a polished electrode sample. The SEM micrographs reveal isolated spherical pores interdispersed throughout the structure, indicative of a closed pore material. The mode of fracture is predominately transgranular and has an identical appearance to the previously processed ZrO_2-based materials.

TABLE 5

DENSITIES, POROSITIES AND PHASE ANALYSIS
OF 85 M/O ZrO_2 - 12 M/O CeO_2 - 3 M/O Y_2O_3

DENSITIES AND POROSITIES

Composition	Green Density	1500°C Firing		1900°C Firing	
		Density	% Open Porosity	Density	% Open Porosity
85 m/o ZrO_2 - 12 m/o CeO_2 - 3 m/o Y_2O_3	3.22 g/cc	5.35 g/cc	4.83	5.37 g/cc	0.13

X-RAY ANALYSIS

Composition	Sample Designation	Crystallinity	Major Phase	Minor Phase
85 m/o ZrO_2 - 12 m/o CeO_2 - 3 m/o Y_2O_3	CZ-WE0201	Poor	Tetragonal * a = 5.158, c = 5.188	CeO_2

* Lattice parameters are tentative due to the broad lines.

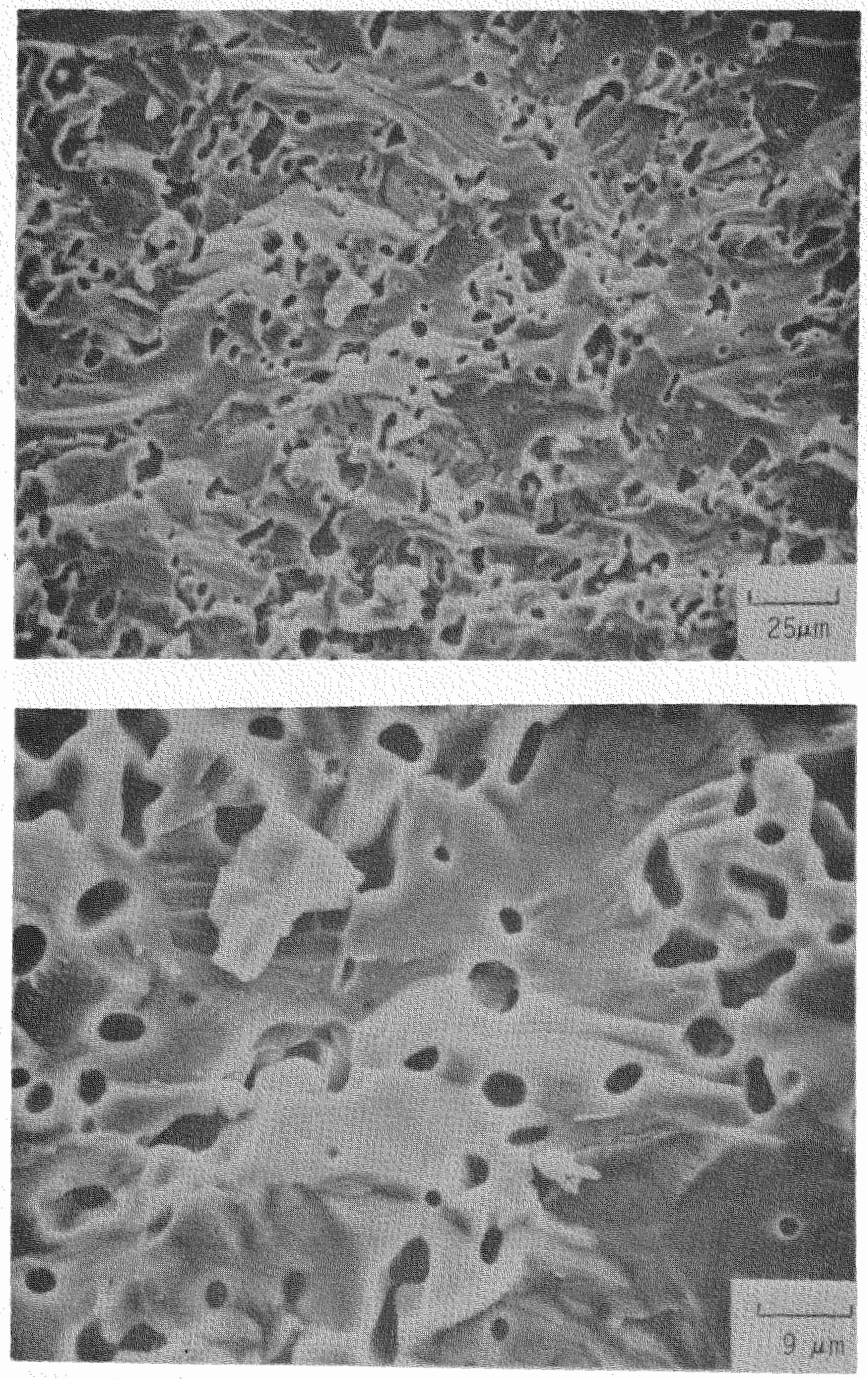

Figure 7. SEM Microphotographs of Fractured Surface of 85 m/o ZrO_2 - 12 m/o CeO_2 - 3 m/o Y_2O_3

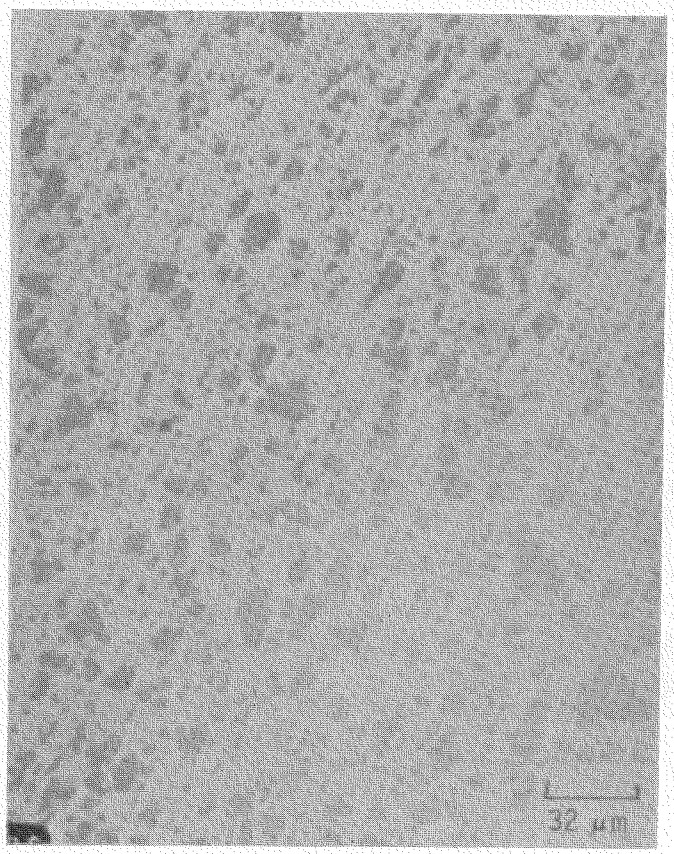

Figure 8. Microstructure of 85 m/o ZrO_2 - 12 m/o CeO_2 - 3 m/o Y_2O_3

1.2 WBS 1.1.2 - Laboratory Screening Tests

1.2.1 Electrochemical Corrosion

Studies are continuing to evaluate the intrinsic corrosion resistance of O^{-2} ion conducting ZrO_2-based materials for use as electrodes under hot slagging conditions. Single crystal fully stabilized ZrO_2 - 12 m/o Y_2O_3 obtained from Ceres Corporation, Waltham, Massachusetts, and a 98 percent dense partially stabilized polycrystalline ZrO_2 -8 w/o Y_2O_3 material from Transtech Corporation, Gaithersburg, Maryland, were used in these current laboratory electochemical tests. A Montana Rosebud slag, W-50 (Reference 2) doped with 10 w/o K_2O served as the electrolyte. The test conditions and results are summarized in Table 6. Anode corrosion losses for the single crystal samples were so low, that the values reported are within measuring error. X-ray diffraction and SEM-EDAX studies of the test samples are, as yet, incomplete.

For the first time in our studies of ceramic electrodes, corrosion reactions especially at the anode were predominately intrinsic in nature. There was little evidence of fluxing or undercutting of the anode by liquid slag. As shown in Figure 9, the single crystal anode from Test 154 appears to be almost unattacked. Under the test conditions given in Table 6, the originally transparent or white colored ZrO_2 cathodes were partially reduced to metallic Zr which in turn gives rise to color darkening and cracking of the cathode matrix. In some locations, these cracked regions tended to be fluxed by the slag, accounting for the much higher corrosion rates at the cathode vis a vis the andoe. Figure 10 is an example of the highly cracked polycrystalline cathode in Test 157. Metallic globules which were predominately iron were universally found in the slag at the cathode/slag interface. This is further evidence that the ZrO_2 cathodes have been partially reduced to metallic Zr. In all these experiments, O_2 gas was not evolved at the liquid slag/anode interface but only at the backface of the anode; i.e., at the Pt lead wire/anode interface. The explanation for this has been discussed previously, Reference 1.

The extent of electrochemical corrosion reported in Table 6 for single crystal ZrO_2 anodes are amongst the lowest ever reported in our experiments with

TABLE 6

SUMMARY OF ELECTROCHEMICAL CORROSION

	Tests on Dense ZrO_2 - Y_2O_3		
Test I. D.	154	155	157
Slag I. D.	W-50	W-50	W-50
Electrode Comp. (% Y_2O_3)	10 m/o*	10 m/o*	8 m/o**
% Theoretical Density	100	100	98
Temperature, °C	1400	1410	1400
Duration, Min.	24	20	25
Current Density, A/cm^2	1.1	1.1	0.83
Corrosion, ΔW μg/Coubmb			
Cathode, ΔWc	33.8	29.4	155.0
Anode, ΔWa	< 4.8	< 5.9	23.8
$\Delta Wc/\Delta Wa$	7.0	5.0	6.5
Test Cell	D2	D2	D2

* Single Crystal

** Polycrystalline

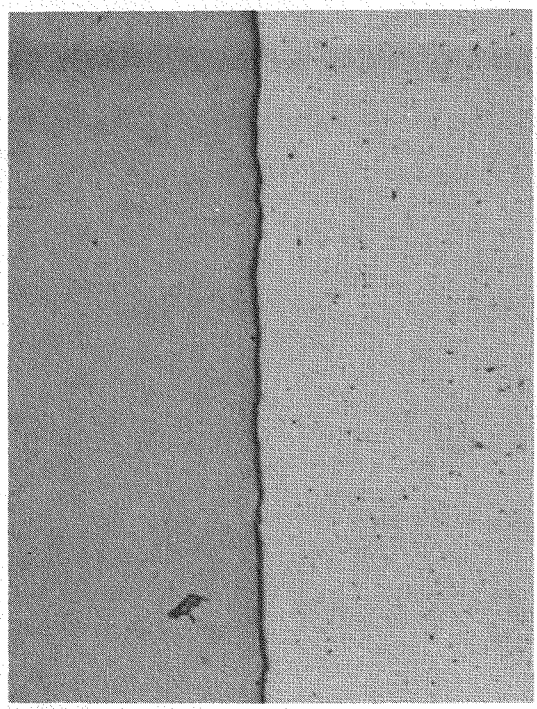

Figure 9. Slag/ZrO_2 Single Crystal Anode Interface from Test 154

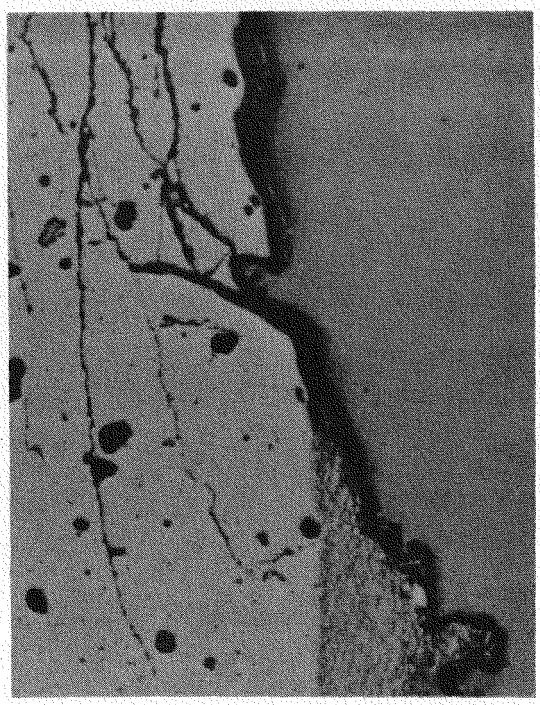

Figure 10. Highly Cracked Slag/ZrO_2 Cathode Interface from Test 157

potential electrode materials. It strongly supports the hypothosis that high quality, dense, pure materials are critically important to the making of long-lived MHD electrodes. Corroborating evidence comes from comparing these most recent results to the ≈200 μg/Coulomb corrosion loss previously reported for an 85 percent theoretically dense ZrO_2 - 10 w/o Y_2O_3 sample tested under the same conditions, Reference 3.

In conclusion, ZrO_2 based materials appear to be extremely promising candidates for use as anodes in MHD channels under hot slagging conditions. They also may seriously be considered as cathode materials provided O_2 can be provided at the backface of the cathode (Pt lead/cathode interface) to minimize the reduction or blackening reactions

1.2.2 Anode Arc Tests

Tests are continuing in our efforts to investigate the parameters effecting anode arc erosion. In this quarter, arc experiments have been run using copper button samples with 5.5 amp arcs at surface temperatures between 250 and 500°C, the principal variables being the chemical coating applied to the copper surfaces. The following coatings (or surface conditions) have been tested:

- K_2SO_4 - H_2O Slurry
- K_2CO_3 - H_2O Slurry
- Deionized H_2O
- Bare Uncoated Copper.

The data from these tests, corrected for oxidation losses, are given in Figures 11 and 12.

The relationships shown suggest the extremely complex nature of anode arc erosion. For example, the results for bare copper should establish the ground state of erosion loss due to the combined mechanisms of arc induced copper oxidation, vaporization, and melting. Erosion values higher or lower than the

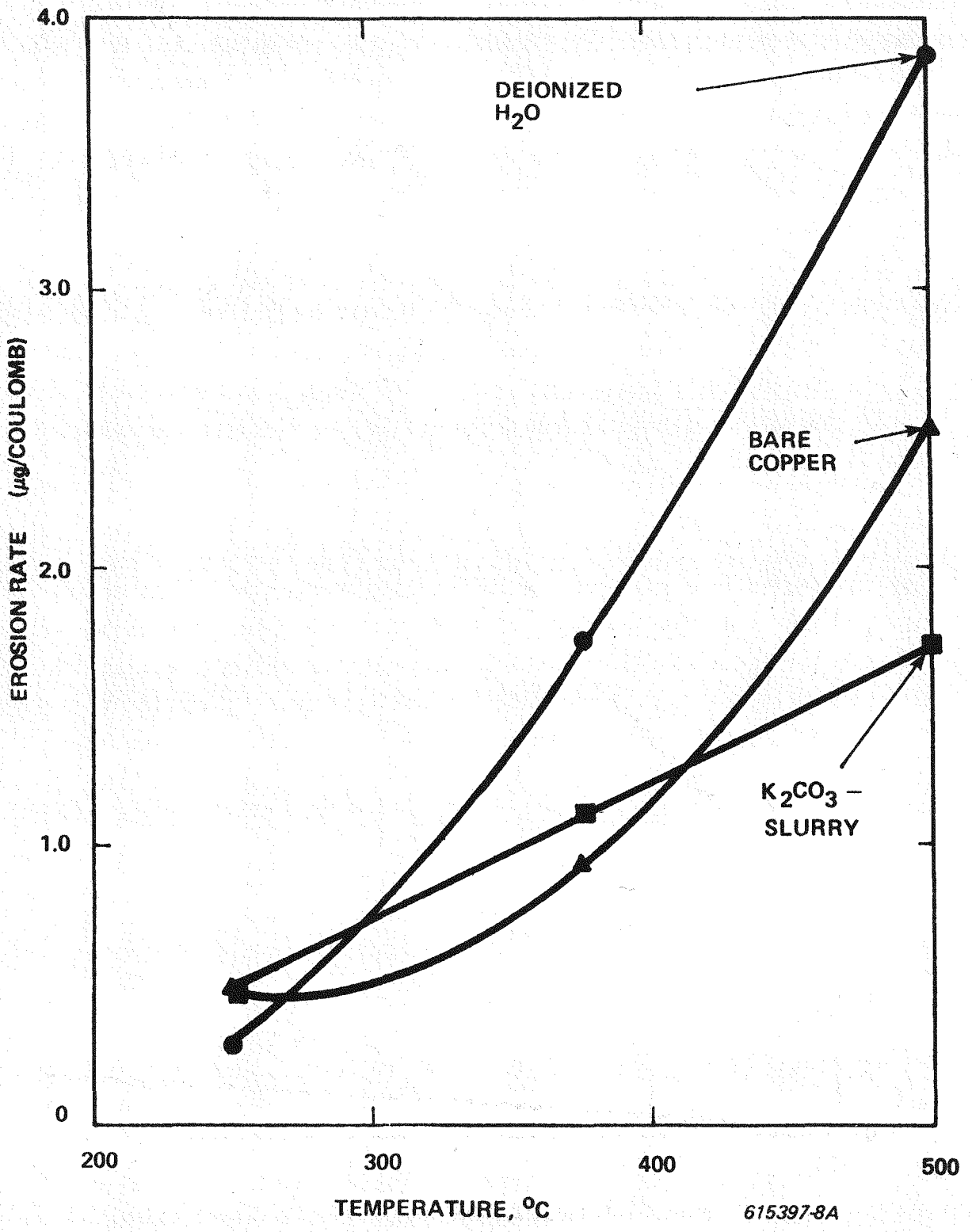

Figure 11. Anode Erosion Rates for a Variety of Surface Coatings or Conditions Versus Anode Surface Temperature

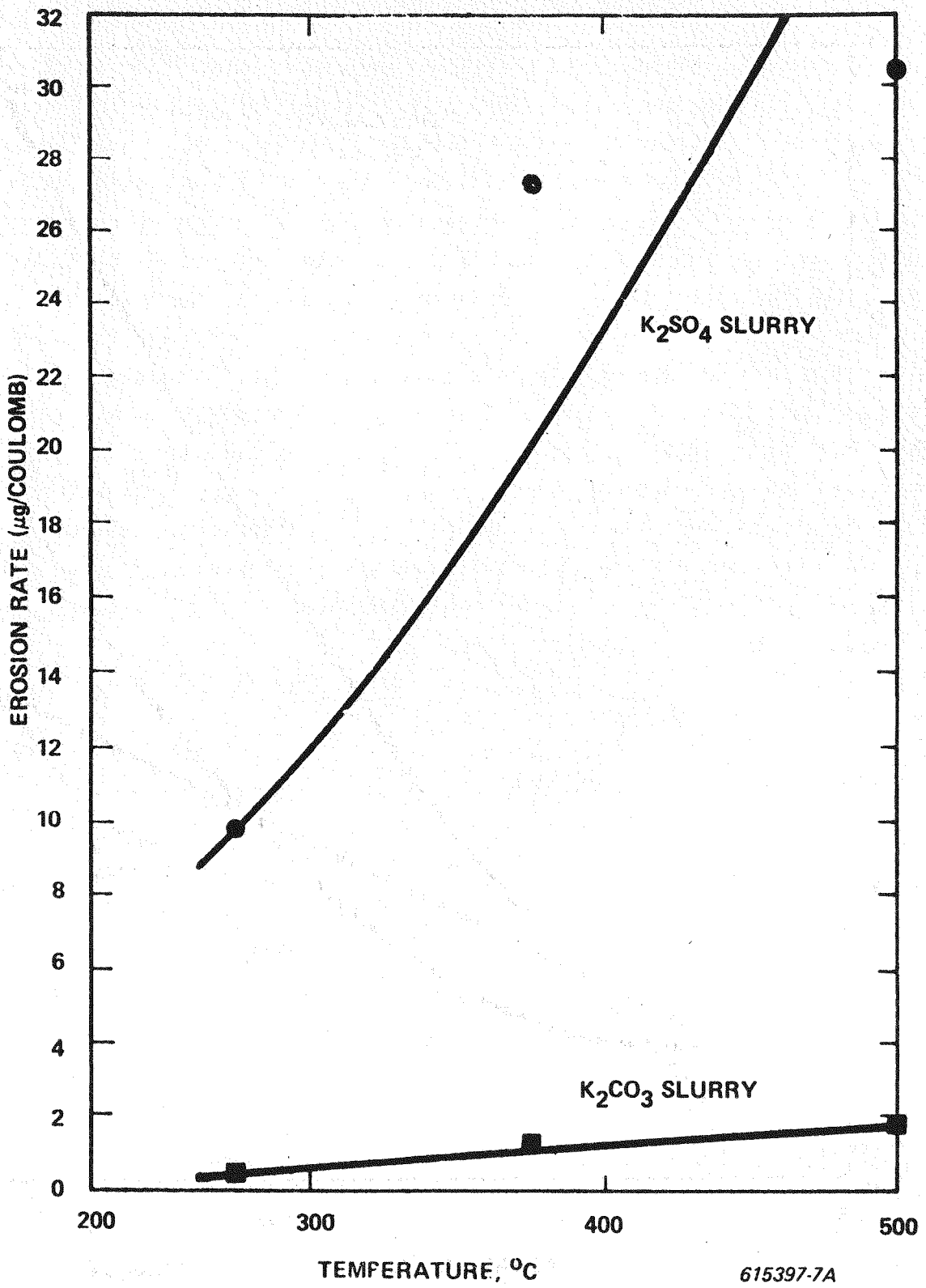

Figure 12. Erosion Rates for K_2SO_4 and K_2CO_3 Water Slurry Coated Anodes Versus Surface Temperature[2]

above may be due to at least two additional phenomena, - dissipation of arc energy resulting from the vaporization of all or part of the chemical coating and promotion of chemical reactions between the applied coating and the copper substrate. The first mechanism listed above should decrease erosion losses while the latter mechanism should increase erosion. Thus the results in Figure 11 suggests that for the case of a pure water coating vis a vis bare copper, chemical corrosion reactions increase faster than the rate at which heat is being removed from the arc. The result that erosion with K_2CO_3 slurry is less than bare copper and much less than that with plain water may be interpreted as indicating , for example, that since the energy of the arc is dissipated much more rapidly in vaporizing K_2CO_3 (or CO_2) and water than what occurs when only pure water is used. There is little excess energy left over to promote chemical reactions. The copper erosion losses from tests using a K_2SO_4 slurry coating are the highest for any coating tested so far and are apparently a result of rapid chemical reactions involving formation of complex sulfates with the copper substrate.

2.0 WBS 1.2 - ENGINEERING TESTS

2.1 WBS 1.2.1 - Test Engineering

2.1.1 Development Requirements

Preliminary test specifications are issued to initiate design activity on the channel for each test. Materials development/procurement and electrode systems development activities are initiated based on the Preliminary Test Specification. Final Test Specifications are issued after completion of all development activities and provide the basis for detail design of the channel and WESTF testing.

During this quarter, revisions to WESTF Test 41 (AVCO electrodes), Final Test Specification, and a Final Test Specification for WESTF Test 42 (Zirconia-based coupons) were issued. The Test 42 specification will be revised again to include hafnia-based coupons that are available from Battelle PNL. A redesign and rebuild of the WESTF Test 41 channel was completed as were manufacturing sketches for all of the components required for WESTF Test 42 (except for the

wall that is to contain the hafnia-based coupons) and for WESTF Test 43. Design and manufacturing priority is being given to WESTF Test 42.

WESTF Test 41

Revision 2 of the Final Test Specification for WESTF Test 41 was issued. This revision pertains to WESTF Test 41, Run 2, a continuation of Run 1 with a redesigned and rebuilt channel using only the electrodes from Run 1.

Run 1 was terminated on March 6, 1979, after approximately fourteen hours at conditions due to a test section leak believed to be caused by loss of insulating titles, overheating of the boron nitride spacer used between the first electrode and the inlet transition section, arc indications in the region of the initial electrode-insulating wall-transition section, and the subsequent degradation of backing materials that resulted in over-temperaturing the G-10 wall and gasket. The channel was redesigned to correct the problems encountered in Run 1 and to improve the electrical insulation of the channel.

Significant features of the redesign are as follows:

- Interlocking ceramic tiles, Harklase refractory MgO, line the transition sections; MONOFRAX "A" Al_2O_3 tiles line the insulating walls in the channel, and spinel brick is relegated to use as a filler in the non-sensitive areas of the insulating walls. Insulating wall design temperatures are 900°C maximum in the channel and 1600-1650°C maximum in the transition section.
- New G-10 electrode support walls have hole locations shifted so that, instead of an ineffectively cooled 0.2 inch thick spacer on each end, a 0.4 inch water cooled spacer will be employed at the exit end of the walls. (The spacer is used to make up for differences in the AVCO electrode dimensions and the effective length of the Westinghouse electrode walls). New boron nitride interelectrode insulation and new tie rods will be in the assembly.

- The insulating walls are redesigned with diagonal heat sinks in the center section that are well insulated from one another and from the anode and cathode walls. The interlocking ceramic tiles extend beyond the electrodes so that they are locked in place and provide better insulation. A schematic diagram showing the design of these walls appears in Figure 13.

WESTF Test 42

A final test specification was issued for WESTF Test 42 on the assumption that the test may be limited to zirconia based coupons and insulation wall materials under super-hot slag/seed conditions. This assumption reflects that some delays have been encountered at Battelle PNL in fabricating and characterizing the candidate hafnia materials.

Since the test specification was issued, satisfactory hafnia-based coupons have been available from Battelle PNL and will be incorporated in the test section, schedule permitting. The test specification will be revised to reflect these changes, as appropriate.

The primary objective of the test is to compare the relative performance of selected materials over a range of temperatures in a super-hot MHD channel environment in the absence of electrical or magnetic fields. There are two walls for electrode materials with six coupon holders on each wall. One wall will have zirconia based coupons, and the other wall will have hafnia based coupons. The zirconia based materials are furnished by Westinghouse, and the hafnia based compositions and the thermal conductivities for all materials are furnished by Battelle PNL. The materials and channel locations as presently known are given in Table 7. The equivalent design information on the hafnia based coupons has yet to be determined since thermal conductivity values are not available.

The insulator walls each have five copper cooling blocks for testing several magnesia materials and a spinel. Surface temperatures are to range from 1500°C at the inlet to 1700°C at the exit of the channel. The materials selected for

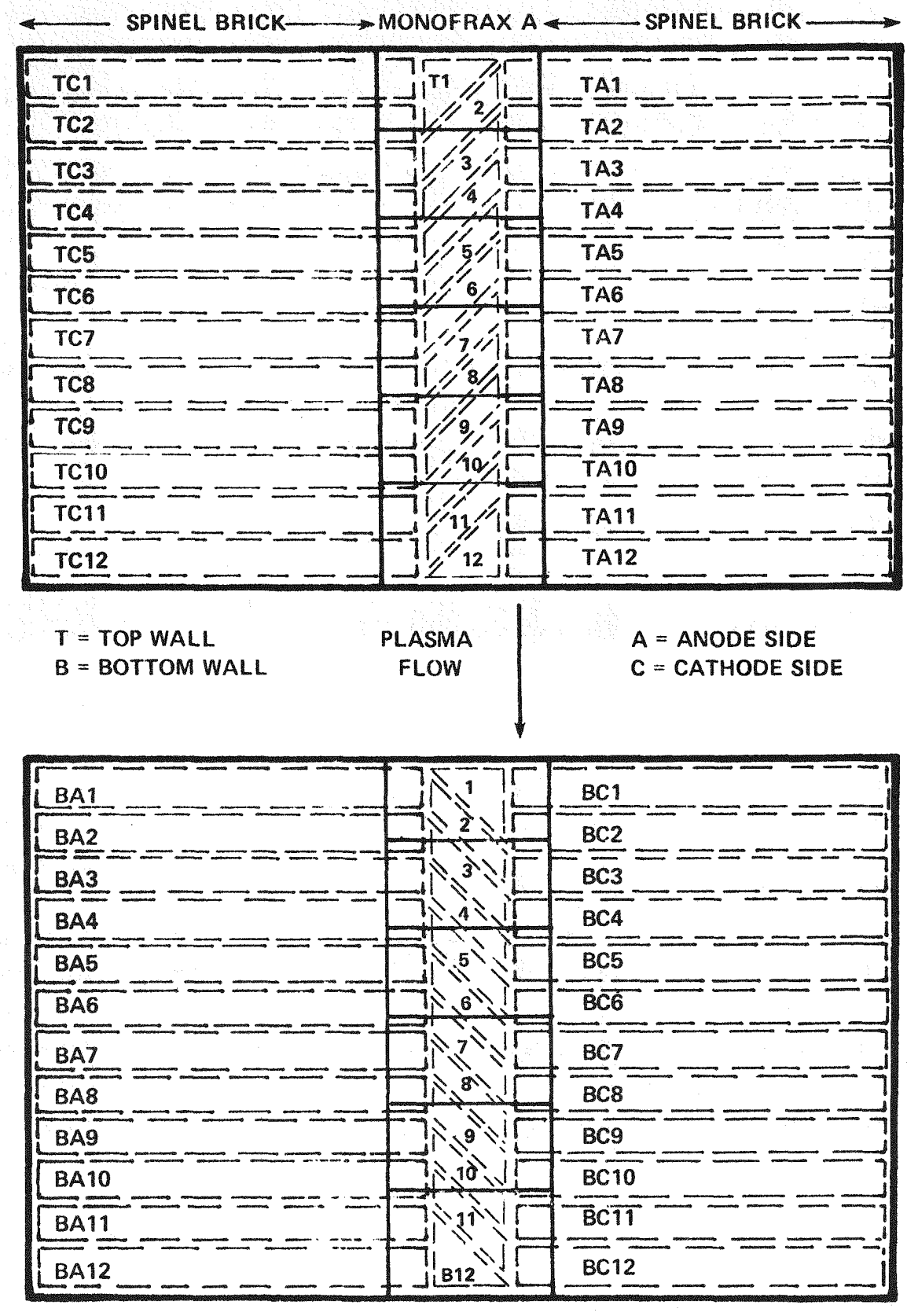

Figure 13. Schematic of Insulating Walls WESTF 41-Run 2 *615397-10A*

TABLE 7

ELECTRODE COUPON MATERIALS AND CHANNEL LOCATIONS

COUPON LOCATION	SURFACE TEMP. (°C)	MATERIALS I.D.[1]	MATERIAL THICKNESS[2]	
			Coupon	MgO Beneath Coupon
A1 (inlet)	1650	YZ-WE0101/YZ-WE0102	0.230	0.050
A2	1650	ZC-WE0101/ZC-WE0102	0.200	0
A3	1750	YZ-WE0101/YZ-WE0401	0.265	0.100
A4	1750	ZC-WE0101/ZC-WE0102	0.300	0.100
A5	1850	YZ-WE0101/YZ-WE0102	0.270	0.050
A6	1850	ZC-WE0101/ZC-WE0102	0.360	0.100
C1 (inlet)	1650	TBD	TBD	
C2	1650	TBD	TBD	
C3	1750	TBD	TBD	
C4	1750	TBD	TBD	
C5	1850	TBD	TBD	
C6	1850	TBD	TBD	

1) YZ = 12 $Y_2 3_0$ - 88 ZrO_2 [WE0401 (mixed particles sizes) and WE0101, WE0102 (fine particle size)]

ZC = 15 $(Mg_{62.5}\ Ca_{37.5})0$ - 85 ZrO_2, [WE0101, WE0102]

2) At a plasma flow rate of 0.11 kg/sec and 0.1 inch of nickel mesh interface material.

the insulating walls and their sizes are shown below (brazed attachments with 0.2 inch nickel mesh interface material):

Surface Temp. (°C)	Material	I.D.	Thermal Cond. (W/cmK)	Thickness (in.)
1500	Harklase MgO	MG-HW0501	0.049	0.39
1625	Norton MgO	MG-NT0501	0.080	0.97
1675	Narco MgO	MG-NA0101	0.051	0.40
1675	Cohart Spinel	MA-CR0101	0.059	0.73

The inlet transition section is lined with high purity MgO (Norton 85 percent dense - MG-NT0501) and designed to run below 1650°C. A conservative design approach gave a thickness of 1.11 inches. However, to maintain the cross-sectional area of the test passage, the maximum ceramic thickness can be only 0.918 inch. Therefore, an even lower surface temperature should be obtained.

The exit transition section provides the opportunity to test some additional commercial materials without contaminating the rest of the test section. It is designed to a 1625°C surface temperature with 1.173 inches thick Harklase surrounding the other test materials. The materials and their design sizes are shown below (silastic attachment to copper):

Surface Temp. (°C)	Material	I.D.	Thermal Cond. (W/GmK)	Thickness (in.)
1625	Harklase MgO	MG-HW0501	0.054	1.16
1625	Chrome-Spinel	CS-CC0101	0.044	0.95
1625	Chrome-Aluminum	CA-CC0101	0.032	0.69
1625	Castable MgO	MG-KA0201	0.043	0.93

A layout of the channel showing materials locations and temperatures is given in Figure 14. Coupon identifications on the wall labelled "cathode" are to be determined.

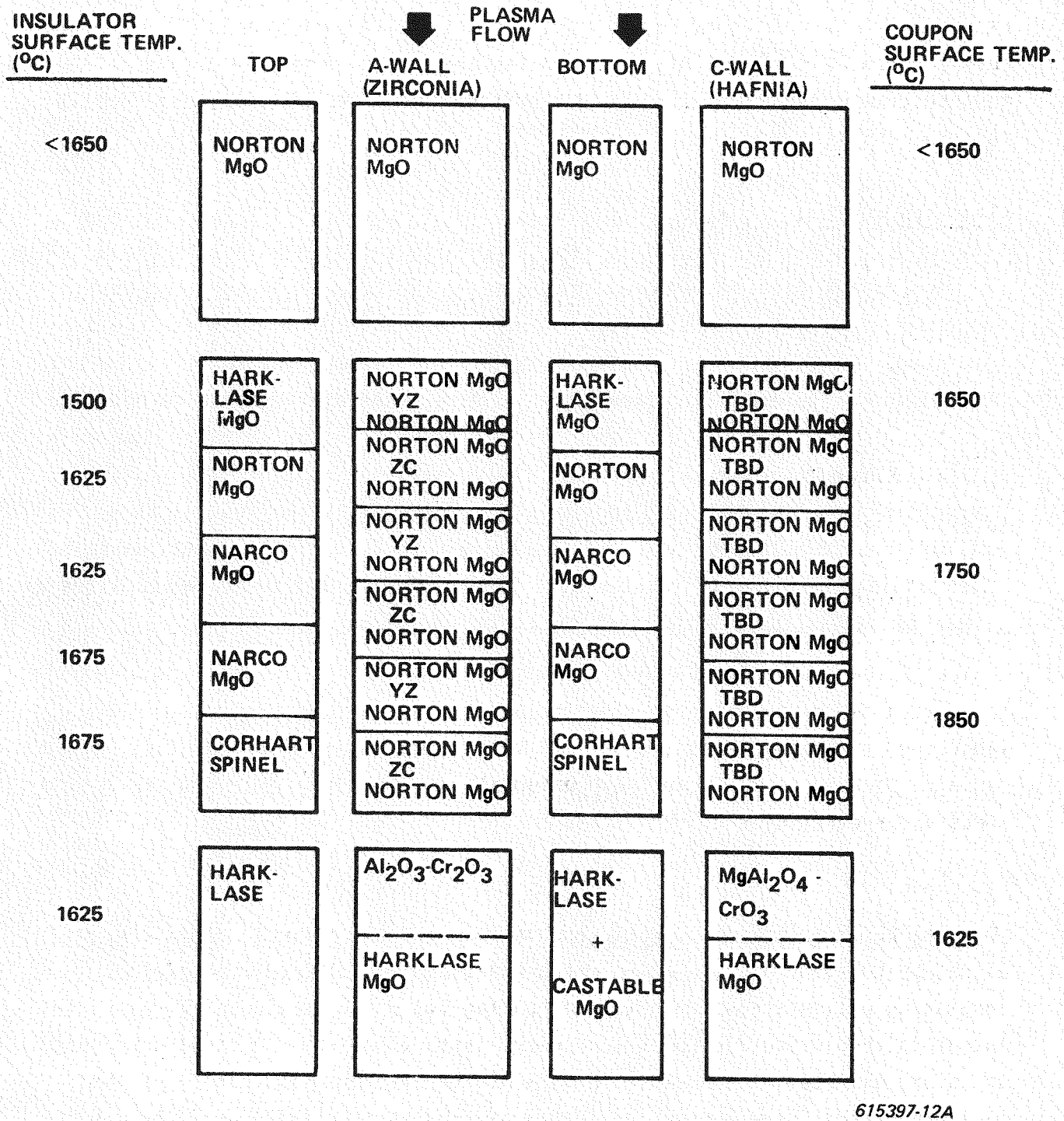

Figure 14. WESTF Test 42 Channel Schematic

WESTF Test 43

WESTF Test 43 is a first test of materials under hot slagging conditions with platinum anodes and iron cathodes. A new definitive preliminary test specification was issued to guide final design activities. The thermal design of the heat section is complete. Engineering sketches of component parts for this test section have been prepared and submitted to the Machine Shop. A final test specification will be issued.

Alternate WESTF Test Sections

Consideration is being given to a number of alternative test section designs to permit increased use of WESTF while providing a bridge between laboratory screening tests and full WESTF tests. Two test sections have been tentatively selected for further consideration, as follows:

- Materials Test Section
- Mini-WESTF Test Section

In each case the size and complexity of the test section would be reduced.

The Materials Test Section would be used to investigage materials under dynamic MHD conditions, exclusive of electrical and magnetic effects. While this type of test is particularly relevant for testing materials, insulator and electrode, to be used under non-slagging super-hot wall conditions where the available laboratory screening tests are partially deficient. The Materials Test Section can also be used to test candidate materials for the other generator operating modes under dynamic test conditions.

The mini-WESTF Test Section would accommodate a reduced number of electrode pairs, up to four, and would support the development of electrode and/or insulating wall systems for ultimate testing via a full scale WESTF test. The intent is to provide for quick turnaround tests of relatively short duration, up to approximately ten hours. In view of the developmental nature of the mini-WESTF tests, the supporting design and analysis activity would be limited in scope and complexity when compared to a full scale WESTF test.

Overall, these test sections will provide a means of effectively expanding the materials and electrode/insulator system data base on a time scale and cost basis which are beneficial to the overall program.

2.1.2 Experiment Design

WESTF Tests 42 and 44

WESTF Tests 42 and 44 are tests of "coupons" of selected materials under super hot slag/seed conditions. The primary objective of these tests is to evaluate and compare the behavior of selected materials in a super hot MHD channel environment (>1900 K temperature regime) in the absence of electrical or magnetic fields. Consequently, electrical and electrochemical considerations are not design criteria for these tests.

The detailed designs of the coupon electrode walls for WESTF Tests 42 and 44 were completed. These results are presented in Tables 8 and 9 for the anode and the cathode walls, respectively. A summary of the test requirements is presented in Table 10.

Figure 15 illustrates the general conceptual electrode coupon design. The detailed design was accomplished via a series of converted finite difference two-dimensional coupon electrode models of unit depth as is illustrated in Figure 16. All elements of the thermal resistance could be appropriately considered in this manner (via the conduction code models) to conservatively establish the coupon dimension, the facility mass flow requirements and the water coolant requirements to satisfy the thermal test objectives. Material thermal conductivity data are compared and illustrated in Figures 17 and 18.

During the next quarter, development of the analytical expressions for on-line test data monitoring will be completed. These will include the relationships for the determination of average coupon surface temperature and heat flux as functions of channel location and indicated thermocouple measurements for both the anode and the cathode walls.

TABLE 8

SELECTED ANODE WALL DESIGN COUPON CONSTRUCTIONS AND RECOMMENDED FACILITY OPERATING POINTS BASED UPON THE SURFACE TEMPERATURE AND THE SINGLE THICKNESS MESH (THERMAL COMPLIANT LAYER) REQUIREMENTS

Coupon Position	Coupon Material (Battelle Designation)	Surface Temperature Requirement (°C)	Coupon Thickness (in.)	MgO Thickness Adjacent to Coupon (in.)	MgO Thickness Below Coupon (in.)	Surface to Nickel Mesh (in.)	Nickel Mesh Thickness (in.)	h(Btu/hr/ft^2 °F)	Average Coupon Surface Flux (W/cm^2)	Average Coupon Surface Temperature (°C)
1	Norton MgO	1600-1650	0.30	0.30	0.10	0.40	0.20	≈110	44.6	1611
	YZ-155		0.25	0.25	0.05	0.30	0.10	≈ 87.5	29.8	1650
	YZ-154		0.20	0.20	0.20	0.40	0.10	≈110	42.6	1645
2	Norton MgO	1650-1700	0.40	0.40	0.10	0.50	0.20	≈107	39.3	1704
	ZC-156		0.20	0.20	0.00	0.20	0.10	≈105	41.8	1659
	YZ-154 [2]		0.20	0.20	0.10	0.30	0.10	≈100	39.8	1696
3	Norton MgO	1700-1750	0.45	0.45	0.10	0.55	0.20	≈105	42.0	1751
	YZ-155		0.29	0.29	0.10	0.39	0.10	≈103	28.6	1725
	YZ-154 [2]		0.24	0.24	0.10	0.34	0.10	≈103	37.8	1725
4	Norton MgO	1750-1800	0.47	0.47	0.47	0.94	0.20	≈103	34.0	1765
	ZC-156		0.30	0.30	0.10	0.40	0.10	≈102	34.0	1797
	YZ-154 [2]		0.30	0.30	0.10	0.40	0.10	≈100	34.7	1786
5	Norton MgO	1800-1850	0.51	0.51	0.10	0.61	0.20	≈100	34.0	1825
	YZ-155		0.25	0.25	0.05	0.30	0.10	≈100	32.6	1825
	YZ-154 [2]		0.35	0.35	0.10	0.45	0.10	≈100	32.2	1825
6	Norton MgO	1850-1900	0.55	0.55	0.10	0.65	0.20	≈ 95	31.4	1875
	ZC-156		0.36	0.36	0.10	0.46	0.10	≈105	31.0	1875
	YZ-154		0.40	0.40	0.10	0.50	0.10	≈100	29.6	1875

Notes:

1) Nickel Mesh Interface to and Cooling Channel 1.25 Inch
2) Cooling Channel Diameter 0.188 Inch
3) Cooling Water Flow Rate 75-95 gph
4) Combustion Product Mass Flow Rate 0.073-0.075 kg/Sec.

TABLE 9

SELECTED CATHODE WALL DESIGN COUPON CONSTRUCTIONS AND RECOMMENDED FACILITY OPERATING POINTS BASED UPON THE SURFACE TEMPERATURE AND THE SINGLE THICKNESS NICKEL MESH (THERMAL COMPLIANT LAYER) REQUIREMENTS

Coupon Position	Coupon Material (Battelle Designation)	Surface Temperature Requirement (°C)	Coupon Thickness (in)	MgO Thickness Adjacent to Coupon (in)	MgO Thickness Below Coupon (in)	Surface to Nickel Mesh (in)	Nickel Mesh Thickness (in)	h(Btu/hr/ft^2 °F)	Average Coupon Surface Flux (W/cm^2)	Average Coupon Surface Temperature (°C)
1	Norton MgO[3] Hafnia Composition A	1600-1650	0.30 0.2	0.30 0.2	0.10 0.1	0.40 0.3	0.20 0.1	110 100	44.6 43.3	1611 1634
2	Norton MgO[3] Hafnia Composition A	1650-1700	0.40 0.25	0.40 0.25	0.10 0.1	0.50 0.35	0.20 0.1	107 100	39.3 40.4	1704 1685
3	Norton MgO[3] Hafnia Composition A	1700-1750	0.45 0.3	0.45 0.3	0.10 0.1	0.55 0.4	0.20 0.1	105 100	42.0 37.5	1751 1736
4	Norton MgO[3] Hafnia Composition A	1750-1800	0.47 0.3	0.47 0.3	0.47 0.15	0.94 0.45	0.20 0.1	103 100	34.0 34.9	1765 1781
5	Norton MgO[3] Hafnia Composition A	1800-1850	0.51 0.3	0.51 0.3	0.10 0.2	0.61 0.5	0.20 0.1	100 100	34.0 32.4	1825 1826
6	Norton MgO[3] Hafnia Composition A	1850-1900	0.55 0.3	0.55 0.3	0.10 0.25	0.65 0.55	0.20 0.1	95 100	31.4 29.8	1875 1871

---

1) Nickel Mesh Interface to and Cooling Channel 1.25 Inch
2) Cooling Channel Diameter 0.188 Inch
3) Cooling Water Flow Rate 75-95 gph
4) Combustion Product Mass Flow Rate 0.073-0.075 kg/Sec.

TABLE 10

WESTF TESTS NO. 42 AND 44 ANODE AND CATHODE WALL MATERIAL AND TEMPERATURE REQUIREMENTS

Material	(Molar) Composition	Coupon Surface Temperature (°C)	Guideline Maximum Insulator (MgO) Surface Temperature (°C)	Generator Axial Location ($\frac{x}{6}$)
Norton MgO	85-90% dense MgO	1600-1650	1475-1550	3.93
YZ (M-155)	12 Y_2O_3 - 88 ZrO_2			
YZ (M-154)	12 Y_2O_3 - 88 ZrO_2			
Hafnia A	$Pr_{0.27}Yb_{0.09}Hf_{0.64}O_2$			
Hafnia B	$Tb_{0.20}Y_{0.10}Hf_{0.70}O_2$			
Norton MgO	85-90% dense MgO	1650-1700	1550-1600	4.77
ZC (M-156)	15 $(Mg_{0.625}Ca_{0.375})$ 0-85 ZrO_2			
YZ (M-154)	12 Y_2O_3 - 88 ZrO_2			
Hafnia A	$Pr_{0.27}Yb_{0.09}Hf_{0.64}O_2$			
Hafnia B	$Tb_{0.20}Y_{0.10}Hf_{0.70}O_2$			
Norton MgO	85-90% dense MgO	1700-1750	1575-1625	5.61
YZ (M-155)	12 Y_2O_3 - 88 ZrO_2			
YZ (M-154)	12 Y_2O_3 - 88 ZrO_2			
Hafnia A	$Pr_{0.27}Yb_{0.09}Hf_{0.64}O_2$			
Hafnia B	$Tb_{0.20}Y_{0.10}Hf_{0.70}O_2$			
Norton MgO	85-90% dense MgO	1750-1800	1600-1650	6.45
ZC (M-156)	15 $(Mg_{0.625}Ca_{0.375})$ 0-85 ZrO_2			
YZ (M-154)	12 Y_2O_3 - 88 ZrO_2			
Hafnia A	$Pr_{0.27}Yb_{0.09}Hf_{0.64}O_2$			
Hafnia B	$Tb_{0.20}Y_{0.10}Hf_{0.70}O_2$			
Norton MgO	85-90% dense MgO	1800-1850	1625-1675	7.28
YZ (M-155)	12 Y_2O_3 - 88 ZrO_2			
YZ (M-154)	12 Y_2O_3 - 88 ZrO_2			
Hafnia A	$Pr_{0.27}Yb_{0.09}Hf_{0.64}O_2$			
Hafnia B	$Tb_{0.20}Y_{0.10}Hf_{0.70}O_2$			
Norton MgO	85-90% dense MgO	1850-1900	1650-1700	8.12
ZC (M-155)	15 $(Mg_{0.625}Ca_{0.375})$ 0-85 ZrO_2			
YZ (M-154)	12 Y_2O_3 - 88 ZrO_2			
Hafnia A	$Pr_{0.27}Yb_{0.09}Hf_{0.64}O_2$			
Hafnia B	$Tb_{0.20}Y_{0.10}Hf_{0.70}O_2$			

[1] Axial location relative to area of constant cross section. That is x = 0 corresponds to the entrance of the transition section, while x = 4 11/16" corresponds to the entrance of the generator channel. The above is based upon the sum of the lengths of the WESTF channel components of identical cross sectional area.

[2] Not a requirement.

[3] U-02 Phase I material

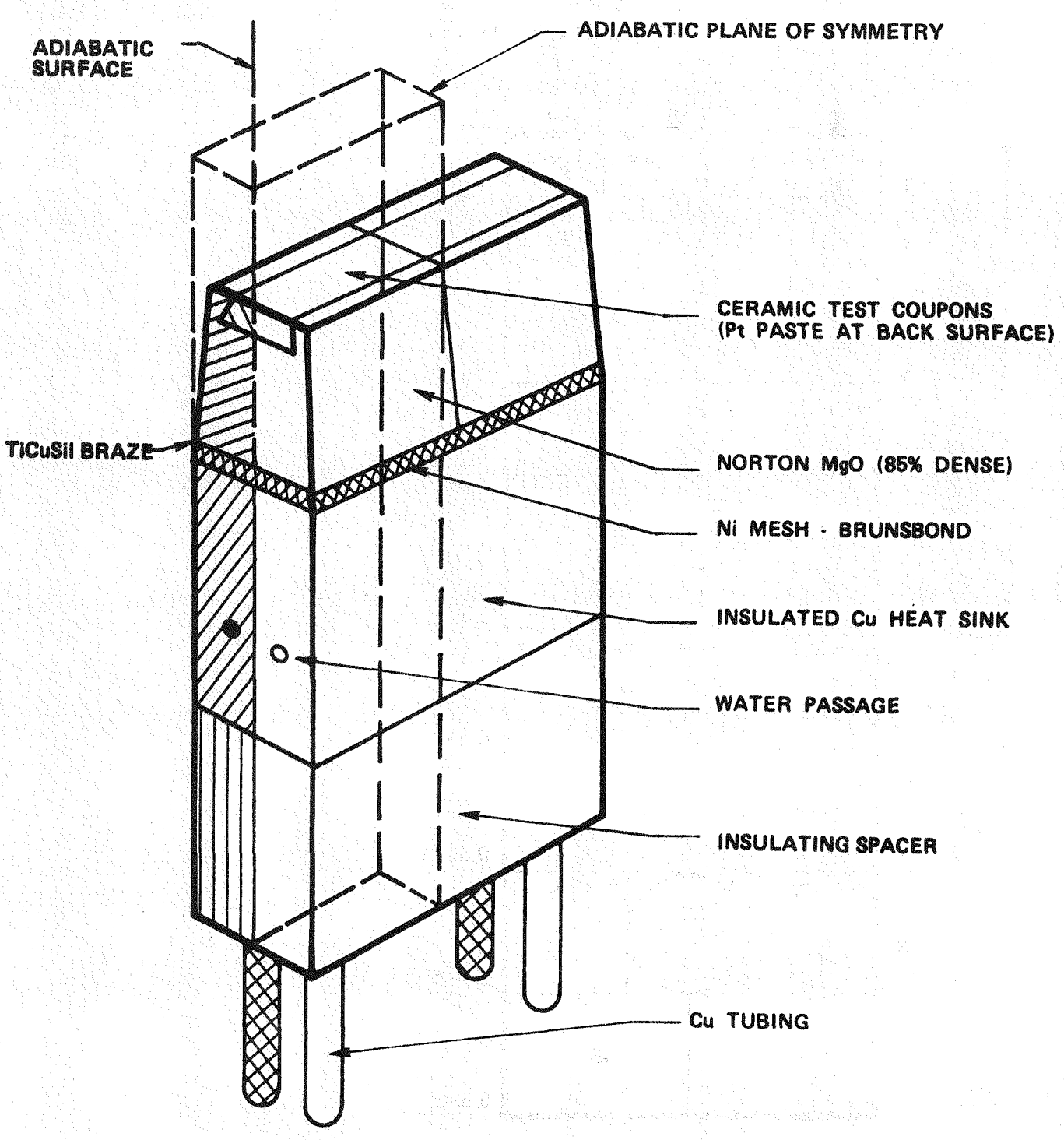

Figure 15. General Coupon Electrode for WESTF Test 42 Electrode Walls

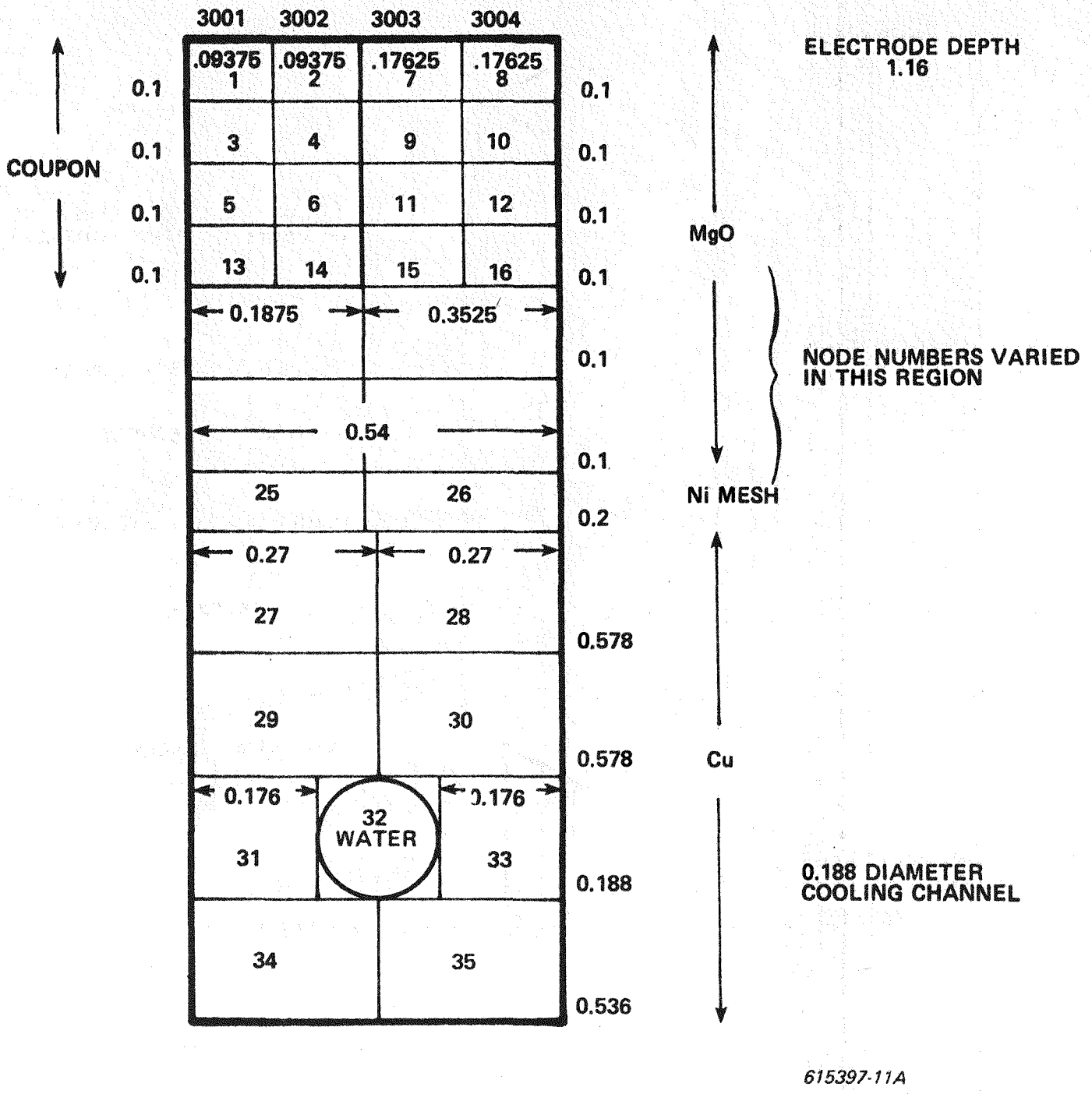

Figure 16. Coupon Electrode Model

M-154

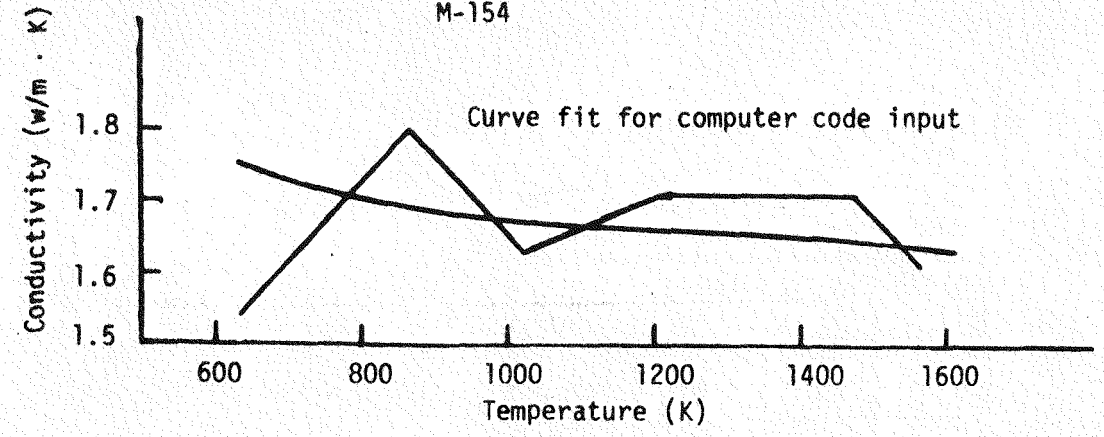

MEASURED (Battelle PNL)

Temp (K)	Conductivity (w/m · K)
682	1.54
870	1.80
1023	1.63
1232	1.71
1480	1.71
1567	1.62

M-156

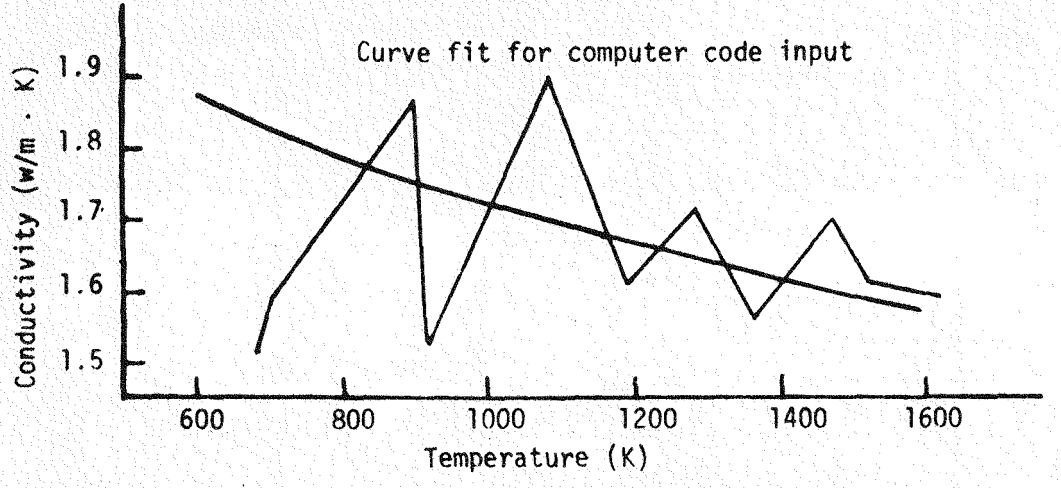

MEASURED (Battelle PNL)

Temp. (K)	Conductivity (w/m · K)	Temp (K)	Conductivity (w/m · K)
683	1.51	1289	1.72
634	1.59	1359	1.56
866	1.87	1473	1.70
950	1.53	1531	1.61
1053	1.89	1629	1.59

Figure 17. Thermal Conductivity Data

M-155

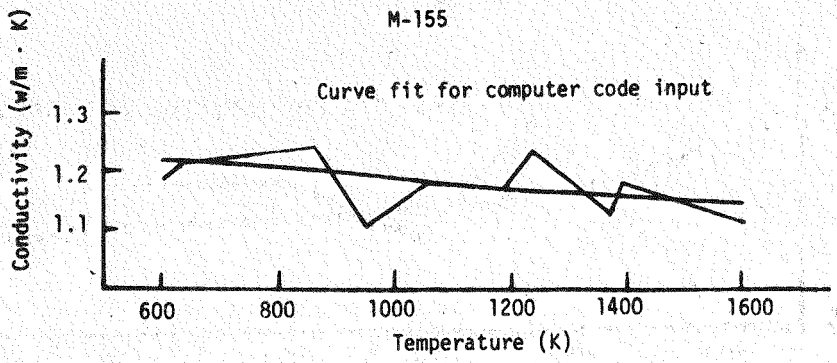

MEASURED (Battelle PNL)

Temp (K)	Conductivity (w/m.K)	Temp (K)	Conductivity (w/m ·K)
611	1.19	1190	1.17
634	1.22	1237	1.24
866	1.24	1379	1.13
950	1.11	1395	1.17
1053	1.18	1606	1.12

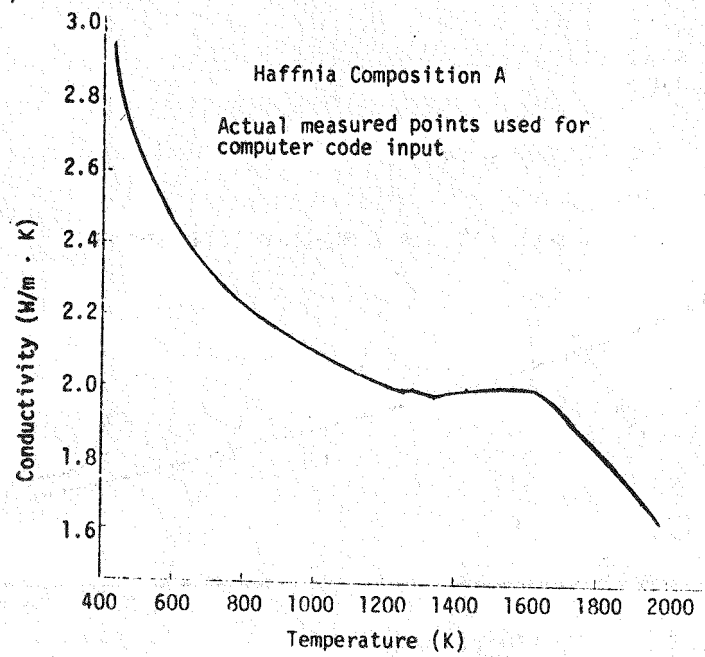

MEASURED (Battelle PNL)

Temp (K)	Conductivity (W/m · K)	Temp (K)	Conductivity (W/m · K)
436	2.97	1340	1.97
618	2.42	1439	2.02
717	2.29	1525	2.02
833	2.23	1633	1.99
962	2.13	1740	1.91
1066	2.06	1830	1.80
1178	2.01	1920	1.68
1278	2.00	1988	1.58

Figure 18. Thermal Conductivity Data

WESTF Test 43

Electrode Walls

The detailed designs of the anode and cathode walls for WESTF Test 43 were completed. These results are presented in Tables 11 and 12 for the anode and the cathode walls respectively.

The principal objective of the WESTF Test 43 is to operate the WESTF duct under hot slagging conditions (1200-1900 K temperature regime) and to assess the durability and the performance of platinum anodes and low carbon steel (iron) cathodes. The different material and temperature design constraints required for each electrode wall necessitated two separate designs and consequently two separate numerical models.

Owing to the geometric and adiabatic symmetry of the conceptual electrode designs (Figures 19 to 21) the detailed design was accomplished via a series of converted finite difference two dimensional electrode models of unit depth as is illustrated in Figures 22 and 23. All elements of the thermal resistance could be appropriately considered in this manner (via the conduction code models) to conservatively establish the electrode dimensions, the facility mass flow requirements and the water coolant requirements to satisfy the thermal and test objectives.

Among the principal assymetrical thermal and structural design considerations for this test were the surface and attachment region temperature requirements associated with the ceramic insulator-steel electrode cathode design and the platinum cap-ceramic substrate anode design. The current leadout problem was intrinsic to both designs.

Figure 24 and 25 illustrate the resultant relationships of surface temperature profile (parallel to the plasma flow) to electrode assembly configuration or total length. It is quite apparent that the high conductivity bulk metallic materials composing the central protion of the electrode assemblies contribute to local temperature minimums. The resultant design dimensions as are presented in Tables 11 and 12 do however result in generally smooth thermal/structural

TABLE 11

NOMINAL DIMENSIONS AND TEMPERATURES - ANODE DESIGN - WESTF TEST NO. 43

Channel Position/ Designation	1 101	2 102	3 103	4 104	5 105	6 106	7 107	8 108	9 109	10 110	11 111	12 112
Average Electrode Surface Temp.[1]		1300 ± 75			1375 ± 75			1450 ± 75			1525 ± 75	
Average Insulator Surface Temp.		1510 ± 50			1545 ± 50			1625 ± 50			1675 ± 50	
Average Insulator Back Face Temp.		730 ± 25			705 ± 25			658 ± 25			645 ± 25	
Average Ceramic Substrate Steel Heat Sink Interface Temp (K)		630 ± 25			610 ± 25			570 ± 25			556 ± 25	
Thickness of Insulator (MgO)		0.440 ± 0.005			0.522 ± 0.005			0.752 ± 0.005			0.802 ± 0.005	
Thickness of Ceramic Substrate (Al_2O_3) (in.)		0.400 ± 0.005			0.482 ± 0.005			0.712 ± 0.005			0.762 ± 0.005	
Nominal Width of Steel Rib (in.)		0.190 ± 0.005			0.190 ± 0.005			0.190 ± 0.005			0.190 ± 0.005	
Nominal Distance of Ceramic-Steel Interface to (O.D.) Outside of Heat Sink Cooling Passage (in.)		0.70			0.70			0.70			0.70	
Hydraulic Diameter of Cooling Passage (in.)		0.125			0.125			0.125			0.125	
Nominal Required Water Flow Rate for Cooling Passage (gph)		50 ± 5			50 ± 5			50 ± 5			50 ± 5	
Nominal Distance from Enter of Cooling Passage to Steel Heat Sink Back Face (in.)		2.1 ± 0.01			2.1 ± 0.01			2.1 ± 0.01			2.1 ± 0.01	
Nominal Width Interelectrode Insulator (in.)[1]		0.118			0.118			0.118			0.118	
Nominal Width Electrode (in.)[1]		0.392			0.392			0.392			0.392	
Total Length Electrode + Insulator Assembly Including Heat Sink		3.513			3.595			3.825			3.875	

[1]Primary electrode design specifications to be satisfied given material candidates and facility test specifications for WESTF Test #43.

[2]Present duct and casing insulation requirements establish a maximum total electrode length not to exceed approximately 5 inches.

TABLE 12

NOMINAL DIMENSIONS AND TEMPERATURES - CATHODE DESIGN - WESTF TEST NO. 43

Channel Position/ Designation	1 201	2 202	3 203	4 204	5 205	6 206	7 207	8 208	9 209	10 210	11 211	12 212
Average Electrode Surface Temperature[1] (K)	1400 ± 75			1475 ± 75			1550 ± 75			1625 ± 75		
Average Insulator Surface Temperature (K)	1625 ± 50			1675 ± 50			1730 ± 50			1785 ± 50		
Average Insulator Back Face Temperature (K)	835 ± 25			795 ± 25			767 ± 25			742 ± 25		
Average Ceramic Substrate Compliant Layer Interface (platinum metallization temp. (K)	1050 ± 25			1035 ± 25			1025 ± 25			1012 ± 25		
Thickness of Insulation ($MgAl_2O_4$) (in)	0.047 ± 0.002			0.107 ± 0.002			0.167 ± 0.002			0.227 ± 0.002		
Thickness of Ceramic Substrate (Al_2O_3) (in.)	0.037 ± 0.002			0.097 ± 0.002			0.157 ± 0.002			0.217 ± 0.002		
Nominal Width of Platinum Metallization (in.)	0.01			0.01			0.01			0.01		
Nominal Thickness of Platinum Metallization of Electrode Surface and at Nickel Mesh Interface (in.)[1]	0.01			0.01			0.01			0.01		
Nominal Thickness of Nickel Mesh Compliant Layer (in.) [1]	0.200 ± 0.02			0.200 ± 0.02			0.200 ± 0.02			0.200 ± 0.02		
Nominal Distance of Ceramic-Steel Interface to (O.D.) Outside of Heat Sink Cooling Passage (in.)	0.70			0.70			0.70			0.70		
Hydraulic Diameter of Cooling Passage (in.)	0.125			0.125			0.125			0.125		
Nominal Required Water Flow Rate for Cooling Passage (gph)	50 ± 5			50 ± 5			50 ± 5			50 ± 5		
Nominal Distance from Center of Cooling Passage to Steel Heat Sink Back Face (in.)	2.1 ± 0.01			2.1 ± 0.01			2.1 ± 0.01			2.1 ± 0.01		
Nominal Width Interelectrode Insulator (in.)[1]	0.118			0.118			0.118			0.118		
Nominal Width Electrode (in.)[1]	0.392			0.392			0.392			0.392		
Total Length Electrode + Insulator Assembly Including Heat Sink (in.)[2]	3.12			3.18			3.24			3.30		

[1]Primary electrode design specifications to be satisfied given material candidates and facility test specifications for WESTF Test 43.

[2]Present duct and casing insulation requirements establish a maximum total electrode length not to exceed 5 inches.

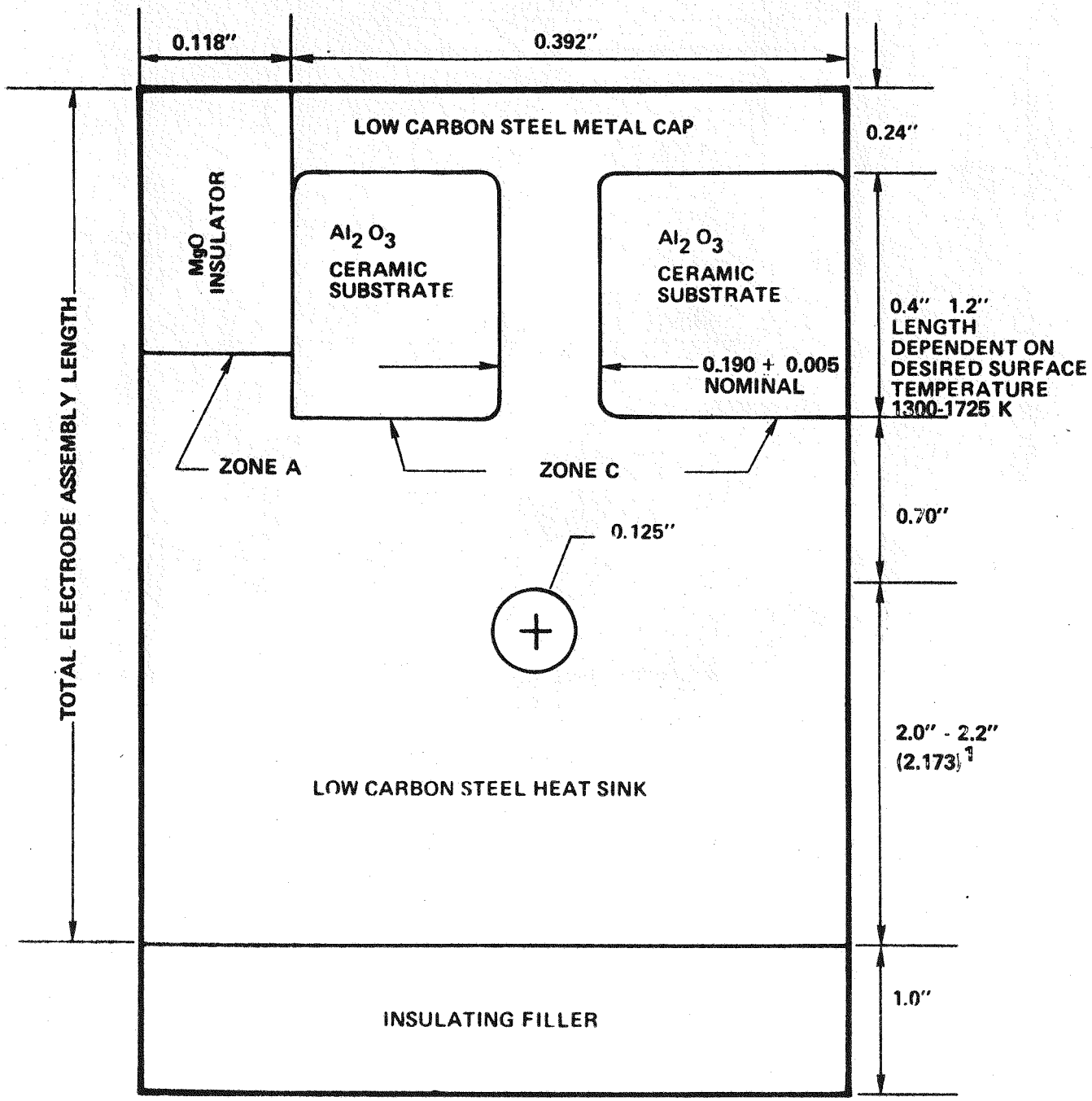

[1]As modeled dimension

Figure 19. Conceptual Design Sketch-WESTF Test No. 43 Iron Cathode

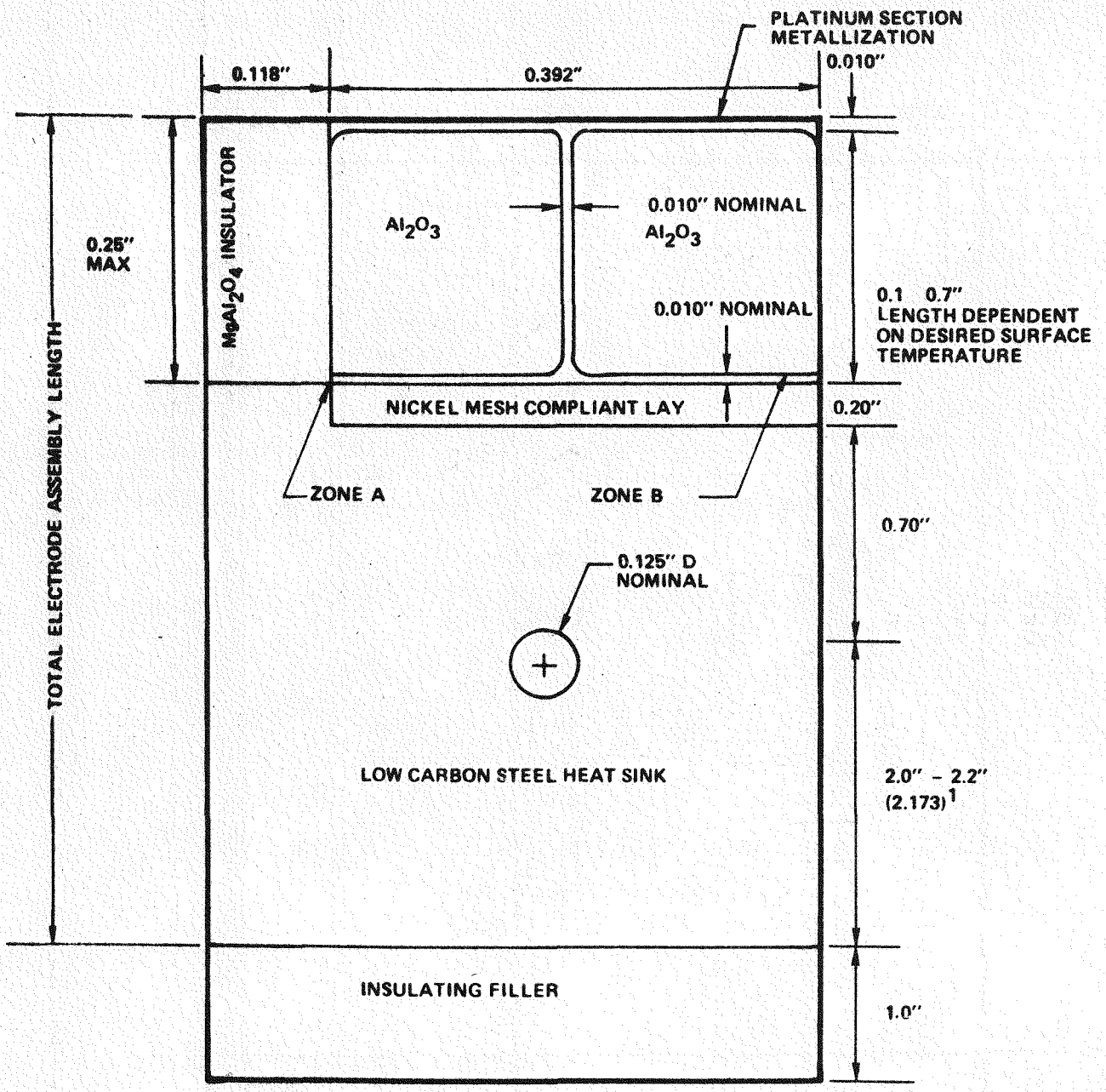

[1]As modeled dimension

Figure 20. Conceptual Design Sketch - WESTF Test No. 43 Platinum Anode

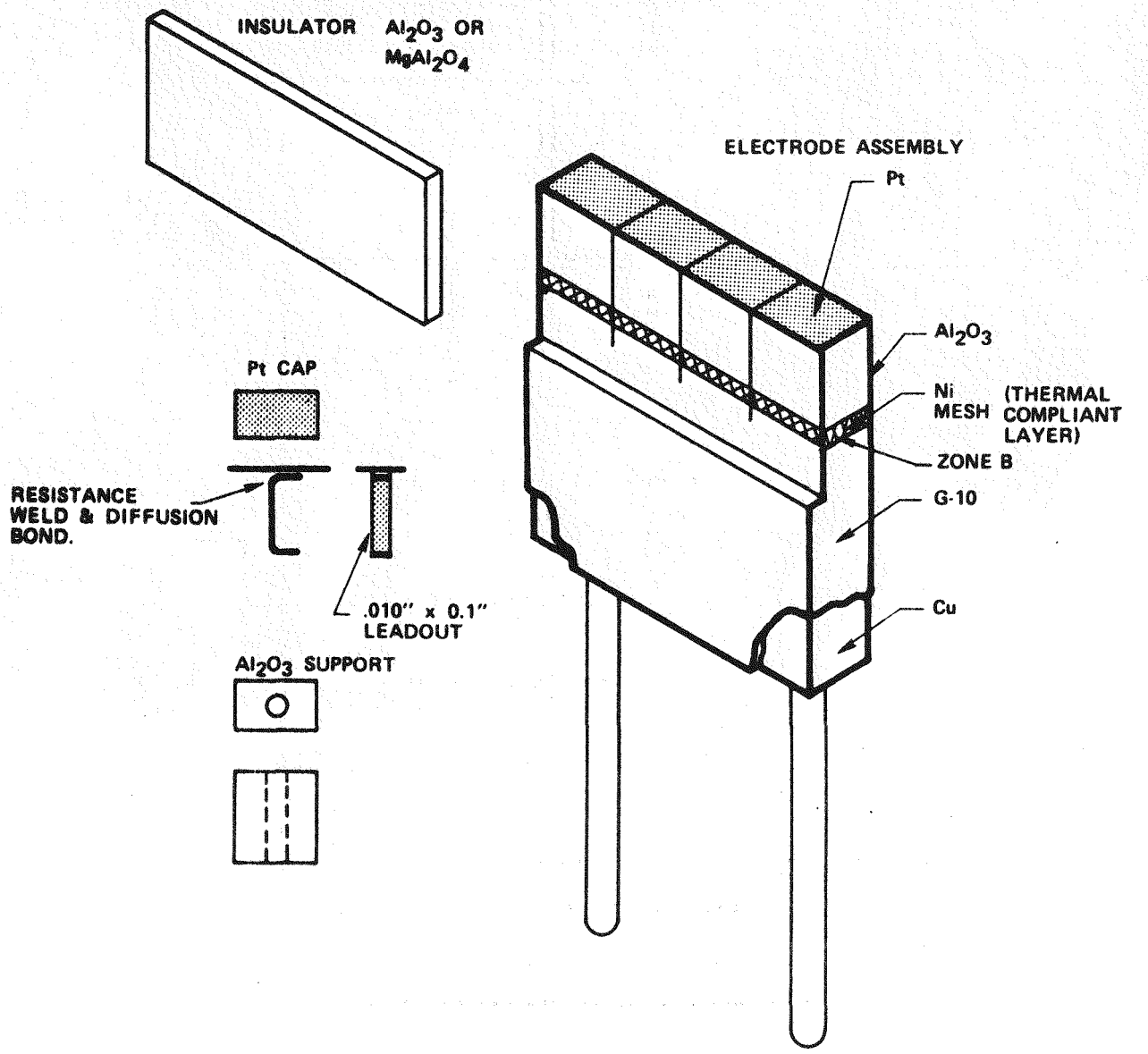

Figure 21, Test 43 Anode

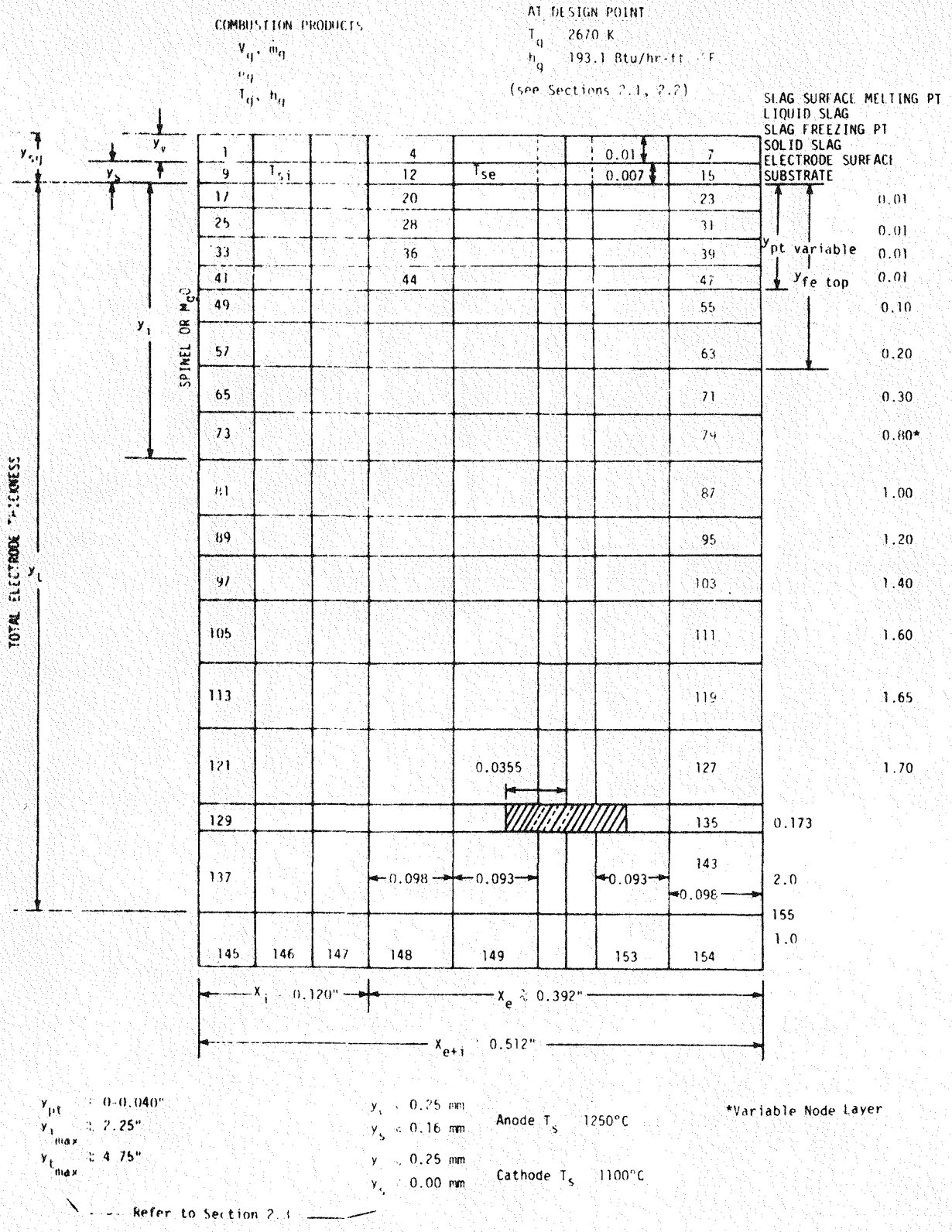

Figure 22. Finite Difference (TAP-A) Modeling for WESTF Test 43 Electrode Wall Design

5	150	160
13	158	168
21	166	176
29	174	184
37	182	192
45	190	200
53	198	208
61	206	216
69	214	224
77	222	232
85	230	240
93	238	248
101	246	256
109	254	264
117	262	272
125	270	280
141	286	296

CENTER NODES KEY

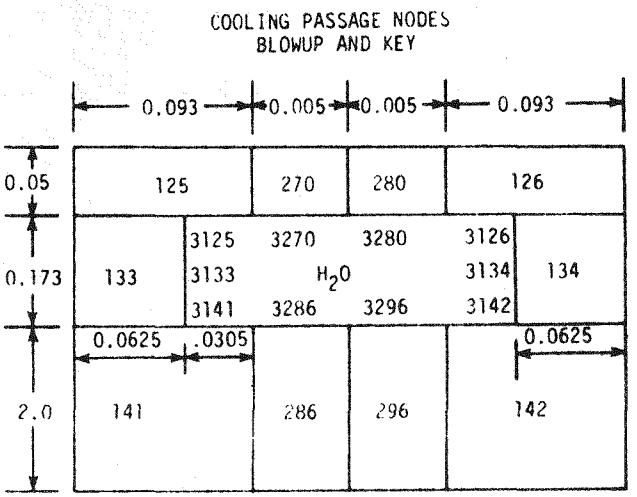

$$A_e = \frac{L_1A_1 + L_2A_2}{L_1 + L_2}$$

Figure 23. Expanded View of Model Center Nodes (Steel Rib or Platinum Metallization) and Cooling Passage Nodes

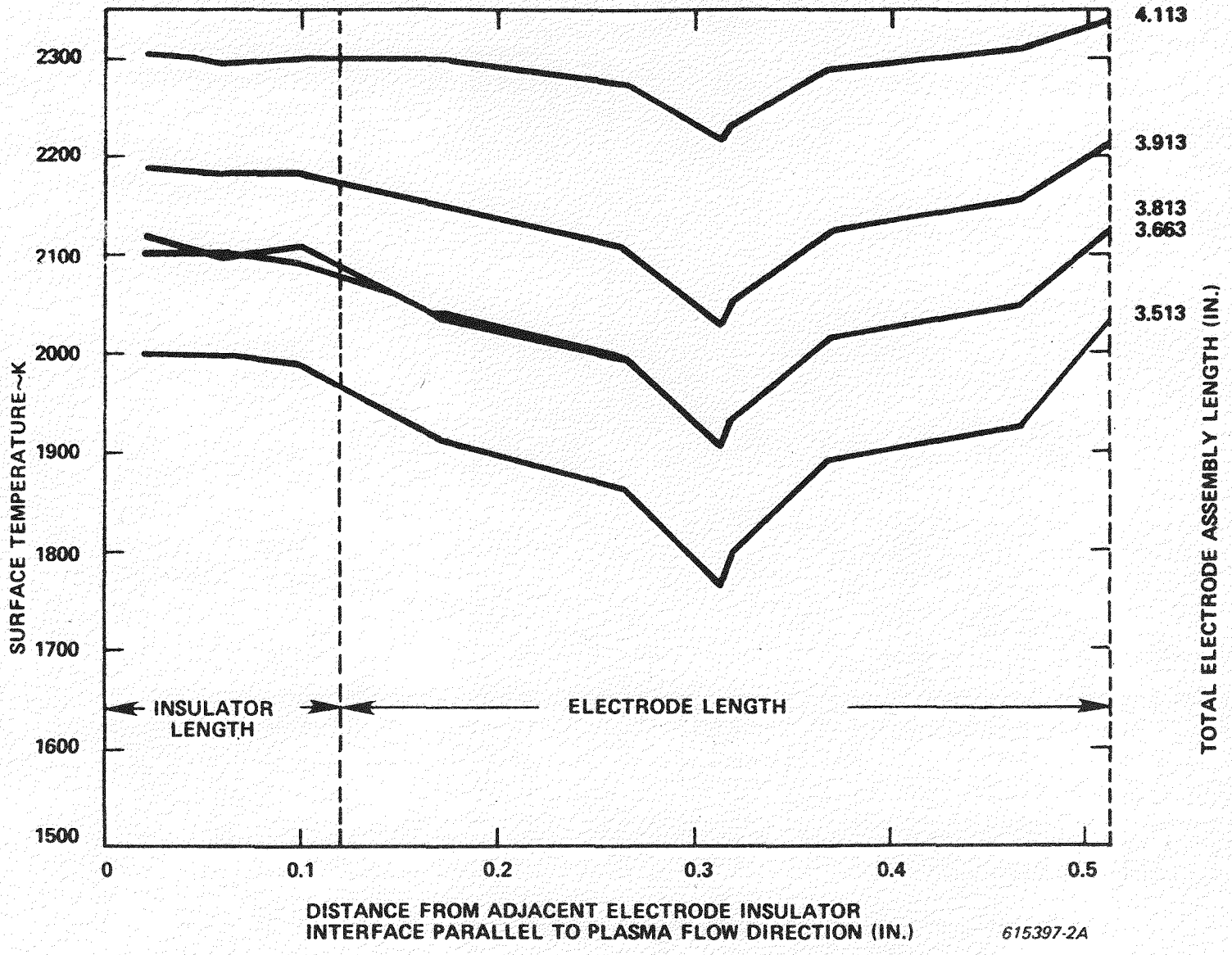

Figure 24. Anodic Temperature Profiles Across the Insulator-Electrode Surface as a Function of Electrode Assembly Total Length - WESTF 43

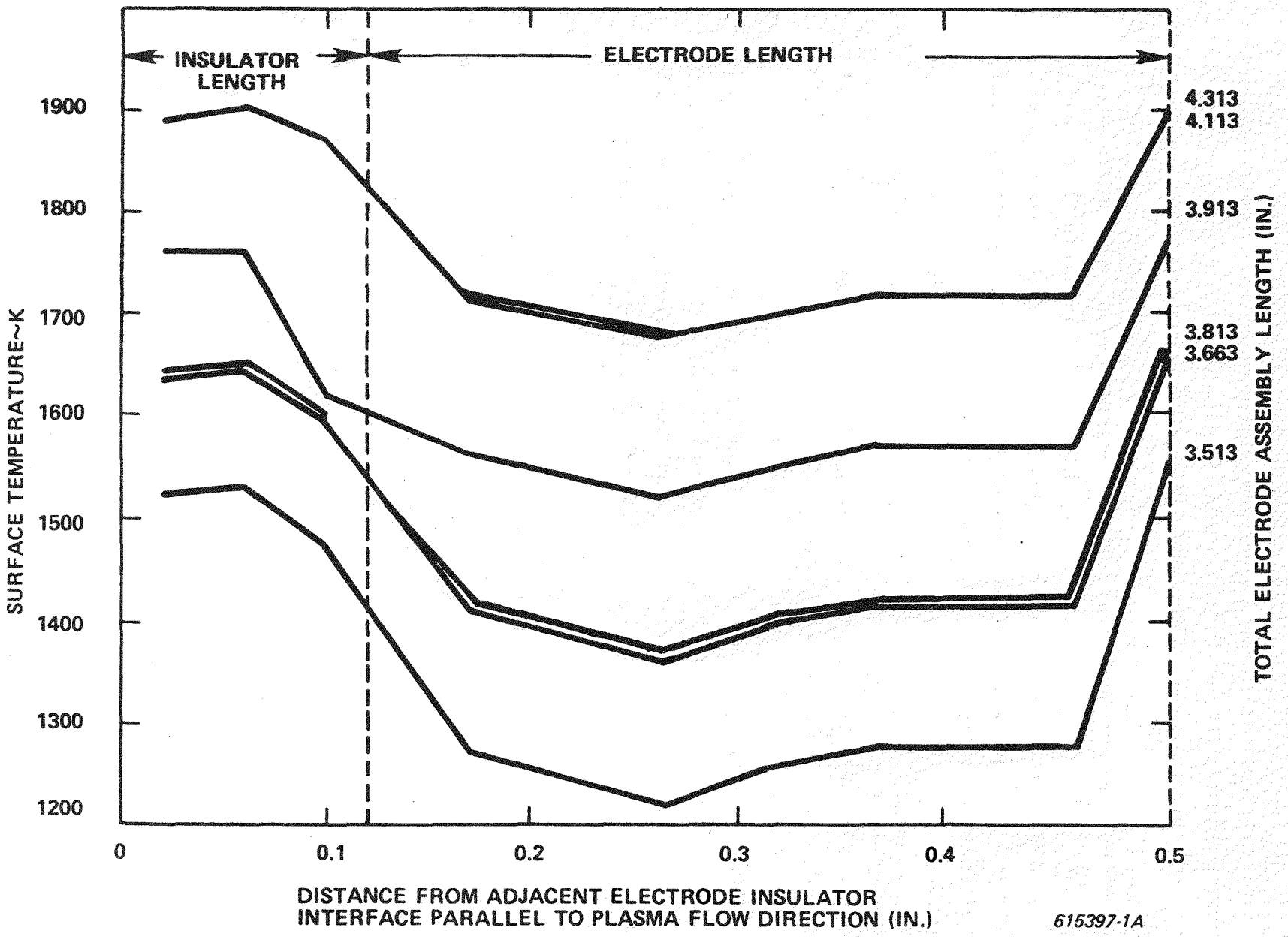

Figure 25. Cathodic Temperature Profiles Across the Insulator-Electrode Surface as a Function of Electrode Assembly Total Length - WESTF 43

transitions between insulator and electrode components. These configurations also ensure interface temperatures for attachment regions consistent with earlier fabrication success in the U-02 Phase III electrode program.

During the next quarter analytical expressions (based upon these design configurations) for surface temperature and system heat flux will be developed for programming the on-line data acquisition system. The resultant programmed functions will provide the required information for the in-test monitoring of dependent thermal parameters.

Transition Sections

The thermal analysis necessary for the design of the entrance and exit transition sections was completed.

The thermal design specification for the Test 43 transition sections is a maximum of 1650°C or a surface temperature compatible with the maximum service ceiling temperature (based upon previous experimental evidence) of the selected ceramic material, so as not to promote any additional heat loss from the incoming plasma.

The material tiles for these transition sections must be designed to ensure a surface temperature compatible with the constraints. That maximum material thickness must also provide the required stiffness for satisfactory material integrity during the entire test duration. This necessitates the choice of a material with a relatively low to moderate coefficient of thermal expansion at high temperatures.

The material and thermal design requirements for the inlet and exit transition sections as a function of candidate materials are listed in Table 13. Those results are based upon a two dimensional programmable calculator model of the transition section wall components. Use of these dimensions for the cooler exit transition section will be conservative for the choices of material thickness.

TABLE 13

TRANSITION SECTION DIMENSIONS FOR WESTF TEST 43

MATERIAL	THICKNESS	TEMPERATURE REQUIREMENT
Harklase Magnesia	0.15 ± 0.03"	1650°C maximum
Monofrax-A-alumina	0.23 ± 0.05"	1650°C maximum
Norton 85% dense magnesia	0.32 ± 0.06"	1650°C maximum
Norton Spinel	0.065 ± 0.013"	1650°C maximum

Additional Thermal Analyses

During this quarter supportive thermal analyses for the slagging electrode test design efforts (principally WESTF 43) were completed. These analyses were concentrated in four principal areas. They were:

1) A simplified analytical model for viscous slagging flow in a MHD channel without power extraction.

2) Development of combustion gas property simulation expressions to aid in plasma characterization and heat transfer/channel design and analyses.

3) Investigation of the radiative heat transfer component in WESTF for the precision design of candidate electrode systems.

4) A simplified analytical model for current conduction modes in the WESTF MHD channel.

Slagging Flow Characterization

The analytical slagging model as is illustrated in Figure 26 is based upon the momentum, energy and continuity equations for slagging flow and energy transport within the liquid slagging layer at steady state facility operating conditions.

The most accurate analytical model is limited by the weakest assumption basis, in this case the energy considerations. The energy considerations are strongly dependent upon the slag property characterization for which available data is not extensive. A summary of some thermal conductivity data for some western slag mixtures typical of these to be employed in WESTF is illustrated in Figure 27. The resultant relationship of liquid and solid slagging lay thicknesses to facility heat flux, based upon the above data are illustrated in Figures 28 and 29, respectively.

Figure 30 illustrates the non-dimensional relationship of the relative slagging thickness ratio (total to liquid conduction layer thickness) as a function of electrode substrate temperature, based upon several different slag melting or slag-plasma interface temperatures.

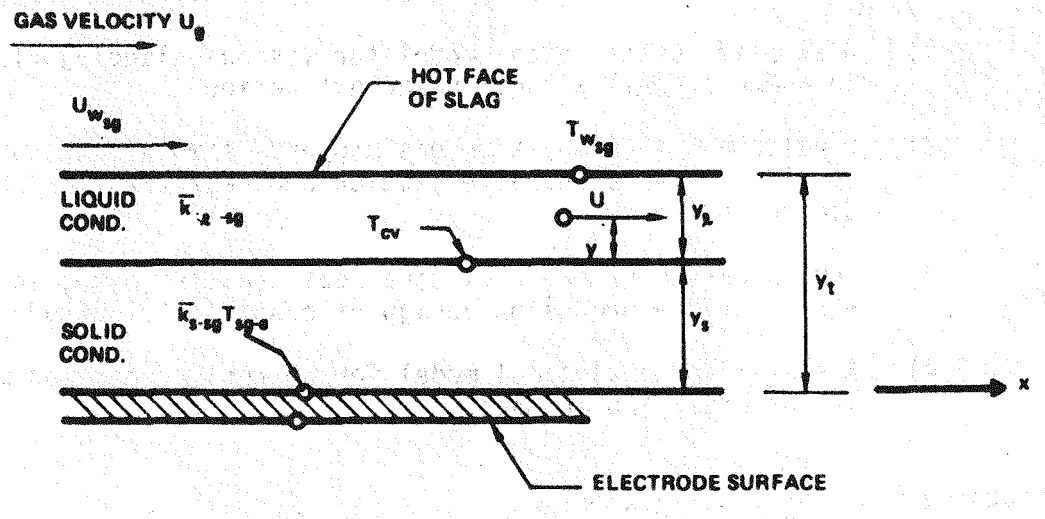

NOTATION

U_g = PLASMA CORE VELOCITY AT ANY CHANNEL CROSS–SECTION

$U_{w_{sg}}$ = PLASMA VELOCITY NEAR THE SLAG GAS INTERFACE

$T_{w_{sg}}$ = SLAG–GAS INTERFACE OR SLAGGING MELTING TEMPERATURE

T_{cv} = TEMPERATURE OF SLAGGING CRITICAL VISCOSITY OR FREEZING TEMPERATURE

Y_ℓ = LIQUID SLAGGING LAYER THICKNESS

Y_s = SOLID SLAGGING LAYER THICKNESS

Y_t = TOTAL EQUILIBRIUM (STEADY–STATE) SLAGGING LAYER THICKNESS

$\bar{k}_{\ell\text{-}sg}$ = AVERAGE THERMAL CONDUCTIVITY OF PARTICULAR SLAGGING COMPOSITION IN THE LIQUID REGION

$\bar{k}_{s\text{-}sg}$ = AVERAGE THERMAL CONDUCTIVITY OF PARTICULAR SLAGGING COMPOSITE IN THE FROZEN (SOLID) REGION

$T_{sg\text{-}e}$ = FROZEN SLAG–METALLIC ELECTRODE INTERFACE TEMPERATURE

Figure 26. Slag Flow on an Electrode Surface (Horizontal MHD Wall)

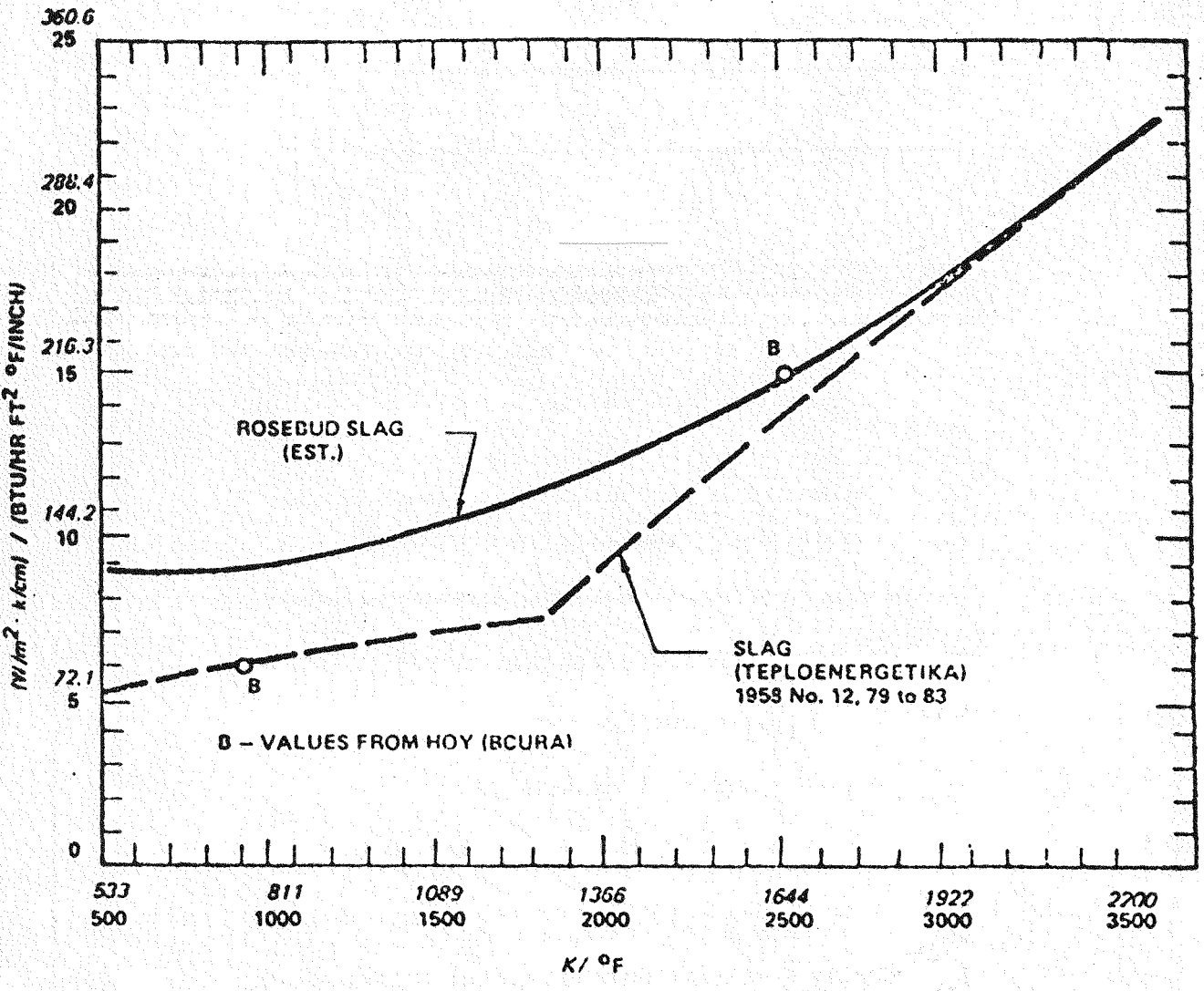

Figure 27. Thermal Conductivity of Slags

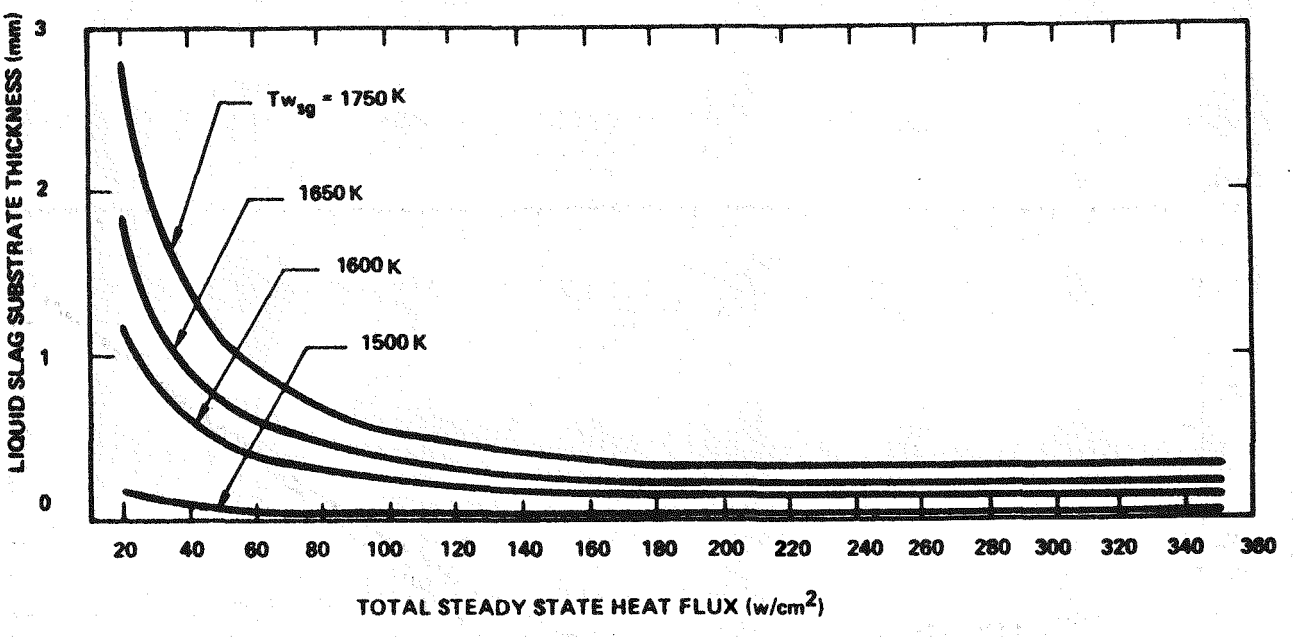

Figure 28. Liquid Slag Substrate Thickness as a Function of Total Electrode Surface Heat Flux and Electrode Surface Temperature

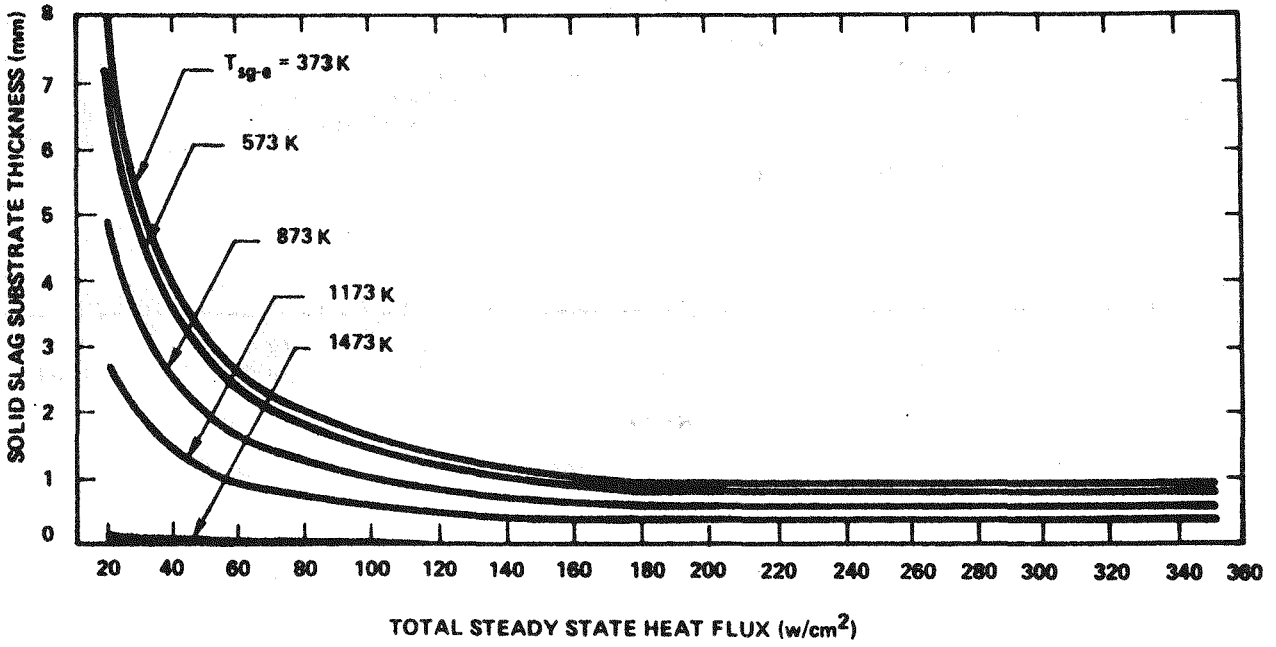

Figure 29. Frozen (Solid) Slag Substrate Thickness as a Function of Total Electrode Surface Heat Flux and Electrode Surface Temperature

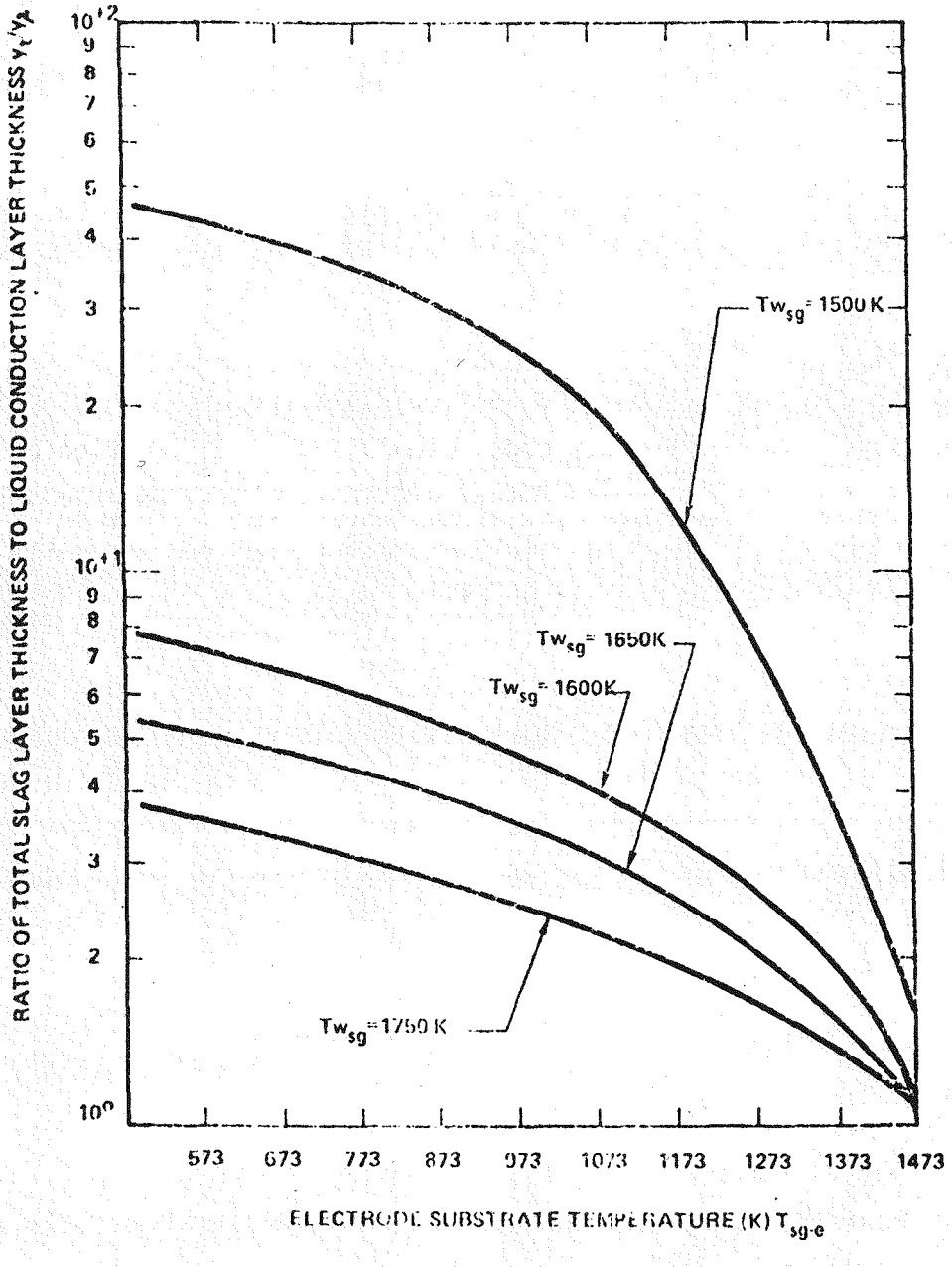

Figure 30. Relationship of Relative Slag Layer Thickness Ratio y/y_T to Electrode Surface Substrate Temperature (T_{sg-e}) for Difference Values of Slag Melting Temperature (Tw_{gg})

Figures 31 and 32 illustrate the relationships of the maximum liquid slag mass flow (Msg) to the liquid slagging layer thickness y_ℓ for various combinations of electrode surface substrate temperature. Comparison of Figues 31 and 32 illustrate the influences of increased heat flux (60 to 100 $\frac{w}{cm^2}$), dependent upon the corresponding increases in facility mass flow rate (o.075 to 0.200 kg/s).

Combustion Gas Expressions

The combustion gas expressions were developed via the use of a proprietary Westinghouse chemical equilibrium code, simulating the combustion products and reactants of a mixture of No. 2 fuel oil, air, ash, seed injection and oxygen at various boundary layer temperatures and at 1 atm pressure (abs.). Table 14 summarizes these analysis property runs.

The main objective of these analyses was to more accurately characterize the thermodynamic and the transport properties of the WESTF combustion gas or plasma products for the future testing sequence. The general simulation gas property expressions so developed (Table 15) for the boundary layer temperature regime, (1500-2000K) will greatly enhance the accuracy of the computation of the plasma-electrode surface heat transfer coefficient in WESTF. The net result would be precisely characterized (temperature of operation) electrode designs for the development of candidate hot wall electrode systems.

Radiation Heat Transfer Model

The results of the radiation heat transfer model has shown that the plasma behaves as an essentially transparent gas if some degree of non-luminosity is assumed.

In general the radiative heat transfer component of the plasma-electrode system constitutes less than 10 percent of the total convective-radiative contribution when any of the standard practice convective correlations are examined and evaluated utilizing gas equilibrium properties.

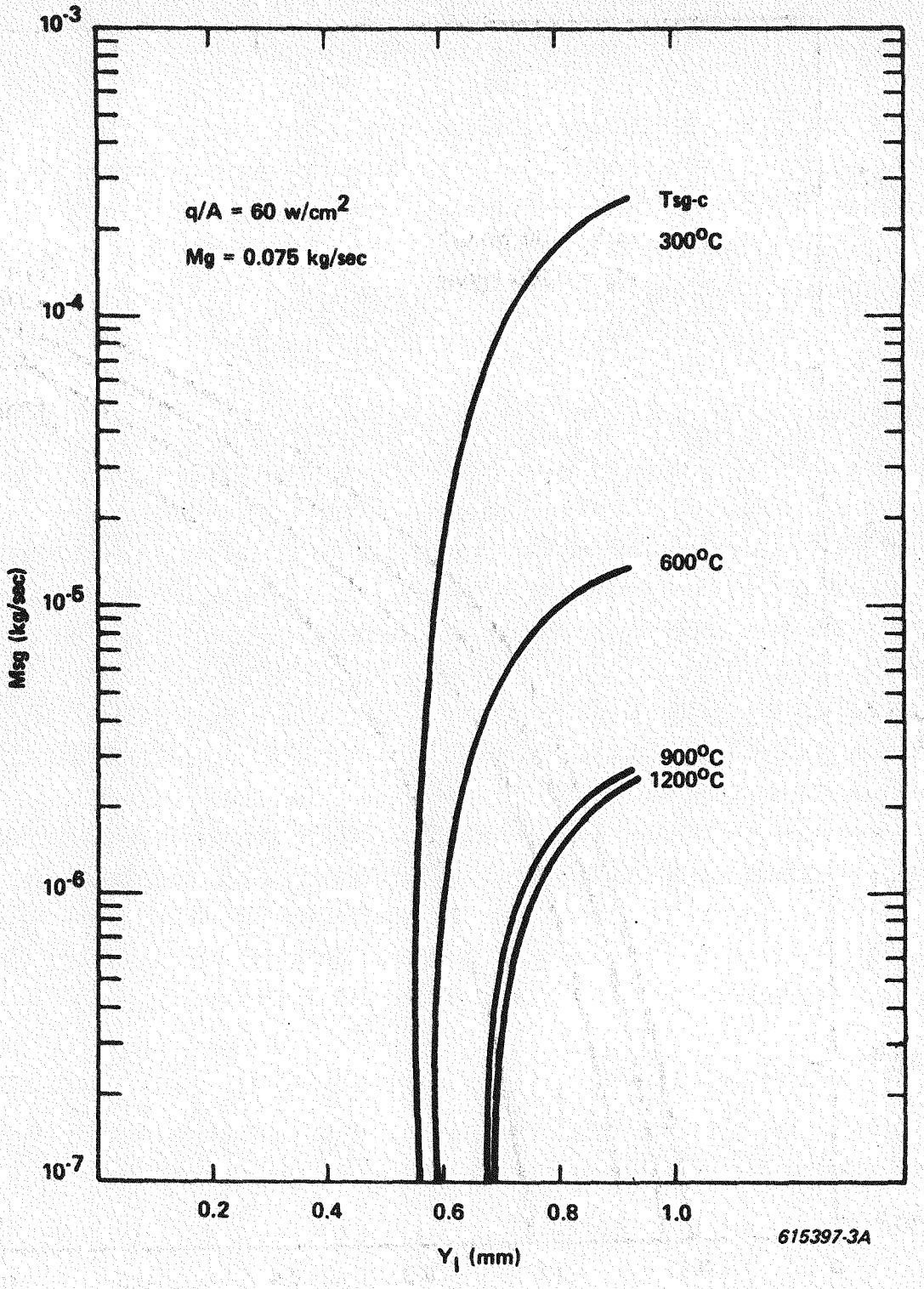

Figure 31. Slag Mass Flow, $\dot{m}_{sg}$, as a Function of the Liquid Slag Layer Thickness, y_ℓ, for a Facility Plasma Mass Flow of 0.075 kg/s

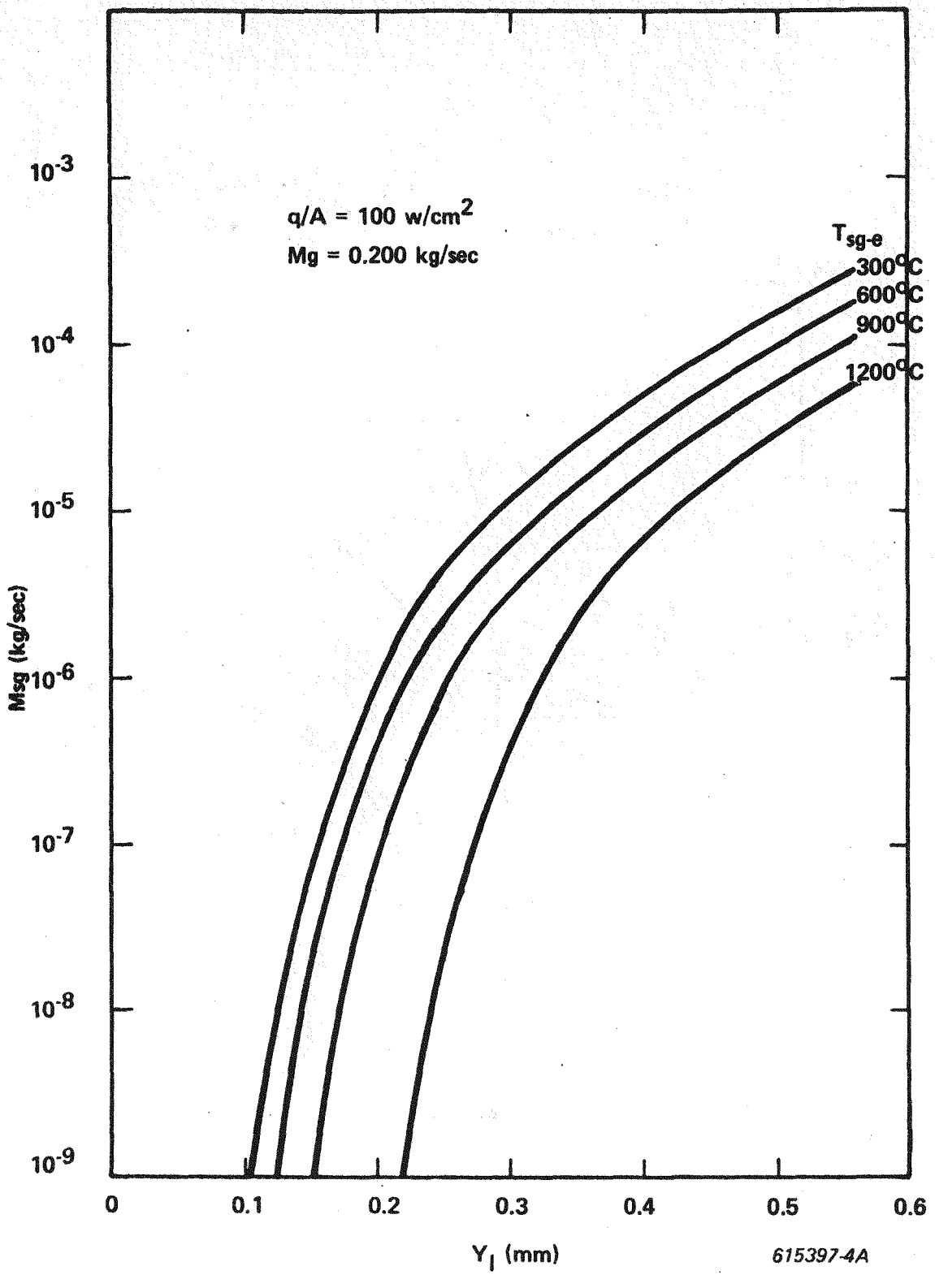

Figure 32. Slag Mass Flow, $\dot{m}_{sg}$, as a Function of the Liquid Layer Thickness, y_ℓ for a Facility Plasma Mass Flow at 0.200 kg/s Illustrating the Influence of Electrode Surface Heat Flux

TABLE 14

DEFINITION OF ANALYSIS PROPERTY RUNS

CASE	PRESSURE (atm. abs.)	TEMPERATURE (K)	(RELATIVE)[1] FLOWS(#/hr) OIL	AIR	ASH	SEED	WATER	OXYGEN
1.1	1	1500	9100	28,500	200	0 (Trace)[1]	0	25,000
1.2	1	1600	9100	28,500	200	0	0	25,000
1.3	1	1700	9100	28,500	200	0	0	25,000
1.4	1	1800	9100	28,500	200	0	0	25,000
1.5	1	1900	9100	28,500	200	0	0	25,000
1.6	1	2000	9100	28,500	200	0	0	25,000
2.1	1	1500	9100	28,500	200	574	574	25,000
2.2	1	1600	9100	28,500	200	574	574	25,000
2.3	1	1700	9100	28,500	200	574	574	25,000
2.4	1	1800	9100	28,500	200	574	574	25,000
2.5	1	1900	9100	28,500	200	574	574	25,000
2.6	1	2000	9100	28,500	200	574	574	25,000
3.1	1	1500	9100	28,500	200	1722	1722	25,000
3.2	1	1600	9100	28,500	200	1722	1722	25,000
3.3	1	1700	9100	28,500	200	1722	1722	25,000
3.4	1	1800	9100	28,500	200	1722	1722	25,000
3.5	1	1900	9100	28,500	200	1722	1722	25,000
3.6	1	2000	9100	28,500	200	1722	1722	25,000

TABLE 15

SUMMARY OF COMBUSTION GAS PROPERTIES SIMULATION EXPRESSIONS FOR TEMPERATURE REGIME 1500-2000 K

PROPERTY	UNITS	GENERAL EXPRESSION	TEMPERATURE RANGE	MAXIMUM DEVIATION FROM CHEMICAL ANALYSES PROGRAM
Thermal Conductivity	hW/M-K	$\kappa(T) = A_0 + A_1 T + A_2 T^2 + A_3 T^3$ a) Coefficients as given in Table 3 b) Graph as presented in Figure 1	1500-2000 K	$< \pm$ 1%
Absolute Viscosity	dPa·s	$\mu(T) = A_0 + A_1 T + A_2 T^2 + A_3 T^3$ a) Coefficients as given in Table 4 b) Graph as presented in Figure 2	1500-2000 K	$< \pm$ 1%
Specific Heat	kJoules/kg-K	$C_p(T) = A_0 + A_1 T + A_2 T^2 + A_3 T^3$ a) Coefficients as given in Table 5 b) Graph as presented in Figure 3	1500-2000 K	$< \pm$ 1%
Prandtl Number	Dimensionless	Pr Graph as presented in Figure 3	1500-2000 K	$< \pm$ 1%
Electrical Conductivity	hS/m or mho/cm	$\sigma(T) = \text{EXP}\,[A_0 + A_1 T + A_2 T^2 + A_3 T^3]$ a) Coefficients as given in Table 6 b) Graph as presented Figure 4	1500-2000 K	$< \pm$ 10%
Density	gm/cm^3	$\rho(T) = A_0 + A_1 T + A_2 T^2 + A_3 T^3$ a) Coefficients as given in Table 7 b) Graph as presented in Table 5	1500-2000 K	$< \pm$ 1%

Current Mode Models

The results of the analysis of the current mode mechanisms for WESTF slagging operation indicates that the plasma-slag system must entail some arcing or discharge mechanism of a significant degree to effect the desired simulated current mode in WESTF. This is especially true for MHD cold wall testing and for current densities as high as 1 to 1.25 A/cm^2.

Incidental to these analyses were the characterization of the resistivity variation of the intervening plasma as a function of temperature. This boundary layer temperature profile is illustrated in Figure 33. The conductivity (resistivity) variation with boundary layer temperature is illustrated in Figure 34.

2.1.3 Post-Test Analysis

WESTF Test 41 - Run 1

Slag Chemical Analysis

After the completion of WESTF 41-1 the slag layer over the downstream section of the channel was quantitatively analyzed for MgO K_2O. Prior WESTF tests had shown an especially large percentage of MgO in the slag, presumably due to the erosion of the upstream components (combustor, mixer, transition section). Figure 35 presents the percentage of MgO and K_2O found in the slag for the WESTF tests run to date, along with the starting flyash analysis. It is apparent from the curves that the MgO content has drastically been reduced from the initial tests, indicating a stabilization of the erosion of the upstream components. The MgO content, however, is still above the starting flyash level (~1 w/o), suggesting some of the frozen slag in the channel may be residue from the earlier MgO rich tests. The K_2O analysis for WESTF 41-1 revealed very little change in content from the previous runs (~2.5 w/o). Unfortunately, this percentage is far below the anticipated value expected for the slag/seed mixture used in the test. This may be due in part to the hydration of the K_2CO_3 immediately after the test and subsequent segregation and separation away from the frozen slag layer. Additional slag samples will be taken for compositional analysis immediately after WESTF 41-2 to try to obtain the representative slag chemistry.

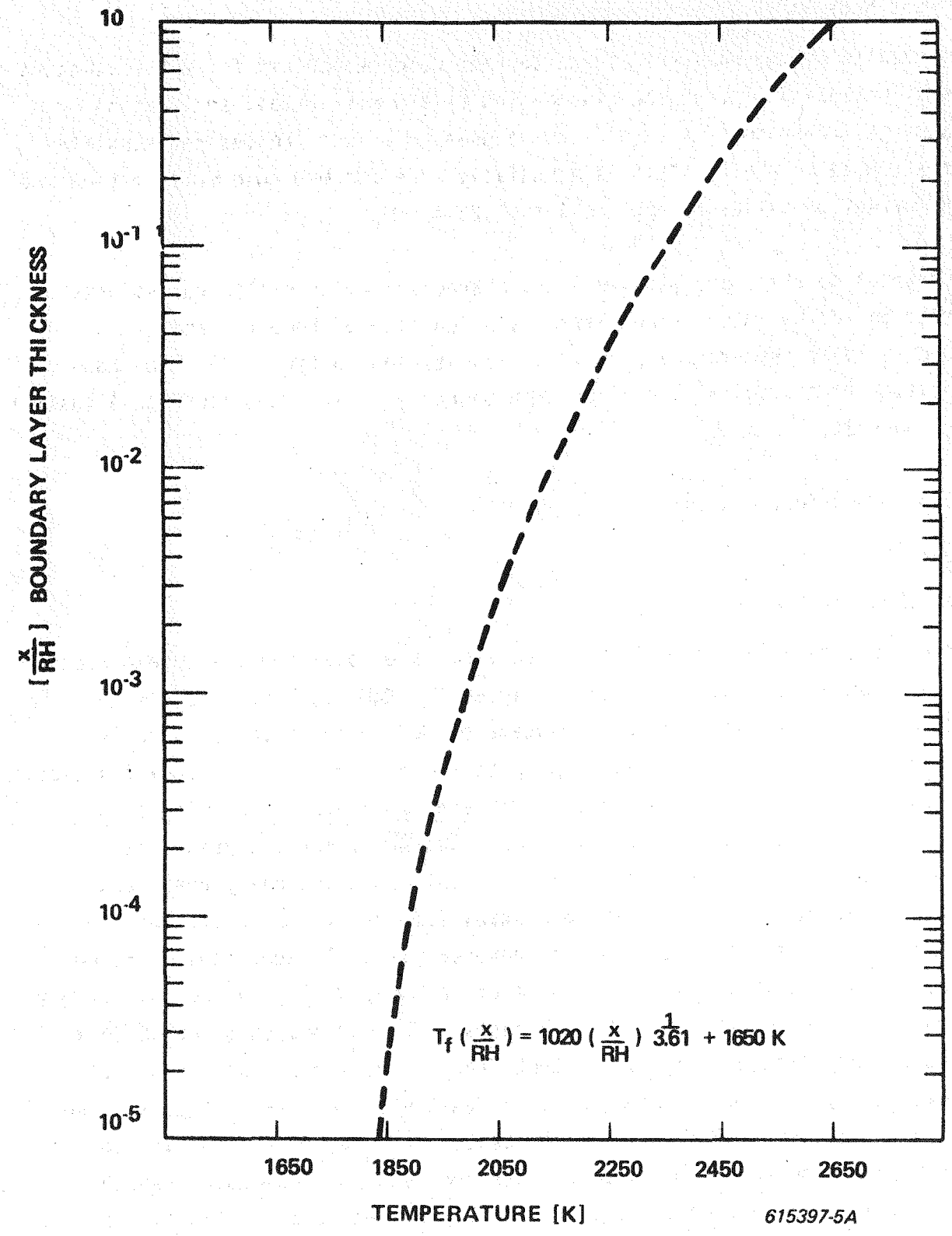

Figure 33. Relative Thermal Boundary Layer Profile for WESTF Test 43

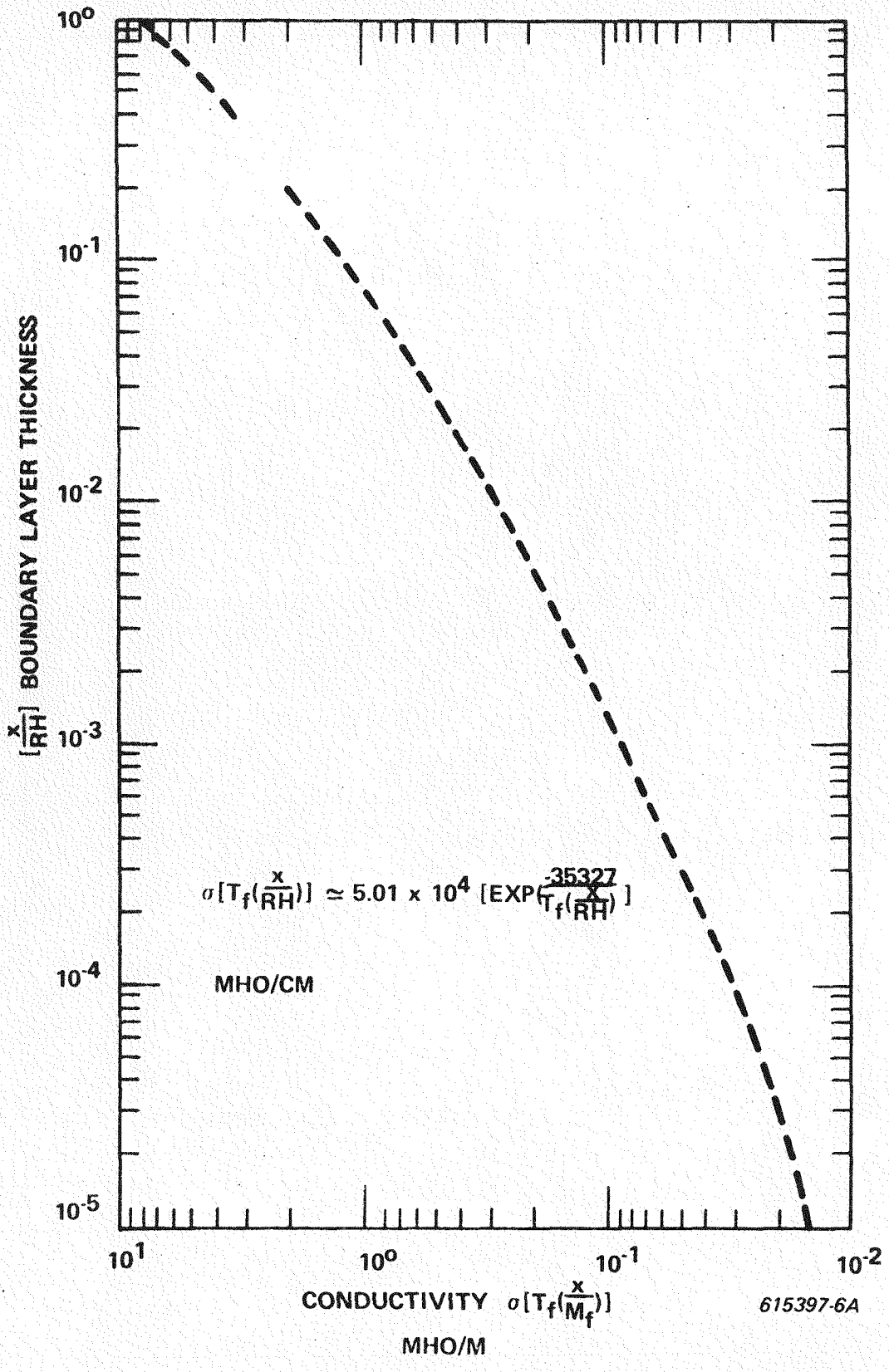

Figure 34. Relative Electrical Conductivity Profile for WESTF Test 43

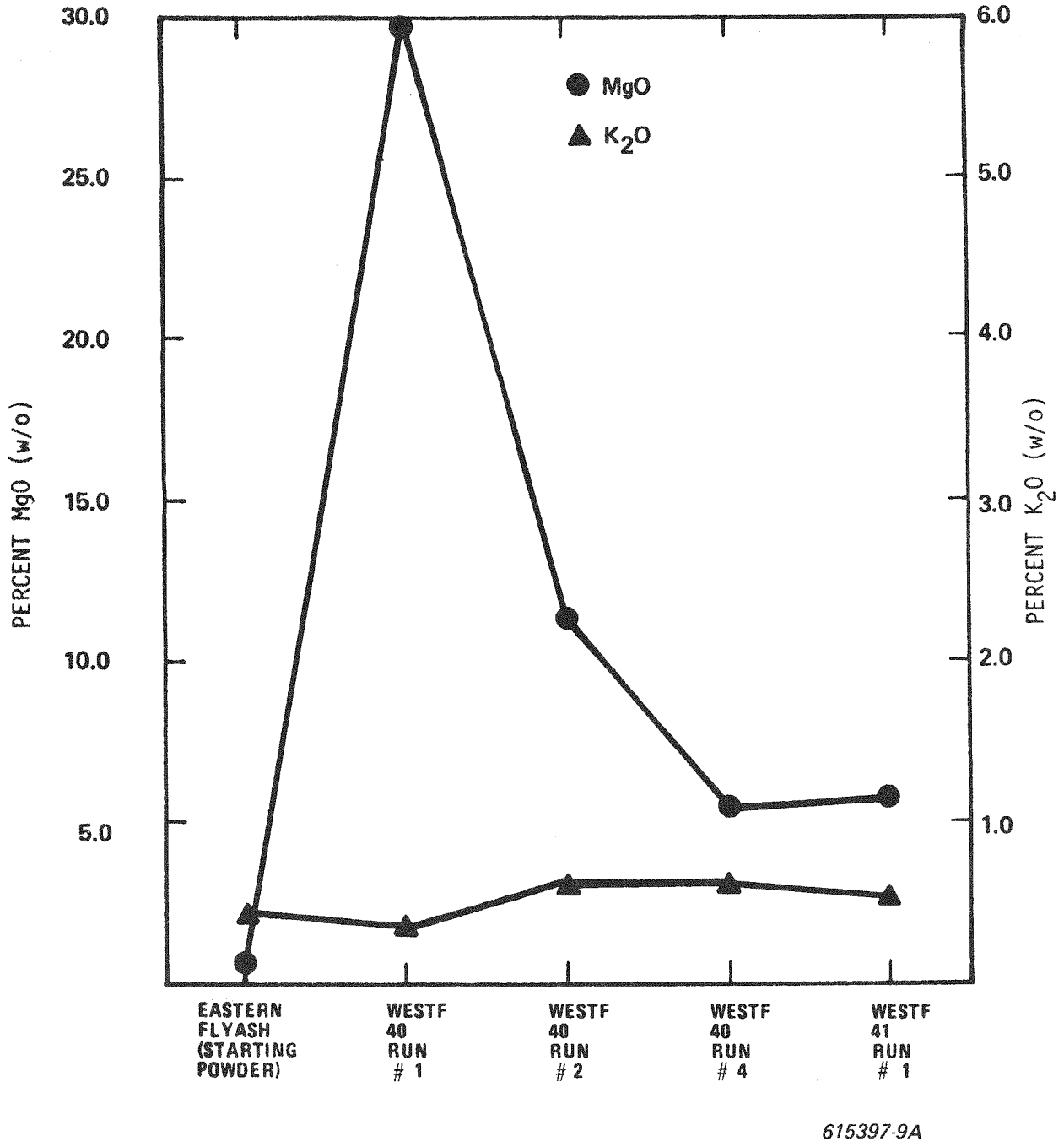

Figure 35. Magnesia and Potassium Oxide Content of Eastern Slag During WESTF Tests

Electrical Analysis

In the prior quarterly report, Reference 1 - Figures 70 to 74, the usual plots of electrode potential as a function of electrode-pair number were amplified to include the floating potentials of individually insulated copper heat sinks mounted in the channel insulating ceiling. Since each of these heat sinks was about 1/5 of the channel length the plots of voltage versus electrode-pair number become a series of individual potential steps. As previously discussed, these heat sinks were not exposed directly to the plasma but were covered with slabs of insulating MgO ceramic. The shape of the potential curves for the heat sinks is a function of the leakage resistances between the individual heat sinks, and between the heat sinks and the various electrical components of the channel, such as the electrodes, and the end flanges.

Similar plots for WESTF Test 41-1, have been prepared and are included in Figures 36 to 43. Figure 44 shows the configuration of electrodes, insulating wall components, and the code for identifying them. The water-cooled heat sinks for Test 41-1 were covered with slabs of spinel ceramic. The insulating walls at the top of the channel and at the bottom of the channel are designated by the symbols T and B, respectively, in Figure 44. The electrical circuit used in Test 41-1 is shown in Figure 45. All of the electrical data were taken with the electrodes floating, i.e., no electrode or circuit element was grounded.

The potential plots for Test 41-1 have been expanded to include all of the heat sinks mounted at the bottom of the channel. The curves plotting the potentials of the heat sinks mounted on the channel ceiling as a function of distance are the curves at the top of Figures 36 to 43. The curves giving the potentials of the heat sinks on the floor of the channel are the middle curves in Figures 36 to 43. The currents observed in the individual circuits are shown at the bottoms of the figures.

In previous reports the curves of electrode potential were plotted as though the measured value of voltage occurred at the center point of each electrode. The present potential plots take into account the finite lengths of the electrodes.

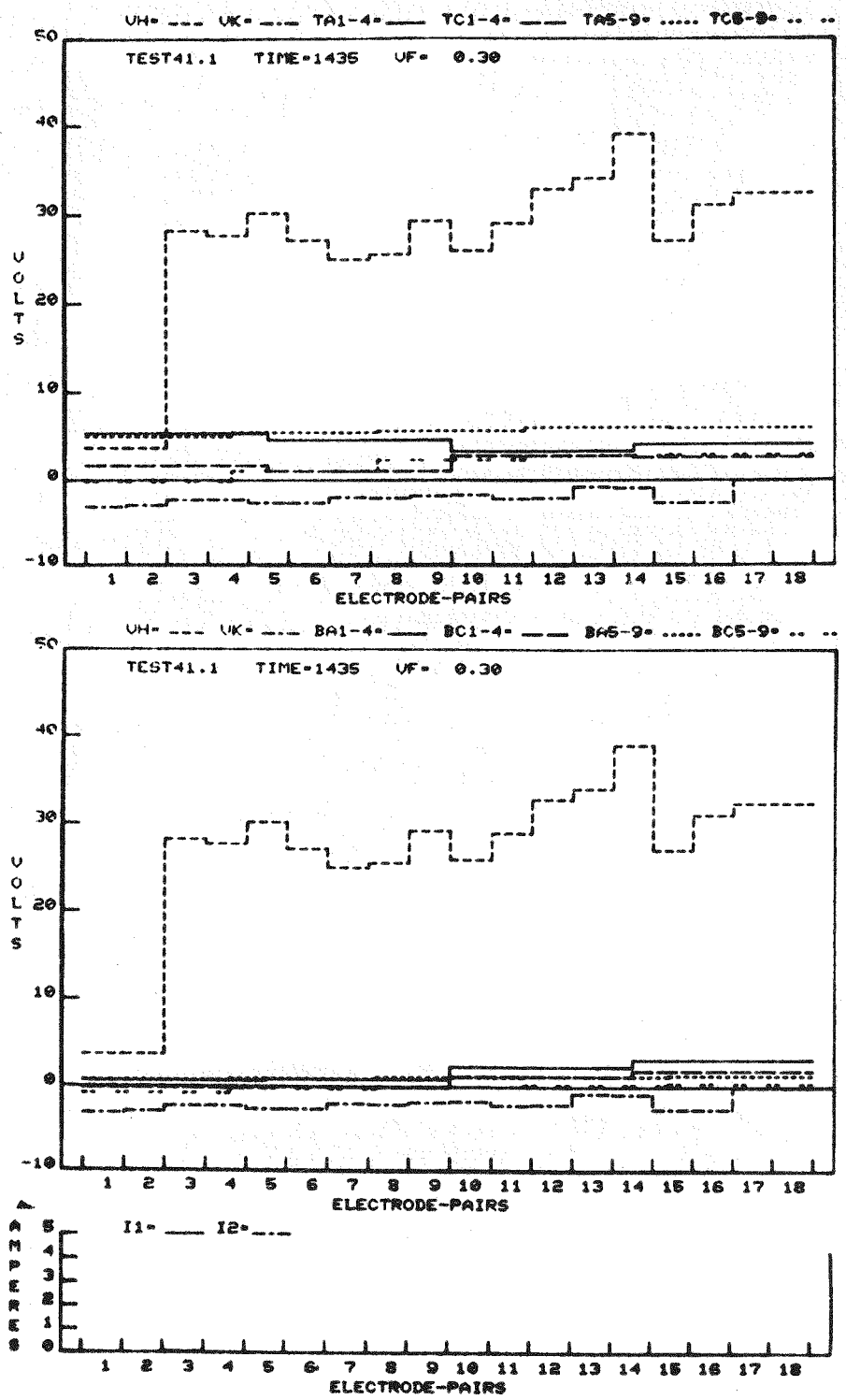

Figure 36. Applied Electrode Voltages, Currents, and Floating Potentials of Water-Cooled Copper Heat Sinks in Top and Bottom Insulating Walls of Channels as Function of Position. No Axial Voltage.

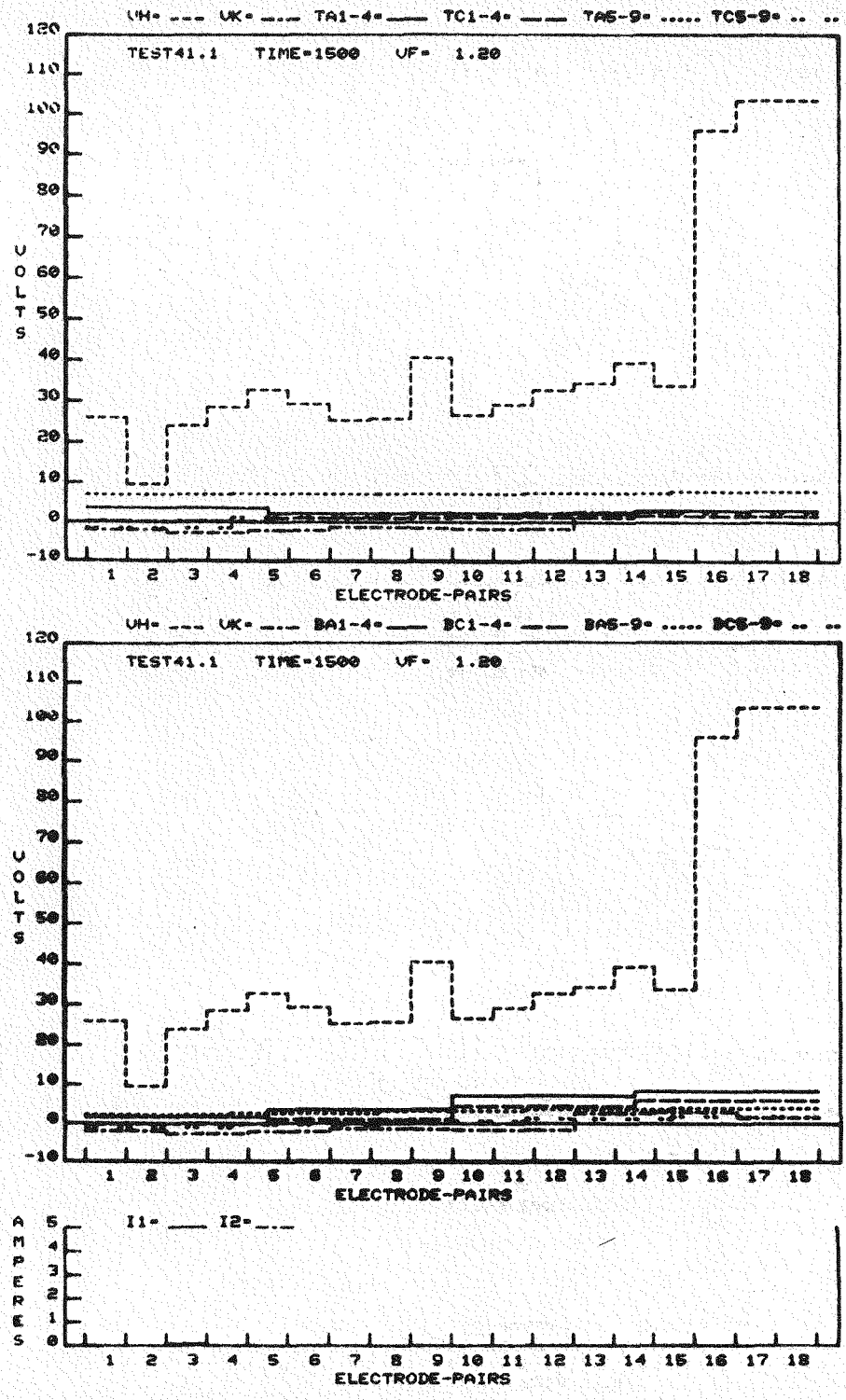

Figure 37. Applied Electrode Voltages, Currents, and Floating Potentials of Water-Cooled Copper Heat Sinks in Top and Bottom Insulating Walls of Channel as Function of Position. Anode Axial Voltage, 72.5 V, 0.06 Amperes.

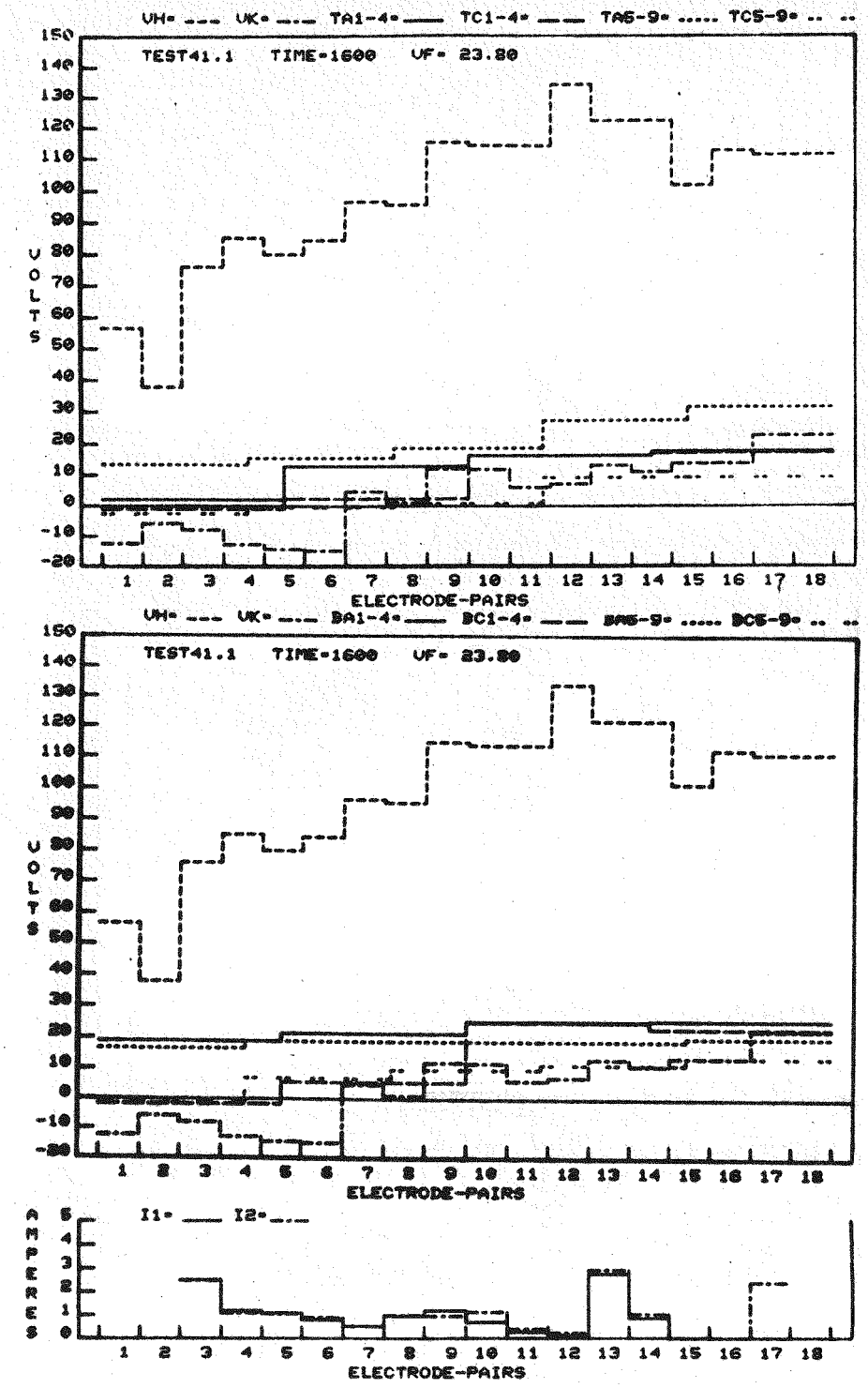

Figure 38. Applied Electrode Voltages, Currents, and Floating Potentials of Water-Cooled Copper Heat Sinks in Top and Bottom Insulating Walls of Channels as Function of Position. Anode Axial Voltage, 31.3 V, 2.4 Amperes.

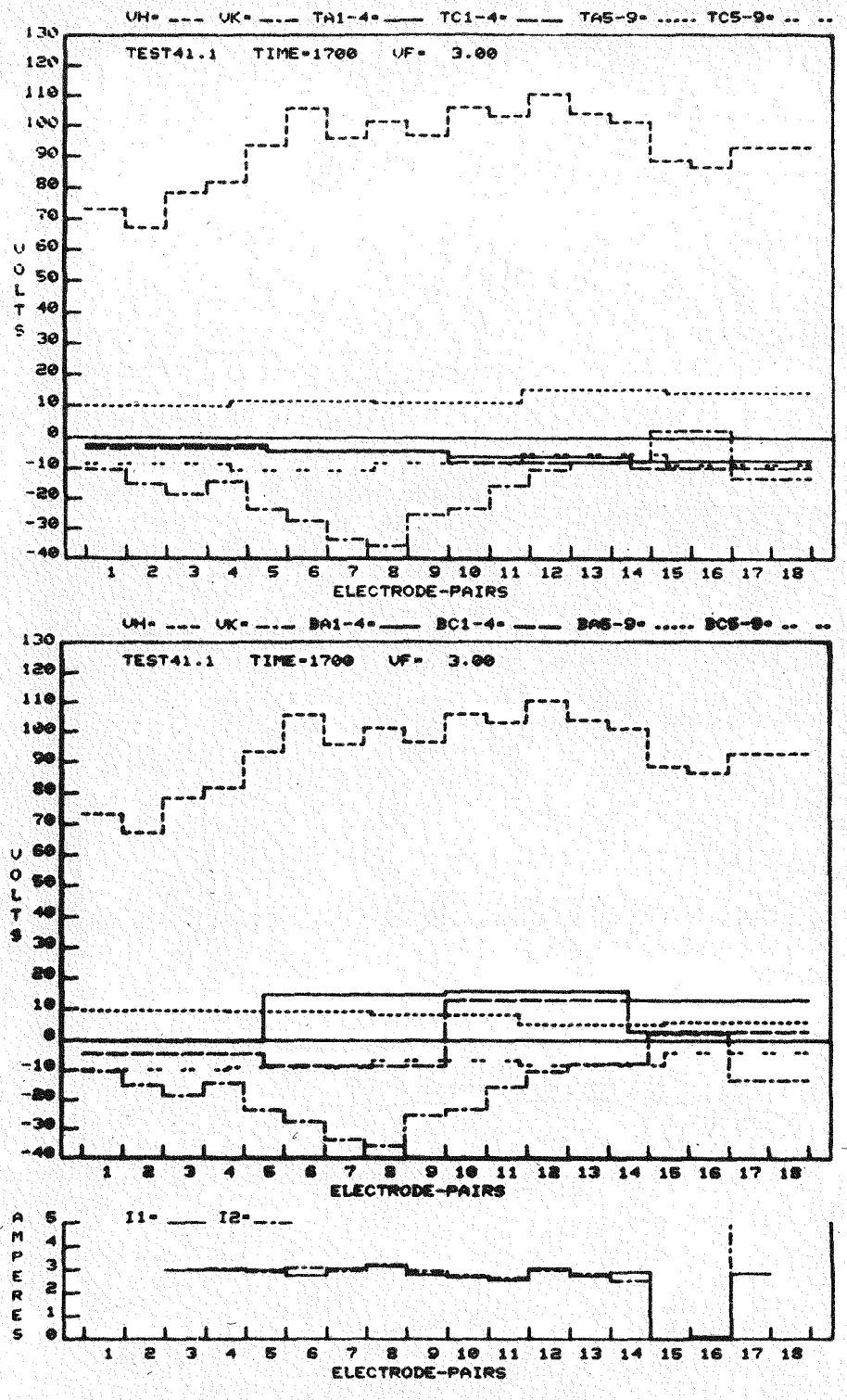

Figure 39. Applied Electrode Voltages, Currents, and Floating Potentials of Water-Cooled Copper Heat Sinks in Top and Bottom Insulating Walls of Channels as Function of Position. Anode Axial Voltage, 7.5 V, 4.8 Amperes.

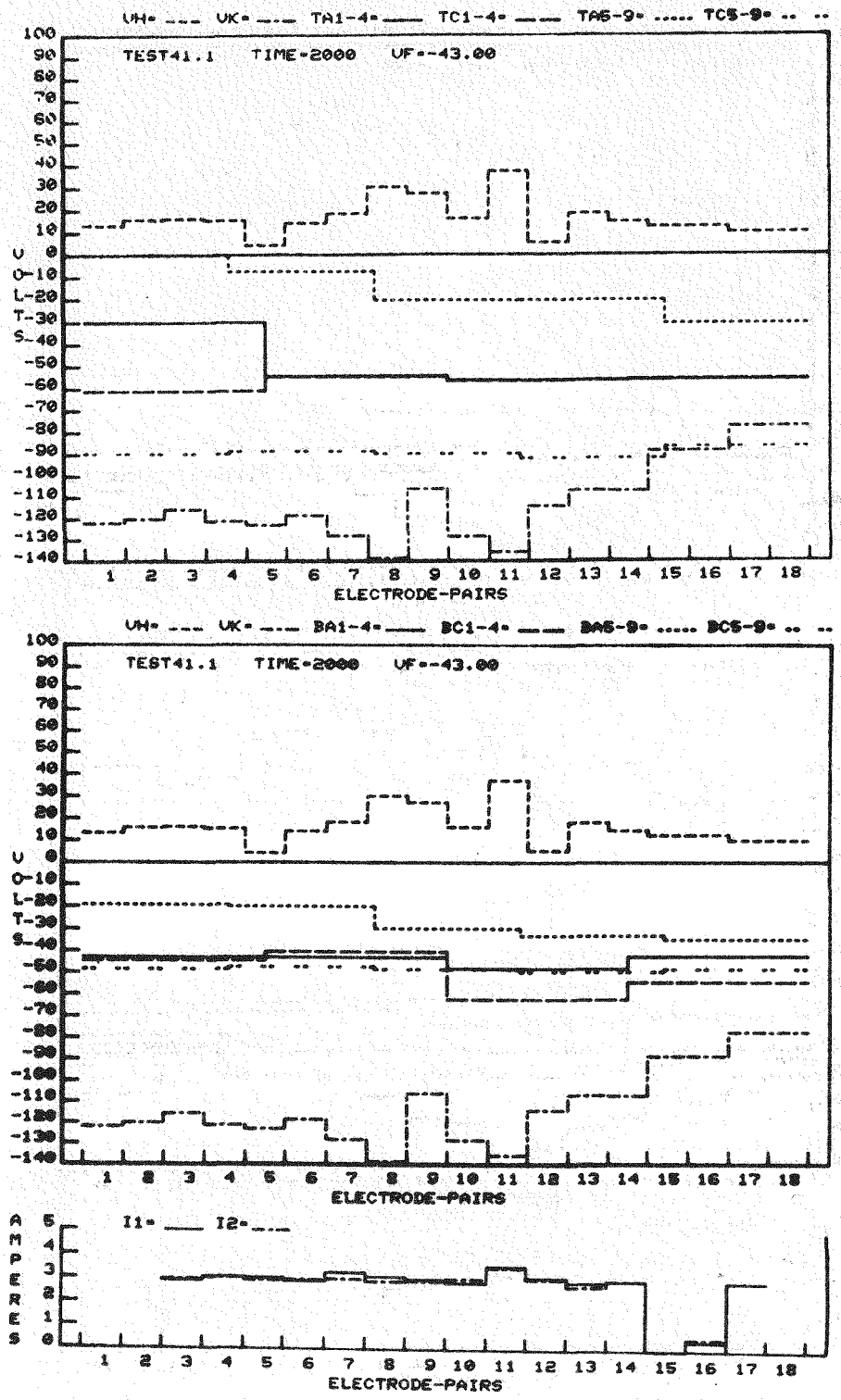

Figure 40. Applied Electrode Voltages, Currents, and Floating Potentials of Water-Cooled Copper Heat Sinks in Top and Bottom Insulating Walls of Channel as Function of Position. Anode Axial Voltage, 1.0 V, 9.2 Amperes.

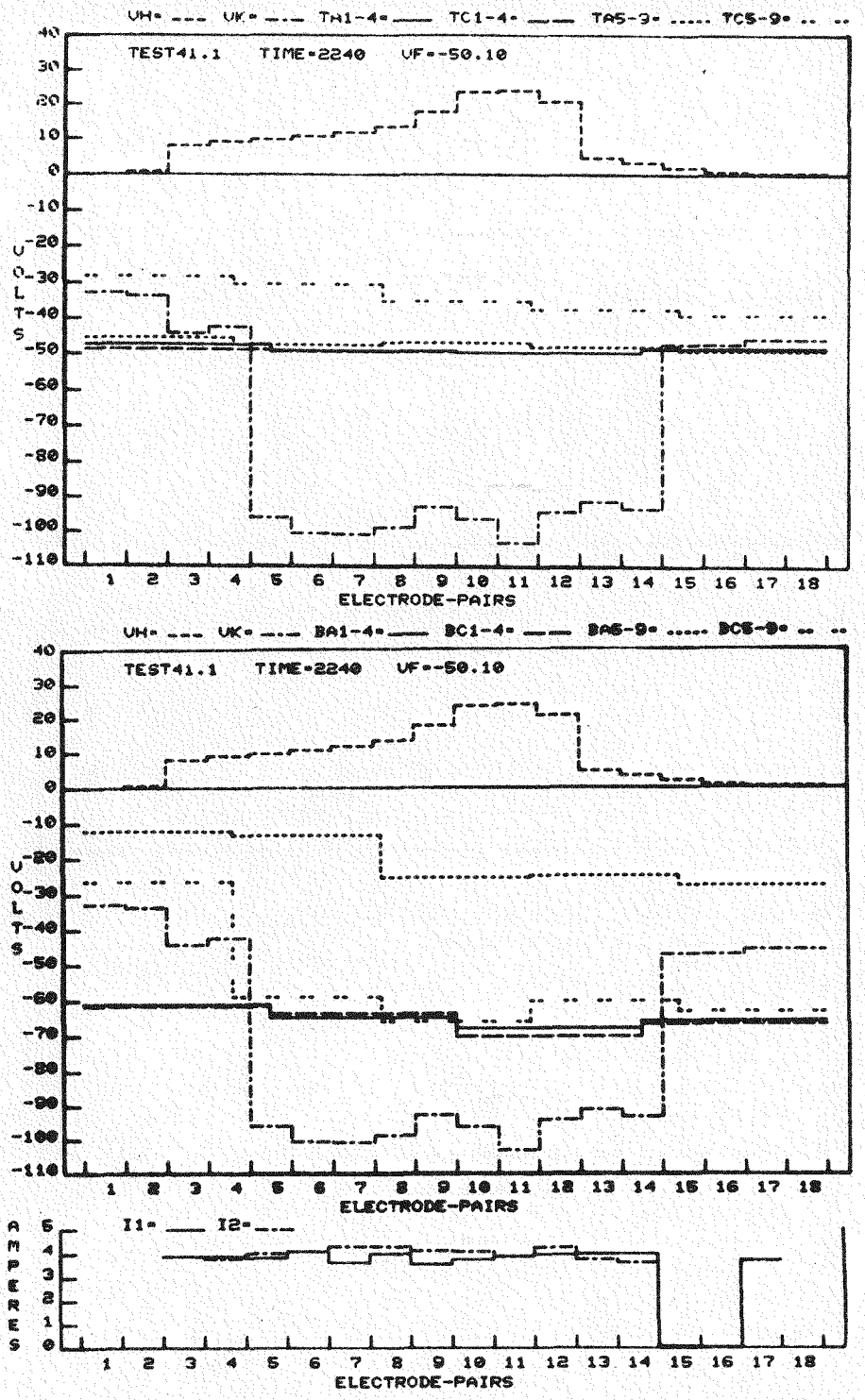

Figure 41. Applied Electrode Voltages, Currents, and Floating Potentials of Water-Cooled Copper Heat Sinks in Top and Bottom Insulating Walls of Channels as Function of Position. No Axial Voltage.

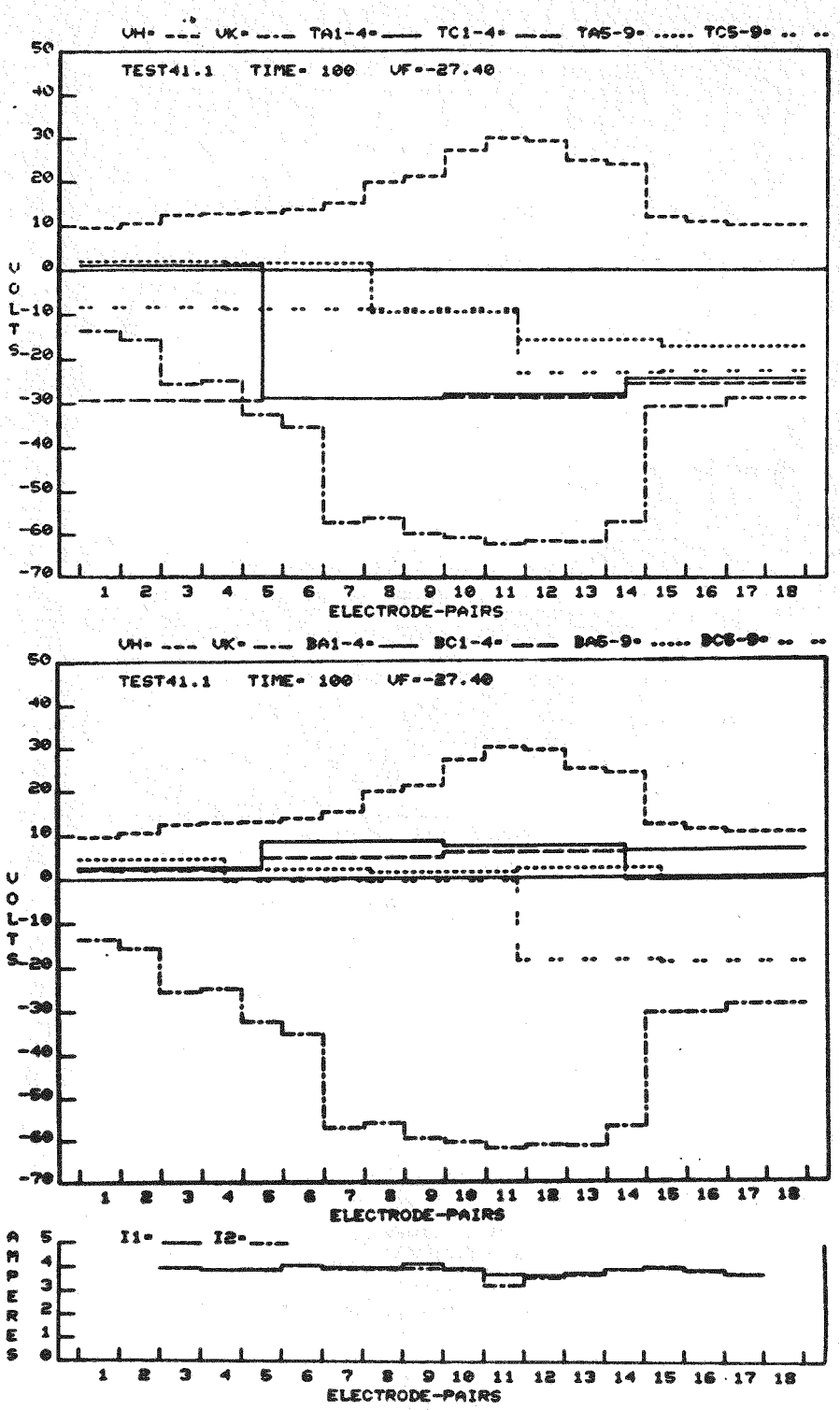

Figure 42. Applied Electrode Voltages, Currents, and Floating Potentials of Water-Cooled Copper Heat Sinks in Top and Bottom Insulating Walls of Channel as Function of Position. No Axial Voltage.

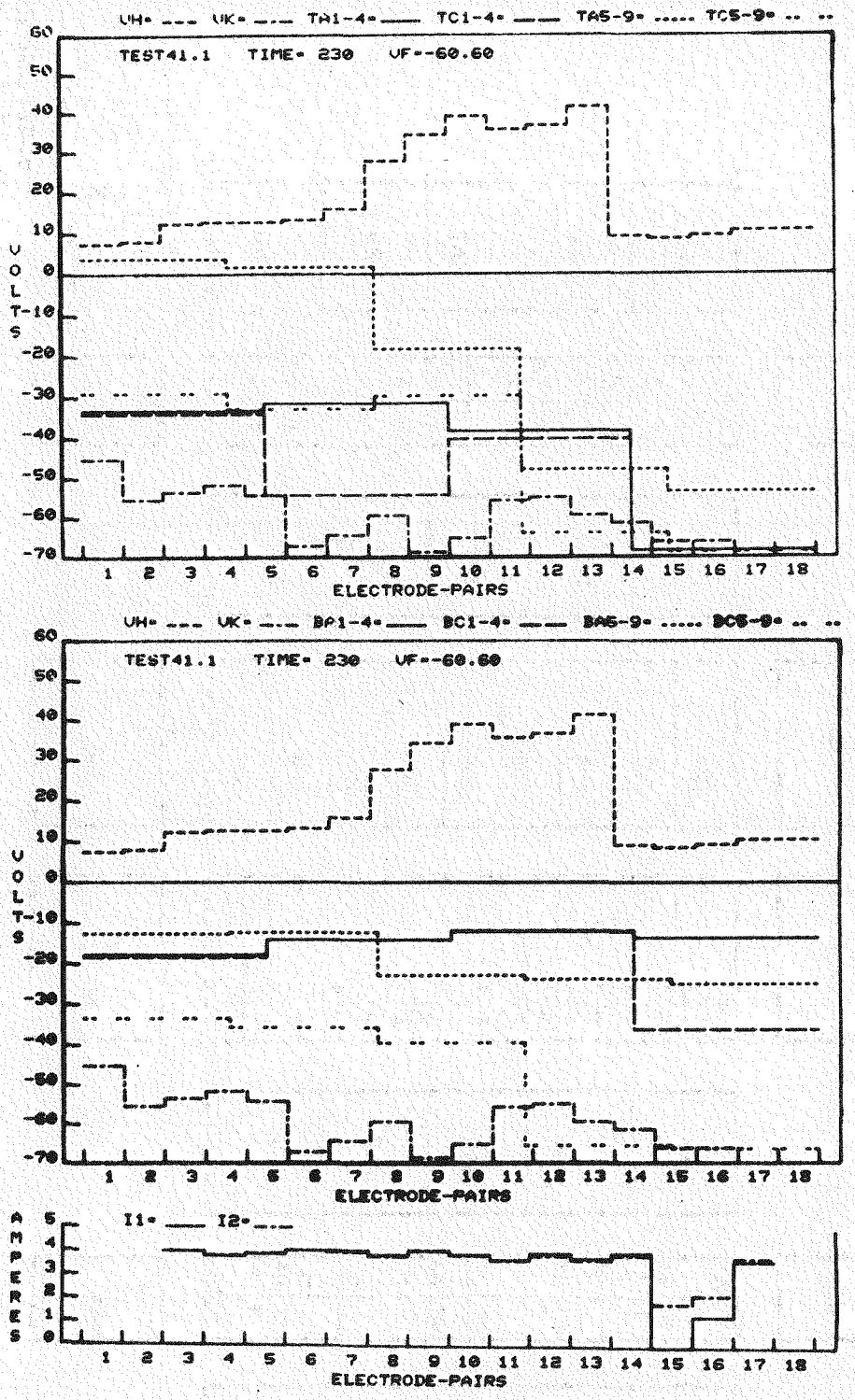

Figure 43. Applied Electrode Voltages, Currents, and Floating Potentials of Water-Cooled Copper Heat Sinks in Top and Bottom Insulating Walls of Channel as Function of Position. No Axial Voltage.

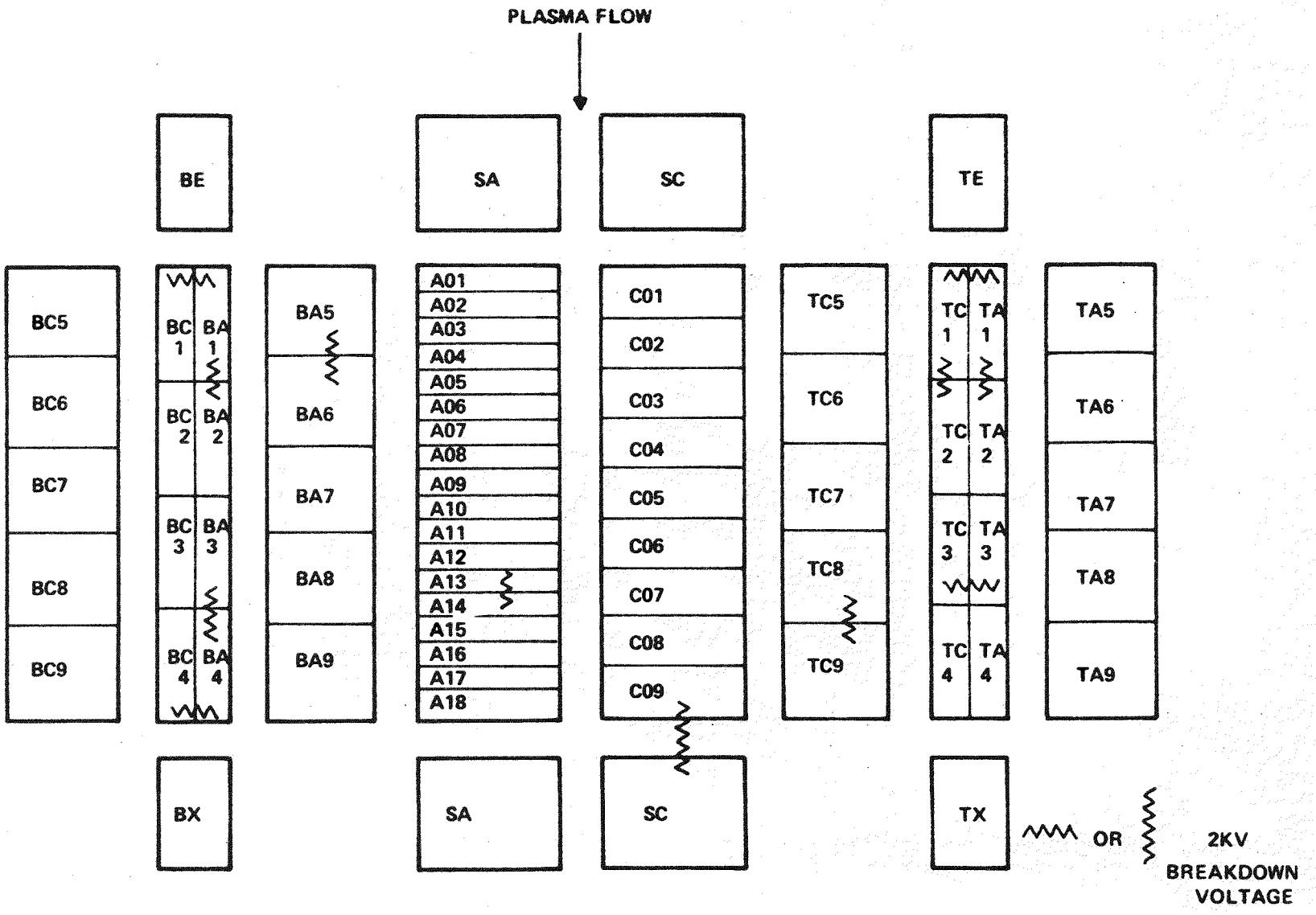

Figure 44. Channel Schematic - Test 41

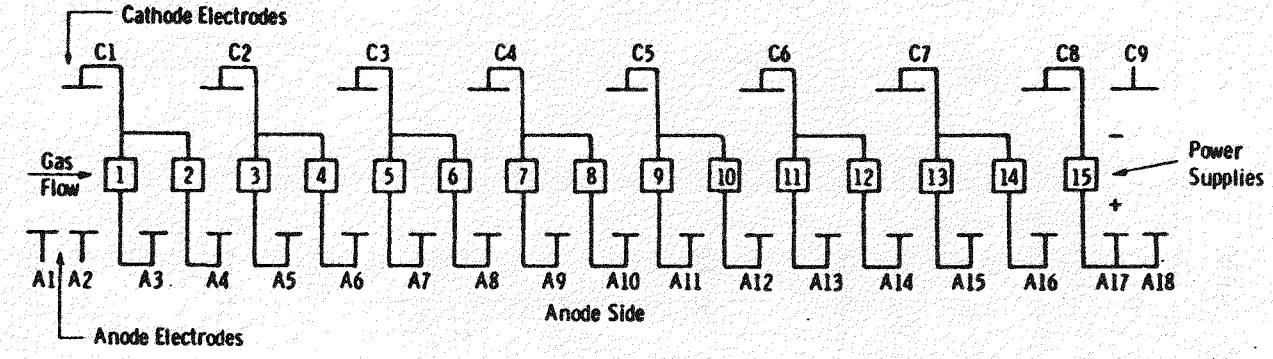

Figure 45. Electrical Circuit Used for Test 41 - Run 1

The plottings of channel components in this way provides a more accurate picture of the electrical field gradients which occur. The curves giving the potential of the positive and negative electrodes has been superimposed into the curves giving the heat sink potentials for both the top and the bottom insulating walls of the channel. The symbol V_H refers to the potentials of the positive electrodes, the symbol V_K the potentials of the negative electrodes. The potential of the exit flange, V_F, in volts, is shown in each graph, as well as the time the data for the graphs were taken.

Test 41-1 was initiated on March 5, 1979. Seed was introduced at 1415. Unlike the beginning of Test 40-4, see Figures 70 to 73 of Reference 1, the ceiling and floor heat sinks, and the cathode electrodes operated near ground potential. In Test 40-4 the heat sinks operated initially at potentials very close to the positive electrodes for the first three hours of the test. They then shifted toward ground potential during the test, see Figure 74 of the last report.

In Figure 36, no axial field was applied. The current resulting from impressing 72.5 volts axially across the anode configuration was initially very low, see Figure 37, indicating a high value of leakage resistance. In addition, most of the axial voltage appeared across the insulation between anode electrodes 15 and 16. Once current was initiated in the channel, see Figure 38, the axial voltages across the anode insulation intended to distribute more uniformly across the anode electrode insulation. The axial leakage resistance decreased rapidly with time, as can be determined from Figures 38 and 39. Starting about 2000 hours, see Figure 40, the potential of the anode electrodes started to approach ground potential and the cathode electrodes became more negative relative to ground. The potential of the various heat sinks, which had been fairly close to system ground tended to go negative. Referring to Figure 41, the five floor heat sinks adjacent to the anode, BA5-BA9, dropped to negative voltages between -12 volts and -27 volts, while the heat sinks adjacent to the cathode electrodes, BC5-BC9, assumed voltages between -26 volts and -63 volts. In the case of the channel ceiling, however, the heat sinks adjacent to the cathode actually became ore positive then the heat sinks adjacent to the anode. This would indicate the presence of one or more leakage paths from some of the cathode heat sinks to the anode electrodes, possibly through the plasma, or vice versa.

In Figure 42 most of the heat sinks in the duct floor insulating wall have shifted in the positive direction toward ground potential, whereas the heat sinks in the channel ceiling tend to operate at somewhat more negative potentials. In Figure 43 the heat sinks in the channel ceiling and floor have again shifted in the more negative direction.

The potential of the downstream flange, V_F, in general has tended to follow the shifts in potentials of the channel heat sinks.

It seems clear from the data taken in these tests so far that wide fluctuations in the potentials of the heat sinks occur as a function of time during a given test run. It is believed that the variations in leakage resistance are a function of the rate of deposition and condensation of seed and slag in the various internal surfaces of the channel. It is not clear why the deposition rates appear to vary and why regions of high leakage appear to shift with time.

In general, the leakage resistance between the heat sinks and the electrodes appears to be higher than the leakage resistance between adjacent heat sinks. This results in a tendency for the heat sinks and the flange to assume roughly the same potentials.

The leakage resistance between adjacent electrodes appears to steadily decrease with continued operation. The net result of this characteristic is that the axial currents gradually become excessively large when axial fields are continuously applied. Turning off the axial fields tends to produce a healing action as discussed in the last quarterly report, Reference 1.

2.2 WBS 1.2.2 - Test Assembly Fabrication

WESTF Test 41

The test section from WESTF Test 41, Run 1, was disassembled and it was determined that only the electrodes themselves would be incorporated in a rebuilt test section. The surfaces of the electrodes were very good and showed only minor arc damage, with most of the damage concentrated on the edges that were

adjacent to the insulating walls. The cooling tubes on the two upstream electrodes were severely damaged and had to be removed and replaced. Otherwise the electrodes were reused as they were removed from the electrode walls.

The WESTF 41-R (rebuilt) test section is composed of inlet and outlet transition sections, a top and bottom insulating wall, and two electrode walls (anode and cathode). The duct in the inlet and outlet transition sections are lined with magnesia brick (MG-HW0501), 0.940 cm (0.370 inch) thick. These tiles are attached to the water-cooled copper transition section with RTV silicone adhesive. The top and bottom tiles are each one piece, 4.5 inches long with a ledge on each side to hold the side tiles in place should the adhesive bond fail. One of the side tiles is also one piece and the other, to accommodate a thermocouple, is made of two interlocking pieces. The top and bottom tiles of the transition section interlock with the tiles on the top and bottom insulating walls.

In order to improve the electrical characteristics of the channel, the insulating walls were completely redesigned and the G-10 support walls were remade to accept the new cooling block arrangement. There are 36 cooling blocks on each wall, 12 long blocks on each side and 12 diagonal blocks within the center of the duct. A nominal 0.040 inch gap separates the blocks. The gap is filled with a low-viscosity heat curable silicone elastomer for electrical isolation. The cooling blocks on each insulating wall are covered with six interlocking fused cast alumina tiles (AL-CC0101), 0.737 cm (0.290 inch) thick in the duct and with 82 percent dense spinel brick (MA-NT0201) of the same thickness on surfaces not exposed to the plasma. The ceramic insulators overlap the copper cooling blocks and are attached to them with RTV silicone adhesive. The center tiles extend beyond the electrodes so that they are locked in place and cannot move should the adhesive fail. A G-7 spacer backs up the cooling blocks and maintains them at a fixed distance from the G-10 outer wall. A schematic of the insulating walls is shown in Figure 13.

The electrode walls are composed of copper anodes with platinum sheet brazed to the surface and TD nickel sheet brazed to the upstream edge and copper cathodes with W-Cu composite brazed to the surface and TD nickel sheet brazed to

the upstream edge. As stated before, these electrodes were recovered from WESTF Test 41, Run 1, for use in the rebuilt test section. New G-10 electrode support walls were made and hole locations shifted so that, instead of an ineffectively cooled 0.2 inch thick spacer on each end, a 0.4 inch water cooled spacer will be employed at the exit end of the walls. (The spacer is used to make up for differences in the AVCO electrode dimensions and the effective length of the Westinghouse electrode walls).

The anode wall holds 18 electrodes on a pitch of 0.89 cm; the cathode wall holds nine electrodes on a pitch of 1.78 cm. The interelectrode insulation is boron nitride. Because many of the insulators cracked in Run 1, new interelectrode insulators were made for 41R. Each anode/insulator assembly is 0.89 cm x 6 cm with an anode surface of 0.79 x 6 cm (4.74 cm^2) exposed to the plasma. Each cathode insulator assembly is 1.78 cm x 6 cm with a cathode surface of 1.55 x 6 cm (9.30 cm^2) exposed to the plasma. The location and identification of electrodes and thermocouples on electrode walls and a sketch of the electrode/insulator assemblies are shown in Figure 2. The flow cross-section of the assembled channel is nominally 2.7 cm x 6.0 cm or 16.5 cm^2.

Excessive leakage was encountered in the pressure test of the rebuilt test section. As a result, the test section was partially disassembled to permit external potting of the channel walls. Following this rework and the successful completion of the pressure test, the completed test section was delivered for final electrical tests and installation in WESTF.

Electrical resistance measurements were made on the individual walls prior to assembly. All measured resistance, except for 17,000 ohms between T11 and T12, were infinite. Electrical measurements made after assembly and prior to test are given in Table 16, with symbols referenced to the schematic diagram shown in Figure 46. These data again show a significant improvement over previous insulating walls.

TABLE 16

ELECTRICAL TESTS - ASSEMBLED CHANNEL FOR WESTF 41, RUN 2

Measured Points(1)	Resistance Megohms	Breakdown
Electrode Walls		
All Points	∞	>2KV
Bottom Insulating Wall		
All Points	∞	>2KV
Top Insulating Wall		
TA1 - TA2	∞	1800
TA5 - TA6	∞	700
TA7 - TA8	∞	1800
T6 - T7	∞	500
T8 - T9	∞	1300
T10 - T11	∞	1600
TC6 - TC7	∞	1800
TC11-TC12	∞	1500

1) Showing resistances between individual components or ground of less than 100 megohms or breakdown voltages of less than 2,000 volts.

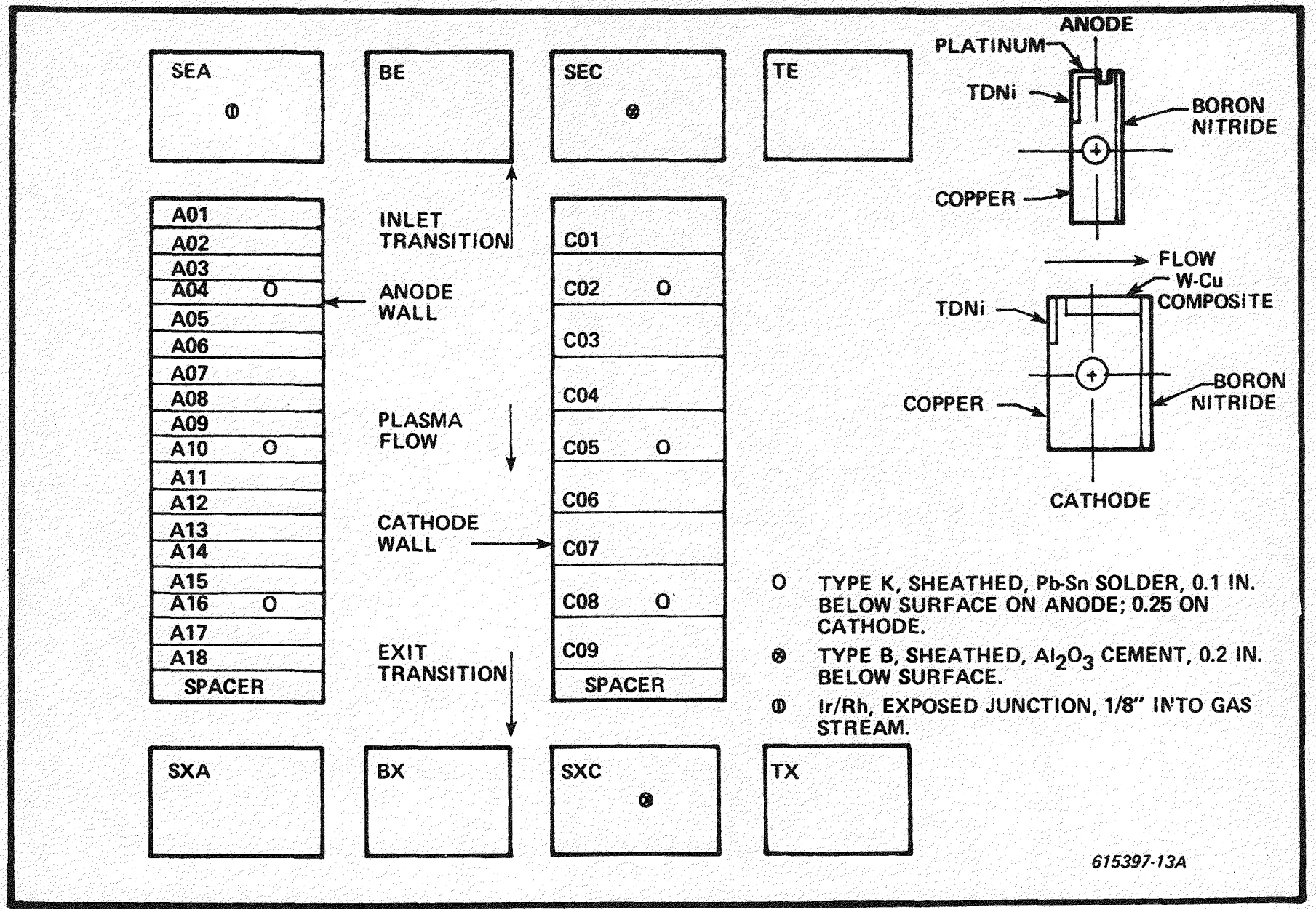

Figure 46. Schematic Diagram of Electrode Walls and Transition Sections - WESTF 41 - Run 2

WESTF Test 42

The scope of WESTF Test 42 has been expanded to include, in addition to zirconia-based coupons, hafnia-based coupons and selected insulator materials. The materials selection was presented in Section 2.1.1. The insulators have been sized based on manufacturer supplied data. The zirconia-based coupons have been sized based on measurements made by Battelle PNL on Westinghouse supplied materials, see Section 2.1.2. Battelle PNL is supplying the hafnia-based coupons and the thermal conductivity data required for the final design of these coupons. All of the components for this test section, with the exception of the hafnia coupon assemblies, have been machined and the preparation of sub-assemblies is underway. A revised final test specification will be issued after final definition of the hafnia-based coupons is obtained.

Tests are made to confirm the attachment of all of the ceramic materials in this test to nickel mesh using TiCuSil brazing alloy. All post-machined, oven-dried specimens are brazed to the mesh with the exception of CORHART spinel. This material was found to have residual sulfur-bearing constituents that attacked the nickel mesh and prevented a good bond from being obtained. It was found necessary to give CORHART spinel a high temperature oxidation treatment to remove the residual sulfur prior to brazing in a vacuum furnace in order to obtain a satisfactory attachment.

WESTF Test 43

WESTF Test 32 is a test of platinum anodes and iron cathodes under hot slagging conditions. Engineering sketches of component parts for this test section have been prepared and submitted to the machine shop. These parts are being machined, but with interruptions due to the priority being given to the WESTF Test 42 components.

2.3 WBS 1.2.3 - WESTF Operations

2.3.1 Pre-Test Activity

During this quarter the rebuilt test section for WESTF Test 41-Run 2 was received and installation initiated. As part of these operations electrical checks were completed; data is presented in Section 2.2.

Normal facility maintenance activities were completed, as required.

A continuing improvement in the mini-computer data acquisition system is being implemented. The system has been modified so that it can now:

- Handle electrical inputs from both the electrode and insulating walls and display the data in graphical form.
- Complete calculation of rates of change of the variables to assist in evaluation of channel performance.
- Display data in formats which are more functional.

With the increasing amount of data being handled by the mini-computer/DAS and the expanded on-line data reduction and calculations, expanded mini-computer memory is required. Equipment has been selected for procurement in this regard.

2.3.2 Test Operations

No WESTF test operations were scheduled or completed during this reporting period.

3.0 WBS 1.3 - WESTF MODIFICATIONS

3.1 Mini-Computer/DAS Expansion

Equipment necessary to effect the mini-computer/DAS expansion has been selected and procurement approval requested.

3.2 Magnet Installation

As a result of the planned installation of a magnet for WESTF, extensive building modifications are required. Figure 47 illustrates to some degree the extent of these modifications as they apply to WESTF.

- The mini-computer, orginally located in the WESTF control room - Room IC5, has been relocated to Room IC2.
- The gas analysis equipment and other non-WESTF equipment, currently located in Room IC6, will be relocated to Room IC7-A.

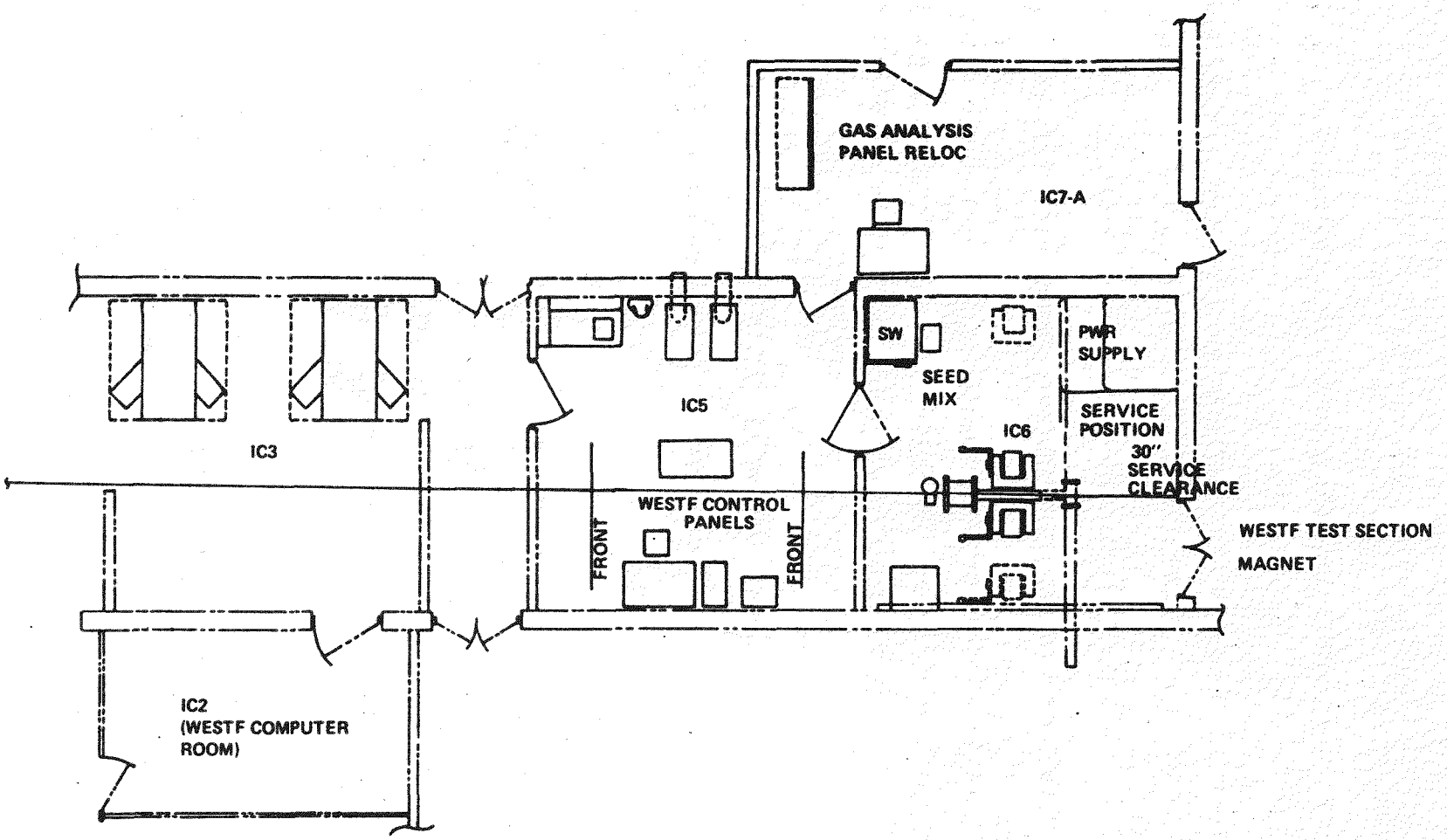

Figure 47. Building 301 Rearrangement (Partial)

- The WESTF flow system will be relocated within Room IC6 to permit magnet installation in such a manner that safe and convenient access is provided to the test section.
- The magnet power supply and safety switch will be installed in Room IC6.

As a result, Rooms IC2, IC5 and IC6 of Building 301 at the Westinghouse Research Center will be devoted to WESTF operations. These modifications will have a positive effect on future WESTF operations.

Purchase orders have been released for a number of long-lead electrical equipment items.

It is planned to complete necessary modifications in parallel with continued WESTF operations to the maximum extent practicable in order to minimize WESTF downtime.

4.0 WBS 1.4 - PROJECT MANAGEMENT AND DOCUMENTATION

The following required project documentation was issued during the reporting period:

- Quarterly Report for the Period January - March 1979.
- Project Management Summary Baseline Report (Original Issue - dated April 1979).

5.0 REFERENCES

1. FE-15529-2, "MHD Electrode Development," Quarterly Report, January-March 1979. DOE Contract DE-AC-01-79-ET-15529, Westinghouse Electric Corporation, Jay 1979.
2. FE-2248-20, "Development, Testing and Evaluation of MHD Materials and Component Designs, Quarterly Report, April-June 1978," DOE Contract EX-76-C-01-2248, Westinghouse Electric Corporation, August 1978.

3. FE-2248-22, "Development, Testing and Evaluation of MHD Materials And Component Designs, Quarterly Report, April-June 1978," DOE Contract EX-76-C-01-2248, Westinghouse Electric Corporation, December 1978.

V. SUMMARY PLANS NEXT REPORTING PERIOD

Summary plans covering significant activities in the next reporting period are presented below according to the Work Breakdown Structure primary tasks.

WBS 1.1 - ELECTRODE AND INSULATOR MATERIALS

- Complete Pt-Fe electrochemical tests in western slag (Rosebud) plus K_2CO_3.
- Complete electrochemical tests of ZrO_2 with various yttria and calcia dopant level in western slag (Rosebud) plus K_2CO_3.
- Prepare insulator materials, MgO, $MgAl_2O_4$ and Al_2O_3, for upcoming WESTF tests.
- Prepare electrode materials, $MgCr_2O_4$, ZrO_2 and $YCrO_3$, for planned Materials Test Section tests in WESTF.
- Continue slag corrosion tests of insulator materials.

WBS 1.2 - ENGINEERING TESTS

- Continue test planning activities and:
  - Revise Test Specification for WESTF Test 42
  - Issue Test Specifications for WESTF Tests 44, 45 and 46
- Complete design of Hafnia coupons for WESTF Tests 42 and 44
- Complete fabrication of channels for WESTF Test 42 and 43
- Complete WESTF Tests 41 and 42
- Initiate fabrication of WESTF Test 44
- Complete detail design of Mini-WESTF and Materials Test Sections
- Complete detailed design of revised WESTF Test Section (for use with magnet).

WBS 1.3 - WESTF MODIFICATION

- Initiate magnet modification
- Continue long lead materials procurement for magnet modification and expansion of DAS

WBS 1.4 - PROJECT MANAGEMENT AND DOCUMENTATION

- Complete technical, schedular and budgetary planning and issue Project Management Summary Baseline Report, FY 80 Revision, for DOE approval.
- Issue March - June 1979 quarterly technical progress report

VI CONCLUSIONS

Two hafnia based materials have been identified by Battelle PNL for inclusion in WESTF Test 42, zirconia/hafnia coupons. These sintered materials are:

- Hafnia A - $Pr_{0.27}Yb_{0.09}Hf_{0.64}O_2$
- Hafnia B - $Tb_{0.2}Y_{0.1}Hf_{0.7}O_2$

Two additional test sections are being considered for use in WESTF. These are:

- Materials Test Section
- Mini - WESTF Test Sections

These test sections will complement the existing WESTF Test Section and permit expanded use of WESTF to develop necessary materials and electrode/insulator systems performance data. Of primary importance in these tests is to evaluate materials as follows:

Electrode Material	vs.	Temperature Current Density Slag/Seed Chemistry
Insulator Material	vs.	Temperature dV/dx Slag/Seed Chemistry

☆U.S. GOVERNMENT PRINTING OFFICE: 1980-640-258 1997